BioMed Research International

Current and Future Novel Treatments for Glioblastoma Multiforme

Guest Editors: Betty Tyler, Francesco DiMeco, Rachel Grossman, and Gustavo Pradilla

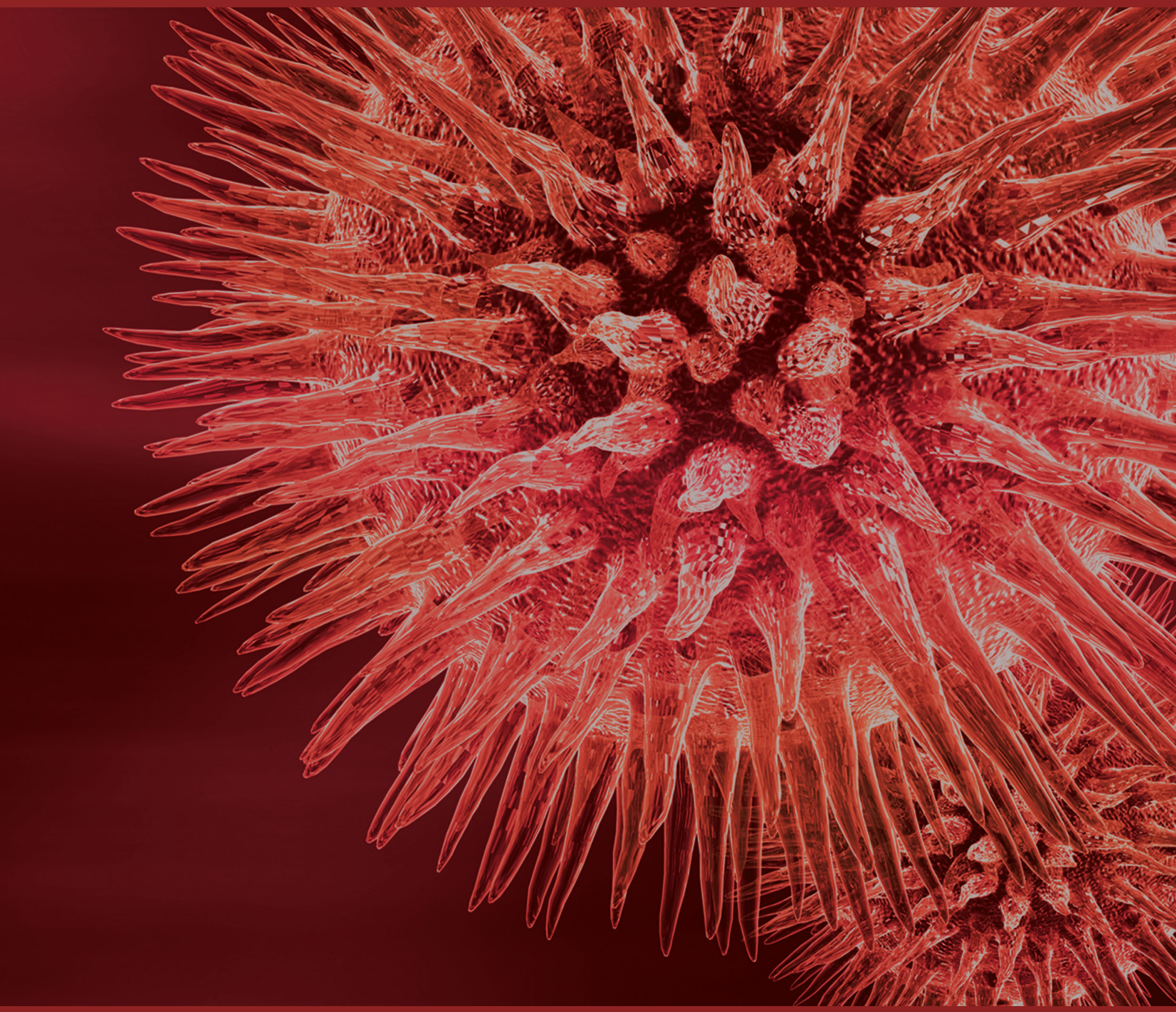

Current and Future Novel Treatments for Glioblastoma Multiforme

BioMed Research International

Current and Future Novel Treatments for Glioblastoma Multiforme

Guest Editors: Betty Tyler, Francesco DiMeco, Rachel Grossman, and Gustavo Pradilla

Contents

Hindawi Publishing Corporation
BioMed Research International
Volume 2014, Article ID 432195, 1 page
http://dx.doi.org/10.1155/2014/432195

Editorial

Current and Future Novel Treatments for Glioblastoma Multiforme

Betty Tyler,[1] Francesco DiMeco,[2] Rachel Grossman,[3] and Gustavo Pradilla[4]

[1]*Department of Neurosurgery, Johns Hopkins University, Baltimore, MD 21231, USA*
[2]*Istituto Nazionale Neurologico "Carlo Besta", 20133 Milan, Italy*
[3]*Department of Neurosurgery, Tel-Aviv Medical Center, 64239 Tel-Aviv, Israel*
[4]*Department of Neurosurgery, Emory University School of Medicine, Atlanta, GA, USA*

Correspondence should be addressed to Betty Tyler; btyler@jhmi.edu

Received 4 November 2014; Accepted 4 November 2014; Published 22 December 2014

After decades of slight to modest changes in outcomes, survival for patients with glioblastoma has shown consistent and sustained improvement. Whether this improvement is due to enhanced imaging technologies, increased diagnostic accuracy, earlier detection, advanced microsurgical techniques, functional tissue preservation, postoperative critical care, targeted radiation, or novel adjuvant therapies is uncertain. What is known is that the field is moving in a more promising direction. In this issue we have selected novel and exciting contributions that represent our current landscape and illustrate new directions, highlighting their opportunities as well as their limitations. The goal of this special issue is to stimulate new understanding and encourage cross-discipline collaborations that will assist in changing the outlook for this disease.

We have invited investigators to contribute original research articles as well as topical reviews that provide updated perspective and present exciting contributions. We have included articles that explore intraoperative technological advances like "*Fluorescence-guided surgery and biopsy in gliomas with an exoscope system*" and combine intraoperative imaging with tissue characterization and biomarker utilization such as "*Intraoperative cerebral glioma characterization with contrast enhanced ultrasound*." Original contributions presenting improved immunotherapy strategies such as "*Interleukin-13 receptor alpha 2-targeted glioblastoma immunotherapy*" and alternative gene therapy approaches were also included such as "*Newcastle disease virus interaction in targeted therapy against proliferation and invasion pathways of glioblastoma multiforme*." The role of cancer stem cells in GBM malignancy and the progress made in its diagnostic and therapeutic implications are nicely reviewed as in "*Stem cell niches in glioblastoma: A neuropathological view*." The impact of the intracranial tumor microenvironment and its pathophysiological implications are also discussed in "*Progesterone induces the growth and infiltration of human astrocytoma cells implanted in the cerebral cortex of the rat*."

It is our intention that this issue will promote discussion of new topics of interest and stimulate interdisciplinary collaborative efforts to improve outcomes for patients with glioblastoma. New modalities of treatment, characterization of the tumor's microenvironment, developing intraoperative innovative techniques, and targeting tumor-specific receptors are all disciplines on the cutting edge of glioblastoma research, the results of which will hopefully lead to marked improvements in outcome.

Betty Tyler
Francesco DiMeco
Rachel Grossman
Gustavo Pradilla

Hindawi Publishing Corporation
BioMed Research International
Volume 2014, Article ID 952128, 8 pages
http://dx.doi.org/10.1155/2014/952128

Review Article

Interleukin-13 Receptor Alpha 2-Targeted Glioblastoma Immunotherapy

Sadhak Sengupta,[1,2] Bart Thaci,[2] Andrew C. Crawford,[3] and Prakash Sampath[1,2]

[1] *Roger Williams Medical Center Brain Tumor Laboratory, 825 Chalkstone Avenue, Prior 222, Providence, RI 02908, USA*
[2] *Department of Neurosurgery, Boston University School of Medicine, Boston, MA 02118, USA*
[3] *University of Illinois College of Medicine, Urbana-Champaign, IL 61801, USA*

Correspondence should be addressed to Prakash Sampath; brain.tumorlab@chartercare.org

Received 3 April 2014; Accepted 5 August 2014; Published 27 August 2014

Academic Editor: Gustavo Pradilla

Glioblastoma (GBM) is the most lethal primary brain tumor, and despite several refinements in its multimodal management, generally has very poor prognosis. Targeted immunotherapy is an emerging field of research that shows great promise in the treatment of GBM. One of the most extensively studied targets is the interleukin-13 receptor alpha chain variant 2 (IL13Rα2). Its selective expression on GBM, discovered almost two decades ago, has been a target for therapy ever since. Immunotherapeutic strategies have been developed targeting IL13Rα2, including monoclonal antibodies as well as cell-based strategies such as IL13Rα2-pulsed dendritic cells and IL13Rα2-targeted chimeric antigen receptor-expressing T cells. Advanced therapeutic development has led to the completion of several clinical trials with promising outcomes. In this review, we will discuss the recent advances in the IL13Rα2-targeted immunotherapy and evaluate the most promising strategy for targeted GBM immunotherapy.

1. Introduction

Despite incremental improvements in survival with the current standard of care for glioblastoma (GBM), which is a tripartite regimen of surgery, radiotherapy, and chemotherapy [1, 2], the prognosis for most patients remains dismal [3, 4]. Major limitations in the treatment of GBM are the tumor's location within the brain that impedes delivery of cytotoxic agents across the blood-brain barrier [2], compounded with a strong immunosuppressive environment [5] and chemo- and radioresistant glioma-initiating cells [6, 7]. As a result, novel strategies are continually being tested to improve patient survival, quality of life, and overall outcomes.

Targeted immunotherapy has thus emerged as promising field of research in the treatment of malignancies and has received a great deal of interest in recent years [8, 9]. Optimism regarding the use of targeted immunotherapy has been even higher recently, since the reported cure of lymphoma patients with engineered or genetically modified T cells targeting CD19 malignant cells [10]. This has increased the focus towards the potential antigens present exclusively in glioma as targets for gene- and immunotherapy. One of the most extensively studied targets is the interleukin-13 receptor alpha 2 (IL13Rα2) [11]. IL13Rα2 is a decoy receptor for interleukin-13 (IL13), lacking the signaling chain that is present on the ubiquitous IL13Rα1, thus preventing any IL13-mediated downstream signaling pathway [12]. Further, higher affinity of IL13 to IL13Rα2 allows for sequestration of the ligand away from IL13Rα1. Increased expression of IL13Rα2 has been reported to promote tumor progression in glioma and other tumor models. IL13Rα2 expression is a prognostic marker for glioma malignancy grade and for poor patient survival [13]. Its selective expression on MG, discovered almost two decades ago, has been a target for therapy ever since [14]. Several targeted therapies have been developed against IL13Rα2 on MG including bacterial toxins conjugated to IL13 [15], nanoparticles [16, 17], oncolytic virus [18, 19], as well as immunotherapies using monoclonal antibodies [20], IL13Rα2-pulsed dendritic cells [21], and IL13Rα2-targeted chimeric antigen receptors [22, 23]. Advanced therapeutic development has led to the completion of phase I clinical trials for IL13Rα2-targeted chimeric antigen receptors and

phase III clinical trials for bacterial toxins [11]. Here we will review the immunotherapeutic modalities that have been developed to specifically target IL13Rα2-expressing GBMs.

2. Using Monoclonal Antibodies to Target IL13Rα2 on GBMs

Both hybridoma technology or phage display libraries have been used extensively to generate monoclonal antibodies against IL13Rα2 [20, 24]. It is to be noted that antibodies generated by phage display technology tend to have a lower affinity of binding to the target than hybridoma generated antibodies. Balyasnikova et al. showed that IL13Rα2-targeting monoclonal antibody generated by hybridoma technology exhibited high affinity towards glioma cells, both *in vitro* and *ex vivo* [20]. This is also the only study that found that the high affinity antibody also prolonged survival in mice when coinjected intracranially with glioma cells. Another clear path indicated by the high specificity targeting of this study is the possibility of delivering antibodies systemically with fewer side effects. Studies have shown that intraperitoneal or intravenous delivery of antibody fragments may successfully home to glioma and reduce its growth in flank or orthotopic models [24]. More work is needed on this approach to determine its potency. One must be wary of trading potency for specificity, as targeting very specific amino acid sequences in highly mutated tumors may result in killing only a subgroup of cells. Also, the advantage of increased specificity via antibody based targeting must be weighed against decreased potency as compared to the IL13 ligand approach. Kioi et al. found that none of the IL13Rα2 antibody fragment variants conjugated to pseudomonas exotoxin (PE) could match the potency of IL13-PE fusion chimera (IL13PE38QQR) *in vitro* or *in vivo*. Keeping that in mind, a better approach might be to generate immune responses towards a variety of specific glioma antigens.

3. Dendritic Cells Pulsed with Tumor-Associated Antigens

One of the strongest immune-evasion techniques employed by GBM is poor antigen presentation by the tumor cells, and most patients with high-grade gliomas have very weak systemic response to the tumor antigens [25]. Dendritic cell based immunotherapy has been used extensively to counteract the GBM immune-evasion characteristics. Recent approaches include *ex vivo* pulsation of dendritic cells with glioma antigens, where cells of interest were sorted from GBM patient's peripheral blood mononuclear cells and exposed to glioma-associated tumor antigens in presence of immunostimulatory cytokines. The loaded cells were then injected back into the respective patients to observe the increased immune response. One must be critical in this approach during the choice of antigens used to stimulate the dendritic cells. Instead of exposing the cells to lysates, which offer complex cocktail of different antigens, more targeted immune response can be affected by pulsation of the dendritic cells with purified tumor-associated peptides such as IL13Rα2, EGFRvIII, or gp100. Dendritic cells pulsed with GBM antigens are being tested in phase I/II clinical trials. Robust immune response has been observed in a subgroup of patients with HLA-A*24/A*02 allele when they were injected with dendritic cells pulsed only with IL13Rα2 peptides [26, 27]. In a recent study with ICT-107, an intradermally administered autologous vaccine, from dendritic cells pulsed with several different antigens including IL13Rα2, showed a statistically significant increase in progression-free survival (NCT01280552). Median progression-free survival increased by 2 months overall. A group of patients that received at least 4 induction vaccinations showed an even longer median progression-free survival [28]. IL13Rα2 peptides have also been part of different cocktails of immunogenic molecules to provide more extensive coverage to different cell populations [21, 29]. Promising results have been observed in some of these antigen-cocktail pulsed dendritic cells being used in clinical trials. The benefits of IL13Rα2 based vaccines are manifold as they are not limited to GBM. Subcutaneous vaccinations with synthetic peptides for tumor-antigen epitopes that include IL13Rα2, WT1, survivin, and EphA2 in a recent study by Okada et al. showed low toxicity and potent immune response in low-grade glioma [30].

4. Chimeric Antigen Receptor-Modified T Lymphocytes

Genetic manipulation of autologous T cells to specifically target a particular tumor antigen is a novel and alternative strategy to bypass the failure of cytotoxic immune response induction by most tumor cells [31–33]. The application of chimeric antigen receptors (CAR) for immunogene therapy of malignant tumors is a promising strategy in which an antibody or ligand binding domain is fused with the zeta signaling chain of the T cell receptor [32–35]. The resulting CAR T cells are redirected by the neospecificity to attack tumors expressing the surface antigen or receptors recognized by the gene-modified T cell receptors and provide cellular therapy that attacks the tumor through normal host immune response in a highly regulated fashion. These cells are free to roam throughout the brain and systemic circulation, making the need for colocalization and bioavailability less of a problem.

The first generation CAR T cells had a single chain variable fragment (scFv) of an antibody specific to the target or a targeting ligand (such as IL13) connected with intracellular signaling zeta-domain of CD3 (CD3ζ). Weak activation levels in these CAR T cells were resolved with the addition of a CD28 costimulatory domain in the second-generation CARs, which enhanced proliferation, cell survival, and memory formation as well as significantly increased cytotoxicity [36].

First- and second-generation CAR T cells have been successfully used in targeting IL13Rα2. These CARs were designed by modifying the IL13 molecule by site-directed mutagenesis to change its affinity to IL13Rα2. Kahlon et al.designed a CAR with an IL13 mutein with a mutation at the E13 site (IL3.E13Y zetakine) [22], while another IL13CAR by Kong et al. was designed to have two mutations, one at site

E13 and another at R109, in IL13 molecule (IL13.E13 K.R109 K) [23]. The double mutation allowed for increased specificity towards IL13Rα2 and decreased affinity towards IL13Rα1. All the studies conducted so far have relied on local intracranial injections to establish efficacy. More studies need to be done to establish risk levels for adverse effects. Table 1 shows the different CARs developed to target IL13Rα2-expressing GBMs.

4.1. IL3 Zetakine. It has been established through early successful preclinical studies on first-generation CAR T cells that the IL13.E13Y zetakine (IL13 zetakine) T cells induced secretion of IFNγ, TNFα, and GM-CSF only in the presence of IL13Rα2-expressing tumor cells. When cultured *in vitro* together with glioma cells, they also lysed only IL13Rα2-expressing U251 glioma cells [22]. Immunodeficient mice, which were given intratumoral injection of IL13 zetakine T cells, were cured of intracranial glioma and also did not show tumor recurrence. The lack of recurrence was predicted to be due to the lack of resistance towards such therapy in glioma. One drawback of most other currently tested therapies is tumor recurrence, as a certain group of cells that is resistant to the therapy becomes the dominant phenotype or acts as a cell pool to originate tumor recurrence. This group of cells, referred to as cancer stem cells or in case of GBMs as glioma-initiating cells, often expresses the classical markers of stem cells, is self-renewing, and can initiate tumor formation *in vivo*. Like many other solid tumors, glioma-initiating cells have been shown to be responsible for resistance to current therapies and for tumor recurrence. However, the glioma-initiating cells derived from IL13Rα2+ tumors express IL13αR2 at levels similar to differentiated cells and were similarly sensitive to *in vitro* IL13 zetakine therapy [41].

The potential for targeting IL13Rα2-expressing GBMs has been demonstrated by early clinical experience at City of Hope in two phase I clinical trials with intracranial administration of first-generation IL13 zetakine T cell clones in patients with high-grade gliomas. In the pilot trial (NCT00730613), 3 consented participants with recurrent/refractory GBM were treated with autologous first-generation IL13 zetakine T-cell clones in escalating cell dose infusion cycles up to 10^8 [37]. In order to facilitate the study, the CAR T cells also expressed a hygromycin resistance gene/herpes simplex virus 1 thymidine kinase fusion (HyTk) and a PET reporter gene. A case study on one of the research participants has been reported with respect to the noninvasive detection of the autologous IL13 zetakine/HyTk+ T cells using 18F-FHGB PET postadoptive transfer [42]. CAR T cells were detected at the site of injection, as well as at a secondary site of recurrence near the corpus callosum, providing evidence for detection of CAR T cells and suggesting the potential of CAR T cells for trafficking to the sites of infiltrative diseases. In the second phase I clinical trial (NCT01082926) involving 6 research participants, an allogenic CAR CD8+ T cell, termed GRm13Z40-2, generated from a healthy donor was modified to express the first generation IL13 zetakine/HyTk CAR as described above [38]. These T cells also had their glucocorticoid receptor sites deleted to make the T cells resistant to steroids following adoptive transfer. All 6 patients had nonresectable recurrent/refractory GBMs. They were treated in conjunction with IL2 with repetitive doses of 10^8 CAR T cells. In all the participants in both clinical trials, the feasibility of this approach was demonstrated clinically, with minimal therapy related side effects and provided evidence for transient antiglioma responses for patients with IL13Rα2-expressing tumors [11].

4.2. IL13 CAR. In a recent publication by Kong et al. [23], a second-generation IL13CAR composed of a mutant IL13 (IL13.E13K.R109K) extracellular domain linked to intracellular signaling elements of the CD28 costimulatory molecule and CD3ζ was reported. In comparison to the Il13.E13Y zetakine, which was designed to be delivered via direct transfection of the CAR-coding plasmids, this IL13CAR was delivered to the T cells by retrovirus, which increased the transduction efficiency to as high as 79%. The double mutant IL13 vastly improved specificity against IL13Rα2+ tumors while showing little affinity for IL13Rα1 expressing cells. IL13Rα2+ glioma targets were accurately targeted and eliminated by the CAR expressing T cells with abundant secretion of cytokines IL2 and IFNγ. Marked increase in animal survival was observed in an *in vivo* test with a human glioma xenograft model with a single intracranial injection of CAR expressing designer T cells into tumor sites.

4.3. HER2.CD28 and IL13Rα2.CD28 biCAR T Cells. Immune escape is often associated with targeted immunotherapy of GBMs due to antigen heterogeneity or unavailability of receptor sites on the surface of solid tumors. Tumor cells also employ immune-evasion techniques to escape immune recognition [5]. GBMs notorious for their antigenic heterogeneity often express varied antigen profile within single tumors and between patients [43, 44]. Hegde et al. performed a tandem expression of anti-HER2 and anti-IL13Rα2 CARs in single T cells and showed that combinational targeting with the bispecific CAR T cells, in comparison to unispecific CAR T cells (anti-HER2 and anti-IL13Rα2 resp.), was able to offset antigen escape and enhanced effector activity against GBM patient tumor cells as well as xenograft murine glioma model [39].

5. Effects of Steroids and Chemotherapy on GBM Immunotherapy

Currently, the most important form of medical treatment for GBM is surgical resection. The success of this surgical intervention is based on perioperative management of the patient. Steroids are commonly used preoperatively to reduce the symptoms of mass effect and edema caused by the tumor [45]. The timing and dose of steroids varies according to surgeon preference. A common regimen for adults is dexamethasone, 6 mg intravenously or orally every 6 hours. If mass effect is profound, doses as high as 20 mg every 4 hours may be considered [45]. Recent studies have shown

Table 1: Chimeric antigen receptors against IL13Rα2.

Chimeric antigen receptors	Mutation	Delivery	Clinical trials
IL13 zetakine [22]	Single (E13Y)	Plasmid	Yes [37, 38]
IL13 CAR [23]	Double (E13K and R109K)	Retrovirus	No
HER2.CD28 and IL13Rα2.CD28 biCAR [39]	E13K	Retrovirus	No
Multiple [40]	E13K, E13Y, E13Y.K105R, E13K.K105R	Retrovirus	No

that dexamethasone reduces tumor-induced disturbances of the microenvironment such as neuronal cell death and tumor-induced angiogenesis, inhibits glioma cell growth in a concentration and species-dependent manner, and executes neuroprotective effects [46–48]. However, surgical removal of the tumor is not curative and must be supplemented with additional therapies to prolong survival and reduce recurrence. Treatment with corticosteroids presents a number of challenges to current immunotherapeutic approaches. One major problem is that the administration of dexamethasone suppresses the immune system by reducing the proliferation of T cells [49]. There is a physical and functional interaction between the glucocorticoid receptor and the T cell receptor (TCR) complex. In its unligated state, the glucocorticoid receptor has an important role in TCR signaling, but, after glucocorticoid-receptor-ligand binding (caused by short-term treatment with the synthetic glucocorticoid dexamethasone), the TCR complex is disrupted, leading to impaired TCR signaling [50]. Dexamethasone acts to functionally suppress immune modulators, which result in fewer IFN-γ-producing Th1 cells and a greater number of IL-4-producing Th2 cells [51]. This becomes an issue for the administration of adoptive T cell therapy as well as the activation of other pathways. One study demonstrates the direct correlation between the use of steroids and the functionality of targeted T-cell immunotherapy. Treatment with D-CAR(+) T cells exhibited specificity for β-glucan which led to damage and inhibition of hyphal growth of *Aspergillus in vitro* and *in vivo*. Treatment of D-CAR(+) T cells with steroids did not compromise antifungal activity significantly [52]. Another problem involves corticosteroid-induced reduction in contrast enhancement on radiographic imaging, which has been seen with gliomas. This finding may represent a diagnostic dilemma. Concern that steroid-induced cytotoxicity obscures histological diagnosis of suspected lymphoma may lead to postponement of a biopsy. If glioma is not considered in the differential diagnosis, reduction in tumor contrast enhancement may be misinterpreted as disease regression rather than a transient radiographic change [53]. Treatment of GBM with corticosteroids has become a double-edge sword. Future studies should be directed towards finding an optimal balance between immune suppression and activation.

A limiting factor for GBM immunotherapy using adoptive cell therapy approach, like engineered T cells, is temozolomide- (TMZ-) induced lymphopenia. FDA-directed GBM standard care must include a tripartite therapy of surgical resection followed by radiation and TMZ chemotherapy, concurrently with radiation and then as an adjuvant [54]. TMZ is a DNA alkylating agent and is the most successful antiglioma drug that has added several months to the life expectancy of GBM patients [55]. TMZ on the other hand is also responsible for inducing lymphopenia and myelosuppression in malignant glioma patients undergoing chemotherapy [56–58]. Although TMZ-induced lymphopenia facilitates antitumor vaccination by inducing passive immune response, it has been also associated with poor immune surveillance leading to opportunistic infections in glioma patients [59]. Reduced expression of DNA-repair enzyme O-6-methylguanine-DNA-methyltransferase (MGMT) in mature monocytes [60, 61] and further deletion of MGMT by TMZ have been determined to be the cause of lymphopenia [58]. Still, the future of chemotherapy-resistant immunotherapy does not look much depressing. In recent developments, it has been shown that genetic modification of MGMT molecule has been shown to render chemoprotection against TMZ [62]. Recent studies have shown promising effects of chemoprotection in hematopoietic cells by mutating the proline residue at 140 of the MGMT peptide to lysine (P140KMGMT) [55]. A calculated approach of using similar chemoprotection during GBM-targeted adoptive T cell-mediated immunotherapy may facilitate concurrent chemotherapy and immunotherapy and thus help reduce therapy time.

Table 2: IL13Rα2-targeted immunotherapy.

Immunotherapy	References	Clinical trials
Monoclonal antibodies	[20, 24]	None
Pulsed dendritic cells	[21, 27]	NCT01280552 [28]
Chimeric antigen receptors	[22, 23, 39, 41]	NCT00730613 [37] NCT01082926 [38]

6. Conclusion

Abundance of IL13Rα2 overexpression in GBM is a well-documented fact [13, 14, 41, 63–65]. IL13Rα2 is expressed in approximately 58% of adult and 83% of the pediatric brain tumors as well as on glioma-initiating cells [13, 41, 65]. This wealth of information has motivated the development of highly effective immunotherapies targeting IL13Rα2 on GBMs as discussed in this review article (Table 2).

High specificity of the hybridoma-derived monoclonal antibody targeting IL13Rα2 [20] is a promising candidate for GBM immunotherapy. The monoclonal antibody can be either delivered directly as antibody fragments with stabilizing agents, as it has been shown that targeting molecules, both antibodies as well as IL13Rα2-targeted peptides has

Table 3: Chimeric antigen receptors targeting GBM.

GBM targets	Preclinical studies	Clinical trials
EGFRvIII	[68–70]	NCT01454596 [71]
EphA2	[72]	None
HER2	[73]	NCT01109095 [74]
IL13Rα2	[22, 23, 39–41]	NCT00730613 [37] NCT01082926 [38]

properties of homing to the tumor sites [24, 66]. Alternatively, delivery of a single chain variable fragment of the high-specificity monoclonal antibody can be achieved by expressing it as a CAR on engineered T cells, thereby increasing the efficiency of the immunotherapeutic procedure.

Dendritic cells pulsed with tumor-associated antigens are a successful GBM immunotherapeutic approach [67]. By loading the dendritic cells with anti-GBM information the immune system is retrained to identify the GBM tumor cells as a threat. GBM patients vaccinated with autologous dendritic cells pulsed with different glioma-associated tumor antigens, including IL13Rα2, have shown significant prolongation of progression-free survival [28]. However, it has to be taken into account that none of the tumor-associated antigens used to pulse the dendritic cells are foreign antigens. This significantly blunts the antitumor immune response due to increased tolerance to the self-antigens, thus limiting the effectiveness of this approach.

Although promising, none of the above findings are as startling as the potency of CAR T cell in other malignancies. While clinical experience with CAR T cells for GBM is limited, recent success in patients with hematological malignancies has highlighted their antitumor potency [10, 75–77]. CARs combine the antigen-binding and lytic properties of monoclonal antibody or a simple ligand-receptor binding properties along with the self-renewing capacities of T cells [32, 34, 78, 79]. CAR T cells act on tumor cells in a MHC-independent fashion and therefore remain unaffected by the major mechanisms by which tumors evade the host immune system [33]. CARs can be designed to express either antibody to target peptide antigens on the tumor surface or ligands to target tumor-specific receptors (in this case IL13 muteins as ligands for IL13Rα2 on GBMs). Because of this advantage CAR T cells have been developed against a plethora of GBM immunotherapy candidates, some of which have progressed onto clinical trials (Table 3). In preclinical tests, CAR T cells designed to target IL13Rα2 produced copious amounts of immunostimulatory cytokines in presence of IL13Rα2-expressing GBM tumor cell lines as well as patient tumor cells indicating the high specificity. In orthotopic xenograft glioma-bearing animal models, the IL13Rα2-targeting CARs showed increased survival of treated animals when compared to untransduced T cells [22, 23]. IL13Rα2-targeting CARs have also been successful against chemo- and radioresistant glioma-initiating cells which otherwise are the cause of recurrent GBM [41]. A recent bispecific CAR T cell developed to target both HER2 and IL13Rα2 has shown promise to curb the immune-escape mechanism often exhibited by GBMs undergoing immunotherapy. Together, it appears that CAR T cells have immense potential as a candidate for targeted immunotherapy of GBM. However, questions, like delivery method of CAR T cells in hosts, survival in presence of lymphopenic chemotherapy drugs, and long-term host immune effect, remain unanswered, which may impose a limitation to this otherwise successful immunotherapeutic approach.

Conflict of Interests

The authors declare that there is no conflict of interests regarding the publication of this paper.

References

[1] C. E. Rolle, S. Sengupta, and M. S. Lesniak, "Challenges in clinical design of immunotherapy trials for malignant glioma," *Neurosurgery Clinics of North America*, vol. 21, no. 1, pp. 201–214, 2010.

[2] L. S. Ashby and T. C. Ryken, "Management of malignant glioma: steady progress with multimodal approaches," *Neurosurgical focus*, vol. 20, no. 4, p. E3, 2006.

[3] R. Stupp, M. E. Hegi, W. P. Mason et al., "Effects of radiotherapy with concomitant and adjuvant temozolomide versus radiotherapy alone on survival in glioblastoma in a randomised phase III study: 5-year analysis of the EORTC-NCIC trial," *The Lancet Oncology*, vol. 10, no. 5, pp. 459–466, 2009.

[4] A. Omuro and L. M. DeAngelis, "Glioblastoma and other malignant gliomas: a clinical review," *JAMA*, vol. 310, no. 17, pp. 1842–1850, 2013.

[5] C. E. Rolle, S. Sengupta, and M. S. Lesniak, "Mechanisms of immune evasion by gliomas," *Advances in Experimental Medicine and Biology*, vol. 746, pp. 53–76, 2012.

[6] S. Bao, Q. Wu, R. E. McLendon et al., "Glioma stem cells promote radioresistance by preferential activation of the DNA damage response," *Nature*, vol. 444, no. 7120, pp. 756–760, 2006.

[7] G. Frosina, "DNA repair and resistance of gliomas to chemotherapy and radiotherapy," *Molecular Cancer Research*, vol. 7, no. 7, pp. 989–999, 2009.

[8] A. F. Carpentier and Y. Meng, "Recent advances in immunotherapy for human glioma," *Current Opinion in Oncology*, vol. 18, no. 6, pp. 631–636, 2006.

[9] D. A. Wainwright, P. Nigam, B. Thaci, M. Dey, and M. S. Lesniak, "Recent developments on immunotherapy for brain cancer," *Expert Opinion on Emerging Drugs*, vol. 17, no. 2, pp. 181–202, 2012.

[10] D. L. Porter, B. L. Levine, M. Kalos, A. Bagg, and C. H. June, "Chimeric antigen receptor-modified T cells in chronic lymphoid leukemia," *The New England Journal of Medicine*, vol. 365, no. 8, pp. 725–733, 2011.

[11] B. Thaci, C. E. Brown, E. Binello, K. Werbaneth, P. Sampath, and S. Sengupta, "Significance of interleukin-13 receptor alpha 2-targeted glioblastoma therapy," *Neuro-Oncology*, 2014.

[12] K. Arima, K. Sato, G. Tanaka et al., "Characterization of the interaction between interleukin-13 and interleukin-13 receptors," *Journal of Biological Chemistry*, vol. 280, no. 26, pp. 24915–24922, 2005.

[13] C. E. Brown, C. D. Warden, R. Starr et al., "Glioma IL13Rα2 is associated with mesenchymal signature gene expression and poor patient prognosis," *PLoS ONE*, vol. 8, no. 10, Article ID e77769, 2013.

[14] W. Debinski, D. M. Gibo, S. W. Hulet, J. R. Connor, and G. Y. Gillespie, "Receptor for interleukin 13 is a marker and therapeutic target for human high-grade gliomas," *Clinical Cancer Research*, vol. 5, no. 5, pp. 985–990, 1999.

[15] W. Debinski, N. I. Obiri, S. K. Powers, I. Pastan, and R. K. Puri, "Human glioma cells overexpress receptors for interleukin 13 and are extremely sensitive to a novel chimeric protein composed of interleukin 13 and Pseudomonas exotoxin," *Clinical Cancer Research*, vol. 1, no. 11, pp. 1253–1258, 1995.

[16] A. B. Madhankumar, B. Slagle-Webb, A. Mintz, J. M. Sheehan, and J. R. Connor, "Interleukin-13 receptor-targeted nanovesicles are a potential therapy for glioblastoma multiforme," *Molecular Cancer Therapeutics*, vol. 5, no. 12, pp. 3162–3169, 2006.

[17] A. B. Madhankumar, B. Slagle-Webb, X. Wang et al., "Efficacy of interleukin-13 receptor-targeted liposomal doxorubicin in the intracranial brain tumor model," *Molecular Cancer Therapeutics*, vol. 8, no. 3, pp. 648–654, 2009.

[18] M. Candolfi, W. Xiong, K. Yagiz et al., "Gene therapy-mediated delivery of targeted cytotoxins for glioma therapeutics," *Proceedings of the National Academy of Sciences of the United States of America*, vol. 107, no. 46, pp. 20021–20026, 2010.

[19] I. V. Ulasov, M. A. Tyler, Y. Han, J. N. Glasgow, and M. S. Lesniak, "Novel recombinant adenoviral vector that targets the interleukin-13 receptor α2 chain permits effective gene transfer to malignant glioma," *Human Gene Therapy*, vol. 18, no. 2, pp. 118–129, 2007.

[20] I. V. Balyasnikova, D. A. Wainwright, E. Solomaha et al., "Characterization and immunotherapeutic implications for a novel antibody targeting interleukin (IL)-13 Receptor α2," *The Journal of Biological Chemistry*, vol. 287, no. 36, pp. 30215–30227, 2012.

[21] H. Okada, P. Kalinski, R. Ueda et al., "Induction of $CD8^+$ T-cell responses against novel glioma-associated antigen peptides and clinical activity by vaccinations with α-type 1 polarized dendritic cells and polyinosinic-polycytidylic acid stabilized by lysine and carboxymethylcellulose in patients with recurrent malignant glioma," *Journal of Clinical Oncology*, vol. 29, no. 3, pp. 330–336, 2011.

[22] K. S. Kahlon, C. Brown, L. J. N. Cooper, A. Raubitschek, S. J. Forman, and M. C. Jensen, "Specific recognition and killing of glioblastoma multiforme by interleukin 13-zetakine redirected cytolytic T cells," *Cancer Research*, vol. 64, no. 24, pp. 9160–9166, 2004.

[23] S. Kong, S. Sengupta, B. Tyler et al., "Suppression of human glioma xenografts with second-generation IL13R-specific chimeric antigen receptor-modified T cells," *Clinical Cancer Research*, vol. 18, no. 21, pp. 5949–5960, 2012.

[24] M. Kioi, S. Seetharam, and R. K. Puri, "Targeting IL-13RA2-positive cancer with a novel recombinant immunotoxin composed of a single-chain antibody and mutated Pseudomonas exotoxin," *Molecular Cancer Therapeutics*, vol. 7, no. 6, pp. 1579–1587, 2008.

[25] C. E. Fadul, J. L. Fisher, T. H. Hampton et al., "Immune response in patients with newly diagnosed glioblastoma multiforme treated with intranodal autologous tumor lysate-dendritic cell vaccination after radiation chemotherapy," *Journal of Immunotherapy*, vol. 34, no. 4, pp. 382–389, 2011.

[26] S. Shimato, A. Natsume, T. Wakabayashi et al., "Identification of a human leukocyte antigen-A24-restricted T-cell epitope derived from interleukin-13 receptor α2 chain, a glioma-associated antigen: laboratory investigation," *Journal of Neurosurgery*, vol. 109, no. 1, pp. 117–122, 2008.

[27] K. Iwami, S. Shimato, M. Ohno et al., "Peptide-pulsed dendritic cell vaccination targeting interleukin-13 receptor alpha2 chain in recurrent malignant glioma patients with HLA-A∗24/A∗02 allele," *Cytotherapy*, vol. 14, no. 6, pp. 733–742, 2012.

[28] "A Study of ICT-107 Immunotherapy in Glioblastoma Multiforme (GBM)," 2012, http://clinicaltrials.gov/show/NCT01280552.

[29] S. Saikali, T. Avril, B. Collet et al., "Expression of nine tumour antigens in a series of human glioblastoma multiforme: interest of EGFRvIII, IL-13Rα2, gp100 and TRP-2 for immunotherapy," *Journal of Neuro-Oncology*, vol. 81, no. 2, pp. 139–148, 2007.

[30] H. Okada, L. Butterfield, R. Hamilton et al., "Robust inductions of type-1 CD8+ T-cell responses in WHO grade II low-grade glioma patients receiving peptide-based vaccines in combination with poly-ICLC," *Neuro-Oncology*, vol. 15, p. iii71, 2013.

[31] Q. Ma, R. M. Gonzalo-Daganzo, and R. P. Junghans, "Genetically engineered T cells as adoptive immunotherapy of cancer," *Cancer Chemotherapy and Biological Response Modifiers*, vol. 20, pp. 315–341, 2002.

[32] M. C. Jensen and S. R. Riddell, "Design and implementation of adoptive therapy with chimeric antigen receptor-modified T cells," *Immunological Reviews*, vol. 257, no. 1, pp. 127–144, 2014.

[33] S. Krebs, T. G. Rodriguez-Cruz, and C. Derenzo, "Genetically modified T cells to target glioblastoma," *Frontiers in Oncology*, vol. 3, article 322, 2013.

[34] R. H. Vonderheide and C. H. June, "Engineering T cells for cancer: our synthetic future," *Immunological Reviews*, vol. 257, no. 1, pp. 7–13, 2014.

[35] T. S. Park, S. A. Rosenberg, and R. A. Morgan, "Treating cancer with genetically engineered T cells," *Trends in Biotechnology*, vol. 29, no. 11, pp. 550–557, 2011.

[36] P. C. R. Emtage, A. S. Y. Lo, E. M. Gomes, D. L. Liu, R. M. Gonzalo-Daganzo, and R. P. Junghans, "Second-generation anti-carcinoembryonic antigen designer T cells resist activation-induced cell death, proliferate on tumor contact, secrete cytokines, and exhibit superior antitumor activity in vivo: a preclinical evaluation," *Clinical Cancer Research*, vol. 14, no. 24, pp. 8112–8122, 2008.

[37] "Cellular Adoptive Immunotherapy Using Genetically Modified T-Lymphocytes in Treating Patients With Recurrent or Refractory High-Grade Malignant Glioma," 2011, http://clinicaltrials.gov/ct2/show/NCT00730613.

[38] "Phase I Study of Cellular Immunotherapy for Recurrent/Refractory Malignant Glioma Using Intratumoral Infusions of GRm13Z40-2, An Allogeneic CD8+ Cytolitic T-Cell Line Genetically Modified to Express the IL 13-Zetakine and HyTK and to be Resistant to Glucocorticoids, in Combination With Interleukin-2," 2013, http://www.clinicaltrials.gov/ct2/show/NCT01082926.

[39] M. Hegde, A. Corder, K. K. Chow et al., "Combinational targeting offsets antigen escape and enhances effector functions of adoptively transferred T cells in glioblastoma," *Molecular Therapy*, vol. 21, no. 11, pp. 2087–2101, 2013.

[40] S. Krebs, K. K. Chow, Z. Yi et al., "T cells redirected to interleukin-13Ralpha2 with interleukin-13 mutein-chimeric antigen receptors have anti-glioma activity but also recognize

interleukin-13Ralpha1," *Cytotherapy*, vol. 16, no. 8, pp. 1121–1131, 2014.

[41] C. E. Brown, R. Starr, B. Aguilar et al., "Stem-like tumor-initiating cells isolated from IL13Rα2 expressing gliomas are targeted and killed by IL13-zetakine-redirected T cells," *Clinical Cancer Research*, vol. 18, no. 8, pp. 2199–2209, 2012.

[42] S. S. Yaghoubi, M. C. Jensen, N. Satyamurthy et al., "Noninvasive detection of therapeutic cytolytic T cells with 18 F-FHBG PET in a patient with glioma," *Nature Clinical Practice Oncology*, vol. 6, no. 1, pp. 53–58, 2009.

[43] G. Z. Jian, J. Eguchi, C. A. Kruse et al., "Antigenic profiling of glioma cells to generate allogeneic vaccines or dendritic cell-based therapeutics," *Clinical Cancer Research*, vol. 13, no. 2, part 1, pp. 566–575, 2007.

[44] Y. Liang, M. Diehn, N. Watson et al., "Gene expression profiling reveals molecularly and clinically distinct subtypes of glioblastoma multiforme," *Proceedings of the National Academy of Sciences of the United States of America*, vol. 102, no. 16, pp. 5814–5819, 2005.

[45] J. A. Cowan and B. G. Thompson, "Chapter 36. Neurosurgery," in *CURRENT Diagnosis & Treatment: Surgery, 13e*, G. M. Doherty, Ed., The McGraw-Hill, New York, NY, USA, 2010.

[46] Z. Fan, T. Sehm, M. Rauh et al., "Dexamethasone alleviates tumor-associated brain damage and angiogenesis," *PLoS ONE*, vol. 9, no. 4, Article ID e93264, 2014.

[47] L. Bavaresco, A. Bernardi, E. Braganhol, M. R. Wink, and A. M. O. Battastini, "Dexamethasone inhibits proliferation and stimulates ecto-5′-nucleotidase/CD73 activity in C6 rat glioma cell line," *Journal of Neuro-Oncology*, vol. 84, no. 1, pp. 1–8, 2007.

[48] S. C. Higgins and G. J. Pelkington, "The in vitro effects of tricyclic drugs and dexamethasone on cellular respiration of malignant glioma," *Anticancer Research*, vol. 30, no. 2, pp. 391–397, 2010.

[49] L. A. Nafe, J. R. Dodam, and C. R. Reinero, "In-vitro immunosuppression of canine T-lymphocyte-specific proliferation with dexamethasone, cyclosporine, and the active metabolites of azathioprine and leflunomide in a flow-cytometric assay," *Canadian Journal of Veterinary Research*, vol. 78, no. 3, pp. 168–175, 2014.

[50] M. Löwenberg, A. P. Verhaar, G. R. van den Brink, and D. W. Hommes, "Glucocorticoid signaling: a nongenomic mechanism for T-cell immunosuppression," *Trends in Molecular Medicine*, vol. 13, no. 4, pp. 158–163, 2007.

[51] J. Liao, X. Wang, Y. Bi et al., "Dexamethasone potentiates myeloid-derived suppressor cell function in prolonging allograft survival through nitric oxide," *Journal of Leukocyte Biology*, 2014.

[52] P. R. Kumaresan, P. R. Manuri, N. D. Albert et al., "Bioengineering T cells to target carbohydrate to treat opportunistic fungal infection," *Proceedings of the National Academy of Sciences of the United States of America*, vol. 111, no. 29, pp. 10660–10665, 2014.

[53] M. D. Mazur, V. Nguyen, and D. W. Fults, "Glioblastoma presenting with steroid-induced pseudoregression of contrast enhancement on magnetic resonance imaging," *Case Reports in Neurological Medicine*, vol. 2012, Article ID 816873, 6 pages, 2012.

[54] "FDA Approval for Temozolomide," http://www.cancer.gov/cancertopics/druginfo/fda-temozolomide.

[55] S. Sengupta, J. Marrinan, C. Frishman, and P. Sampath, "Impact of temozolomide on immune response during malignant glioma chemotherapy," *Clinical and Developmental Immunology*, vol. 2012, Article ID 831090, 7 pages, 2012.

[56] C. S. Brock, E. S. Newlands, S. R. Wedge et al., "Phase I trial of temozolomide using an extended continuous oral schedule," *Cancer Research*, vol. 58, no. 19, pp. 4363–4367, 1998.

[57] A. B. Heimberger, W. Sun, S. F. Hussain et al., "Immunological responses in a patient with glioblastoma multiforme treated with sequential courses of temozolomide and immunotherapy: case study," *Neuro-Oncology*, vol. 10, no. 1, pp. 98–103, 2008.

[58] M. Gander, S. Leyvraz, L. Decosterd et al., "Sequential administration of temozolomide and fotemustine: depletion of O6-alkyl guanine-DNA transferase in blood lymphocytes and in tumours," *Annals of Oncology*, vol. 10, no. 7, pp. 831–838, 1999.

[59] M. C. Kizilarslanoglu, S. Aksoy, N. O. Yildirim, E. Ararat, I. Sahin, and K. Altundag, "Temozolomide-related infections: review of the literature," *Journal of B.U.ON.*, vol. 16, no. 3, pp. 547–550, 2011.

[60] M. Briegert, A. H. Enk, and B. Kaina, "Change in expression of MGMT during maturation of human monocytes into dendritic cells," *DNA Repair*, vol. 6, no. 9, pp. 1255–1263, 2007.

[61] M. Briegert and B. Kaina, "Human monocytes, but not dendritic cells derived from them, are defective in base excision repair and hypersensitive to methylating agents," *Cancer Research*, vol. 67, no. 1, pp. 26–31, 2007.

[62] N. Sawai, S. Zhou, E. F. Vanin, P. Houghton, T. P. Brent, and B. P. Sorrentino, "Protection and in vivo selection of hematopoietic stem cells using temozolomide, O6-benzylguanine, and an alkyltransferase-expressing retroviral vector," *Molecular Therapy*, vol. 3, no. 1, pp. 78–87, 2001.

[63] W. Debinski, D. M. Gibo, B. Slagle, S. K. Powers, and G. Y. Gillespie, "Receptor for interleukin 13 is abundantly and specifically over-expressed in patients with glioblastoma multiforme," *International Journal of Oncology*, vol. 15, no. 3, pp. 481–486, 1999.

[64] B. H. Joshi, G. E. Plautz, and R. K. Puri, "Interleukin-13 receptor chain: a novel tumor-associated transmembrane protein in primary explants of human malignant gliomas," *Cancer Research*, vol. 60, no. 5, pp. 1168–1172, 2000.

[65] M. Kawakami, K. Kawakami, S. Takahashi, M. Abe, and R. K. Puri, "Analysis of interleukin-13 receptor α2 expression in human pediatric brain tumors," *Cancer*, vol. 101, no. 5, pp. 1036–1042, 2004.

[66] H. Pandya, D. M. Gibo, S. Garg, S. Kridel, and W. Debinski, "An interleukin 13 receptor α 2-specific peptide homes to human Glioblastoma multiforme xenografts," *Neuro-Oncology*, vol. 14, no. 1, pp. 6–18, 2012.

[67] C. J. Wheeler and K. L. Black, "DCVax-brain and DC vaccines in the treatment of GBM," *Expert Opinion on Investigational Drugs*, vol. 18, no. 4, pp. 509–519, 2009.

[68] S. S. Bullain, A. Sahin, O. Szentirmai et al., "Genetically engineered T cells to target EGFRvIII expressing glioblastoma," *Journal of Neuro-Oncology*, vol. 94, no. 3, pp. 373–382, 2009.

[69] B. D. Choi, C. M. Suryadevara, P. C. Gedeon et al., "Intracerebral delivery of a third generation EGFRvIII-specific chimeric antigen receptor is efficacious against human glioma," *Journal of Clinical Neuroscience*, vol. 21, no. 1, pp. 189–190, 2014.

[70] R. A. Morgan, L. A. Johnson, J. L. Davis et al., "Recognition of glioma stem cells by genetically modified T cells targeting EGFRvIII and development of adoptive cell therapy for glioma," *Human Gene Therapy*, vol. 23, no. 10, pp. 1043–1053, 2012.

[71] "White Blood Cells With Anti-EGFR-III for Malignant Gliomas," 2014, http://www.clinicaltrials.gov/ct2/show/NCT01454596.

[72] K. K. Chow, S. Naik, S. Kakarla et al., "T cells redirected to EphA2 for the immunotherapy of glioblastoma," *Molecular Therapy*, vol. 21, no. 3, pp. 629–637, 2013.

[73] N. Ahmed, V. S. Salsman, Y. Kew et al., "HER2-specific T cells target primary glioblastoma stem cells and induce regression of autologous experimental tumors," *Clinical Cancer Research*, vol. 16, no. 2, pp. 474–485, 2010.

[74] "CMV-specific Cytotoxic T Lymphocytes Expressing CAR Targeting HER2 in Patients with GBM (HERT-GBM)," 2014, http://www.clinicaltrials.gov/ct2/show/NCT01109095.

[75] M. Kalos, B. L. Levine, D. L. Porter et al., "T cells with chimeric antigen receptors have potent antitumor effects and can establish memory in patients with advanced leukemia," *Science Translational Medicine*, vol. 3, no. 95, Article ID 95ra73, 2011.

[76] D. L. Porter, M. Kalos, Z. Zheng, B. Levine, and C. June, "Chimeric antigen receptor therapy for B-cell malignancies," *Journal of Cancer*, vol. 2, no. 1, pp. 331–332, 2011.

[77] S. A. Grupp, M. Kalos, D. Barrett et al., "Chimeric antigen receptor-modified T cells for acute lymphoid leukemia," *New England Journal of Medicine*, vol. 368, no. 16, pp. 1509–1518, 2013.

[78] J. Maher, "Immunotherapy of malignant disease using chimeric antigen receptor engrafted T cells," *ISRN Oncology*, vol. 2012, Article ID 278093, 23 pages, 2012.

[79] M. Sadelain, R. Brentjens, and I. Rivière, "The basic principles of chimeric antigen receptor design," *Cancer Discovery*, vol. 3, no. 4, pp. 388–398, 2013.

Hindawi Publishing Corporation
BioMed Research International
Volume 2014, Article ID 386470, 11 pages
http://dx.doi.org/10.1155/2014/386470

Review Article

Newcastle Disease Virus Interaction in Targeted Therapy against Proliferation and Invasion Pathways of Glioblastoma Multiforme

Jafri Malin Abdullah,[1,2,3] Zulkifli Mustafa,[2] and Aini Ideris[4]

[1] *Center for Neuroscience Services and Research, Universiti Sains Malaysia, Health Campus, 16150 Kubang Kerian, Kelantan, Malaysia*
[2] *Department of Neurosciences, School of Medical Sciences, Universiti Sains Malaysia, Health Campus, 16150 Kubang Kerian, Kelantan, Malaysia*
[3] *Department of Neurosciences, Hospital Universiti Sains Malaysia, Jalan Sultanah Zainab 2, Kubang Kerian, 16150 Kota Bharu, Kelantan, Malaysia*
[4] *Faculty of Veterinary Medicine, Universiti Putra Malaysia, 43400 Serdang, Selangor, Malaysia*

Correspondence should be addressed to Jafri Malin Abdullah; brainsciences@gmail.com

Received 10 February 2014; Revised 5 June 2014; Accepted 25 June 2014; Published 27 August 2014

Academic Editor: Betty Tyler

Glioblastoma multiforme (GBM), or grade IV glioma, is one of the most lethal forms of human brain cancer. Current bioscience has begun to depict more clearly the signalling pathways that are responsible for high-grade glioma initiation, migration, and invasion, opening the door for molecular-based targeted therapy. As such, the application of viruses such as Newcastle disease virus (NDV) as a novel biological bullet to specifically target aberrant signalling in GBM has brought new hope. The abnormal proliferation and aggressive invasion behaviour of GBM is reported to be associated with aberrant Rac1 protein signalling. NDV interacts with Rac1 upon viral entry, syncytium induction, and actin reorganization of the infected cell as part of the replication process. Ultimately, intracellular stress leads the infected glioma cell to undergo cell death. In this review, we describe the characteristics of malignant glioma and the aberrant genetics that drive its aggressive phenotype, and we focus on the use of oncolytic NDV in GBM-targeted therapy and the interaction of NDV in GBM signalling that leads to inhibition of GBM proliferation and invasion, and subsequently, cell death.

1. Introduction

Oncolytic viruses are viruses that selectively eradicate tumour cells without harming the normal surrounding tissues [1–3]. They are used to recognise and infect mutated cancerous cells, where they replicate and then release new virions that directly amplify the input dose. Newly produced virions can also spread and infect the adjacent cancerous cells. Consequently, infected cells often undergo pathological programmed cell death, known as apoptosis [4].

Grade IV glioma, or glioblastoma multiforme (GBM), is one of the most lethal forms of human brain cancer, despite multiple modern approaches that have been developed to combat the disease [5]. Current bioscience has now begun to depict more clearly the signalling pathways responsible for high-grade glioma initiation, migration, and invasion, thus opening the door for molecular-based targeted therapy [6]. Targeted therapy is a therapeutic approach that uses a specific molecule inhibitor or activator to hinder or reboot the aberrant signalling observed in cancerous cells.

The application of viruses as a novel biological bullet to specifically target aberrant signalling in GBM has brought new hope. Newcastle disease virus (NDV), a chicken pathogen that exhibits selective oncolytic properties, is one of the most intensively studied oncolytic viruses, affecting many types of human cancer [7, 10, 11]. We previously presented the therapeutic potential of NDV to induce apoptosis in GBM cell cultures and induce GBM regression in in vivo and ex vivo models [7, 12]. As a mode of therapy, oncolytic NDV has been shown to be a potent and safe anticancer agent for treating

human brain cancer [2]. As such, in the present review, we describe the therapeutic potential pathways associated with oncolytic NDV tropism in human GBM, which display the natural selectivity of NDV towards GBM and the interaction of NDV in GBM proliferation and invasion signalling.

2. Malignant Brain Cancer

Brain cancer is a mixed group of neoplasms that originate in intracranial tissue and meninges and display multiple levels of malignancy [13, 14]. Glial cancers, or glioma, the most common types of primary brain cancer, are derived from mutated glial cells and consist of astrocytes, oligodendroglial cells, and ependymal cells. As a form of cancer, gliomas are defined as pathological tumours that display histological, immunohistological, and ultrastructural evidence of glial differentiation [8, 14]. Among gliomas, GBM brain cancer is the most dangerous type of brain tumours, and no cure has been identified.

Malignant brain cancer is characterised by highly invasive multifocal growth, histologic and genetic heterogeneity, and local relapse [15, 16]. The complex characteristics of GBM explain its resistance to current therapeutic intervention.

As indicated by the name glioblastoma multiforme, this type of tumour is grossly multiformed and often haemorrhaging, with necrotic regions. It is also multiformed microscopically, with pleomorphic nuclei and cells, microvascular proliferation, and regions of pseudopalisading necrosis [15, 17, 18].

Another hallmark of high-grade brain cancer is its invasive nature. Due to the massive growth of the brain cancer focus, peripheral cancerous cells invade the adjacent brain parenchyma, and the core of the tumour becomes necrotic, forming a region in which tumour cells, oedema, and normal tissue coexist, making it difficult to estimate the tumour margin to ensure complete therapeutic removal [5, 19]. The tumour is also surrounded by a penumbra of invasive tumour cells that are detectable several centimetres away from the main tumour mass. These locally invasive glioma cells, which are often found at the margins of the tumour resection, are the most common sites of malignant glioma recurrence [20].

Brain cancers are relatively rare compared to other tumours, with an estimated 25,000 new patients diagnosed in North America in 2009 [21]. The majority of these patients have gliomas (>15,000), and of those, approximately 70% are GBM (WHO grade IV), 15% are anaplastic astrocytomas (WHO grade III), and the remainder are low-grade gliomas [2, 5]. In Malaysia, the incidence of cancers of the brain and nervous system, as reported by the Malaysian Cancer Registry, was 3.3 per 100,000 persons in 2006. This number reflects an increase from 2.4 per 100,000 in 2003, and the frequency is higher in males. Brain cancer is currently reported as the third most common paediatric cancer in Malaysia [7, 22, 23].

Despite the impressive advances in imaging, surgery, and therapy methodologies over the past 25 years, the median survival rate of GBM patients remains only 12–15 months [2]; thus, an urgent, proficient solution is needed.

3. GBM Genetic Aberrations

Generally, a cancer consists of mutated cells that divide or survive when, instead, they should undergo cell cycle arrest or apoptosis cell death due to internal aberrations. Thus, due to several genetic abnormalities, most cancers, including GBM, remain alive and can form tumours. The discovery that cancer is an aberrant genetic disease, arising when defects occur in genes involved in cell death and growth regulatory processes, has revolutionised our understanding of tumorigenesis [14, 24].

Several genetic aberrations in the genes governing cell cycle control and growth factor signalling pathways have been well described in human brain cancers [6, 25]. Genes that are mutated or amplified to lead to the enhancement of cellular growth are referred to as oncogenes. Glioma oncogenes have provided new insights into tumorigenesis, and therefore, the deregulated cell signalling pathways that have been identified are now becoming the focus of specific molecular targeted therapies [26].

Several deregulated signalling pathways have been described in GBM, mainly in proliferation signalling, including the MEK/ERK, PI3K/Akt, and PLC/PKC pathways. The deregulation of these signalling pathways is driven by the mutation, overexpression, or amplification of multiple genes, such as epidermal growth factor (EGFR), platelet-derived growth factor (PDGF), phosphatase and tensin homologue (PTEN), p53, retinoblastoma (Rb), and mammalian target of rapamycin (mTOR) [14, 16, 27]. A summary of the signalling regulations is shown in Figure 1.

Specifically, EGFR and the loss of chromosome 10 are the primary alterations found in GBM. EGFR amplification is found in nearly 92% of astrocytomas. By contrast, 62% of grade IV gliomas show an increased expression of EGFRvIII, a constitutively active mutant receptor. The complete loss of chromosome 10 has been reported in 70% of primary GBMs, whereas the other 30% display an aberrant tumour suppressor gene p53 [6, 25, 28].

Regardless of the cellular receptor or ligand status, up to 100% of GBMs show the activation of Ras, and nearly 70% show activated Akt. The loss of the tumour suppressor gene PTEN on chromosome 10, which normally represses Akt activation, is also typically observed.

As summarised in Figure 1, proliferation signalling of GBM is initiated after appropriate mitogenic signals, such as EGF or PDGF activation. Activated EGF receptor (EGFR) or PDGF receptor (PDGFR) triggers the synthesis of cyclin D, which enables cyclin-dependent kinase (CDK) via the Raf/ERK/MAPK or PI3K/Akt pathway. Active CDKs, such as CDK4, further phosphorylate and inactivate the tumour suppressor protein Rb. In turn, Rb is unbound from E2F, allowing this transcription factor to lead the cell through the G1 restriction point [18, 29, 30], subsequently allowing the cell to undergo genomic synthesis and mitosis to produce new cells. Furthermore, Rb is a major regulator of cell cycle progression; the mutational inactivation of Rb leads to unscheduled cell cycle entry, and Rb mutation is found in approximately 25% of GBMs [6, 8, 14].

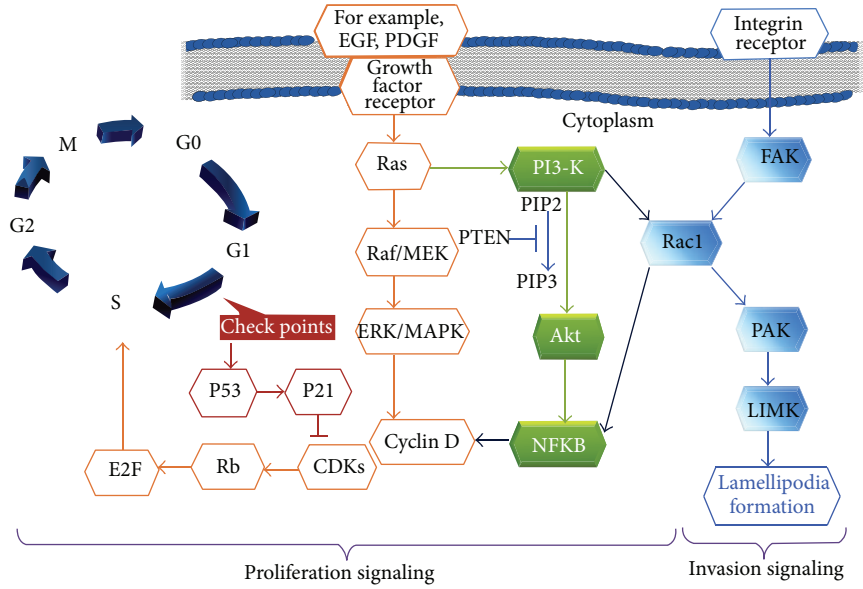

FIGURE 1: Genomic aberration of the proliferative and invasive pathways of glioma signalling. The extrinsic activation of growth factor receptors triggers the major signal transduction crossroad Ras-GTP, which conveys the message into the Raf-MAPK-ERK pathway or the PI3K-AKT or PI3K-Rho GTPase Rac1 pathway and leads the cell through the G1 restriction points of cell cycle. This signalling activation promotes an aberrant cell cycle that continuously produces mutated cells and promotes invasion signalling, resulting in an aggressive phenotype [6–8]. The control over cell division at checkpoint 1 is normally maintained by p53, a tumour suppressor that also contributes to DNA repair and cell death pathways.

In an overexpressing Rac1 NIH3T3 mutant cell, cyclin D transcription can be activated directly by the downstream of Rac1 (Figure 1) via the nuclear factor kappa-light-chain-enhancer of activated B cells (NFKB) [31, 32] to promote cell cycle progression [33, 34]. Aberrant cell proliferation associated with the constitutive activation of NFKB in response to PDGF overexpression has also been reported in gliomas. This NFKB activation is mediated via the PI3K pathway in association with PTEN inactivation [6, 14].

Another concerning feature of GBM cells is their ability to invade the normal brain parenchyma individually. This ability is achieved through the dual signalling of proliferation and invasion pathways via PI3K/Rac1 signalling (Figure 1) [9, 14, 33], which maintains tumorigenic cell survival.

Due to this variability, which indicates that gliomas comprise multiple diseases, unique and different therapeutic tools are required [24, 35], which has driven the development of targeted therapies. The overexpression of these genes provides an opportunity for oncolytic viruses such as oncolytic NDV, which require the Rac1 protein in their replications in human cancer cells [36].

4. Oncolytic NDV

NDV is a highly contagious pathogen that affects avian species and causes severe economic losses to the poultry industry worldwide. NDV outbreaks were first reported in poultry from Java, Indonesia, followed by Newcastle-upon-Tyne in 1926 [11, 37]. Eighteen NDV strains from four lineages were later identified and classified as velogenic, mesogenic, and lentogenic according to their pathotypes [38, 39]. NDV is classified as a member of the Paramyxoviridae family of the Mononegavirales superfamily, in the *Avulavirus* genus [37].

The NDV genome consists of 15 kb pairs of nonsegmented, single-stranded RNA, which code for six main structural proteins. These genes, nucleocapsid (NP), phosphorylation (P), matrix (M), fusion (F), hemagglutinin-neuraminidase (HN), and RNA-dependent RNA polymerase (L) proteins, are found in a 3′ NP-P-M-F-HN-L 5′ arrangement [40, 41].

In researching human brain cancer, preclinical studies of oncolytic viruses in glioma emerged in the 1990s, when the first attenuated herpes simplex viruses (HSVs) and adenoviruses were used, followed by oncolytic reovirus. To date, four viruses have completed the phase 1 clinical trials: herpes simplex virus (strains HSV-1, HSV-1716, and HSV-G207), Newcastle disease virus (strains MTH-68/H and NDV-HUJ), adenovirus (Onyx-015), and reovirus. As a result of the trials, the viruses were declared safe to be injected directly into the brain, and no maximum tolerated dose (MTD) was reached. Some antiglioma activities were also observed. NDV showed the most promising benefits, as six patients exhibited tumour regression and three patients exhibited long-term survival [2].

The lentogenic NDV strain OV001/HUJ has been used in the treatment of patients with stage IV brain cancer. In the third stage of phase I/II clinical testing, the NDV-HUJ strain was intravenously administered in two parts to patients with primary GBM. In the first part, escalation steps at doses of 0.1, 0.32, 0.93, 5.9, and 11 BIU of NDV-HUJ were given in one cycle of five consecutive daily doses, followed by three additional cycles of 55 BIU. In the second part, maintenance

doses consisting of two doses of 11 BIU weekly were given. The MTD was not reached. One patient maintained a near complete response 30 weeks after the start of dosing, and a second patient maintained stable disease for 26 weeks [42].

Several strains of NDV infection are known to induce multicascade, self-suicide apoptosis in many human neoplastic cells [4, 12, 43].

5. Natural Selectivity of Oncolytic NDV towards GBM

It is well known that mutations in multiple genes promote tumour evolution and contribute to a malignant phenotype [6, 44]. Features of transformed cells, including altered receptor expression, defective signalling pathways, oncogene activation, and increased cell cycling, have been shown to augment the capacity of viruses to replicate within cancerous cells [45].

In normal brain cells responding to viral infections, microglia and astrocytes respond to foreign nucleic acids, leading to the stimulation of the pattern-recognition receptors (PRRs), such as TLR-3, TLR-7, and TLR-9. The activation of PRRs subsequently activates type 1 interferon (IFN) [2], which further binds and activates the Janus kinases JAK1 and TYK2, which in turn phosphorylate the activators for STAT1 and STAT2 transcription. The STAT proteins then heterodimerize and form a complex with IRF9. This complex, known as ISGF3, further provides DNA recognition and simultaneously produces the IFN-stimulated genes (IGSs) that create the antiviral state in the target cells and block viral replication [11, 46]. This is particularly important because the normal IFN mechanism prevents oncolytic virus amplification within normal brain parenchyma.

In the study of Miyakoshi et al. [47], the activation of oncogenes in human cancer increased the activation of protein kinases, leading to interferon synthesis and the inhibition of tumorigenesis. In glioma, however, the antitumour IFN response is impaired by glioma-derivative immunosuppressing factors such as TGF-b, IL-10, prostaglandin E2, and gangliosides. TGF-b, the most prominent immune suppressor, plays a major role in glioma biology, where it is often overexpressed and has become a hallmark of gliomas [2].

IFNβ is the principle antiviral factor secreted by infected cells in response to NDV infection. Therefore, IFN-defective tumour cells provide a greater opportunity than normal cells for NDV to replicate effectively. Thus, this replication-competent virus-selective mechanism is associated with the defect of the host IFN [10, 46].

As NDV is very sensitive to IFN, its replication is inhibited in IFN-competent normal cells, but not in transformed cells that fail to develop an appropriate antiviral state [48]. However, it has been reported that many transformed cells that do not show deficiencies in IFN signalling are still selectively destroyed [48]. Consistent with this finding, melanoma cells with a functional IFN system were infected with NDV-HUJ, indicating that IFN is not solely involved in NDV-induced oncolysis [49]. Thus, selective cellular catastrophe by NDV seems to vary according to cell type and NDV strain pathotype.

Nevertheless, NDV has been used in immunotherapy to trigger IFN signalling against transformed cells [40]. Previous reports have reported that NDV infection was a thousandfold more efficient in Ras-transformed cells [36, 50, 51]. Consistent with those findings, the aberrant signalling of GBM, as discussed above, indicated that more than 50% of GBMs were identified with high Ras expression and EGFR overexpression [6, 52, 53], leading to increased cell proliferation, especially in the primary GBMs [14]. This result might explain why NDV targets cancerous cells more efficiently than normal cells.

It would be of great interest to address the recent report that placed new interest on the Ras downstream protein Rac1. Puhlmann et al. [36] identified Rac1 as a protein with activity that is critical for both oncolytic virus sensitivity and the autonomous growth behaviour of Ras-transformed skin carcinoma cells.

6. Rac1 Signalling in the Proliferation and Invasion of GBM

Rac1, a Ras-related C3 botulism toxin substrate 1, is a member of the monomeric G-protein Rho GTPases. In proliferation signalling, this protein is involved in the regulation of gene transcription and G1 cell cycle progression [14, 29, 33, 54]. Gjoerup et al. [55] reported that in an embryonic mouse fibroblast NIH3T3 cell line, activated Rac1 and Cdc42 promoted the inactivation of Rb to allow E2F-mediated transcription, thus permitting the cell cycle progression from G1 into the S phase [30, 55–57].

Rho GTPase activity also affects cell cycle progression or inhibition via the activation of NFKB-dependent gene expression. NFKB activation by the Rac1 protein occurs when Rac binds to p67 (phox) to increase the activation of the NADPH oxidase system and the production of reactive oxygen species (ROS) [33, 56].

In GBM, Rac1 is a key contributor to cell survival, most likely via multiple signalling pathways [27]. For example, in an analysis of a set of erlotinib-resistant GBM cell lines in an expression analysis of 244 prospectively selected genes, Rac1 expression was shown to associate significantly with erlotinib-resistant glioblastoma. Erlotinib is a small molecule of tyrosine-kinase inhibitor that targets the EGFR. It has been studied as a targeted therapeutic strategy to take advantage of EGFR overexpression and its subsequent downstream (Figure 1) in GBM. While experimental GBM analysis showed favourable results; however, six clinical trials failed to prove any significant benefit, suggesting that different associated signalling pathways might regulate the proliferation of GBM. Therefore, interference with this Rac1 gene might enhance the proliferation inhibition of erlotinib against glioblastoma [27, 58].

Another study, using a Rac1 inhibitor in a retinoblastoma-deficient breast cancer cell line, demonstrated that Rac1 suppression leads to apoptosis [59]. This observation is consistent with the findings of an earlier study, in which the suppression of Rac1 led to glioma inhibition [54].

In addition to proliferation signalling, Rac1 is known as a key regulator of cell migration and invasion. This concept was

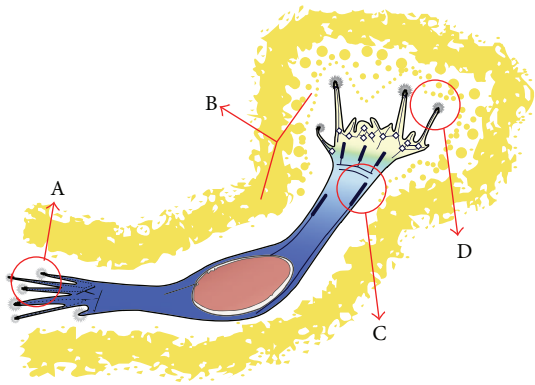

Figure 2: Schematic illustration of GBM cell. (A) Focal adhesion and (B) pseudopodium that is regulated by Rho GTPases to modulate actin cytoskeleton activity; (C) focal adhesions and actin cytoskeleton that support cell morphology and anchorage of the cell; (D) filopodia-ECM interactions that modulate actin-driven protrusions (adapted from O'Neill et al., 2010 [9]).

proven by Chan et al. [60], who showed that the depletion of Rac1 in SNB19 and U87 glioblastoma cells lines strongly inhibited lamellipodia formation and cell migration.

During migration, the actin fibers of the cell become polarised to form membrane protrusions through sheet-like extensions, such as pseudopodia, lamellipodia, filopodia, and invadopodia (Figure 2), which extend from the edges of the cells. These protrusions involve several signalling proteins that regulate filamentous actin and numerous structural membranes. The establishment of membrane anchors allows cytoskeletal contraction symphony, which finally moves the cell forward [17, 61]. Rac1 has been shown to localise at the leading edge of the moving cell, where it is activated by integrin-mediated cell adhesion and growth factors [9]. The role of Rac1 in cell migration is mediated through the formation of lamellipodia via the reorganisation of the actin cytoskeleton to generate locomotive force [62].

Rac1 activity has also been implicated in the aggressive phenotype. The aberrant activation of Rac1 stimulates neoplastic cell invasion via the activation of matrix metalloproteinase (MMP). MMP-2 and MMP-9 are examples of MMPs known to be upregulated in gliomas [62].

Cellular focal adhesions are points of linkage among the extracellular matrix (ECM), transmembrane integrin receptors, and the internal actin cytoskeleton. The integrin receptors are heterodimeric transmembrane complexes [9]. During tumour development, changes in integrin receptor expression, intracellular control of integrin function, and signals perceived from integrin receptor ligand binding influence the cell's ability to interact with the environment, enabling metastatic cells to convert from a sessile, stationary phenotype to a migratory and invasive phenotype [9].

Via this activity of focal adhesion kinases and their subsequent downstream molecules, a signalling network is established that culminates in the activation of GTPase proteins, such as Rac1. In turn, this determines the dynamic state of the actin cytoskeleton that is essential to the morphological progression of cell migration and adhesion [9].

Thus, Rac1 has been found to be involved in several pathways, explaining why it is so important in inducing a malignant phenotype. Several proteins act as effectors of Rac1 or are downstream of this gene region, including the p21-activated kinases (PAKs). For example, PAK1 is targeted by Rac1 to phosphorylate and activate the LIM kinase (LIMK), which phosphorylates cofilin. Cofilin phosphorylation triggers actin depolymerisation, resulting in the alteration of the cell structure [33].

The Rac1-associated activation of the actin-related protein-2/3 (ARP2/3) complex also activates actin polymerisation in lamellipodia. This polymerisation is triggered via Rac1 signalling, which binds to the WASP family verprolin homology domain-containing protein (WAVE) complex to release active WAVE and subsequently activates ARP2/3 [33, 57].

Other downstream targets of Rac1 are IQ motif containing GTPase activating protein-1 (IQGAP1), partner of Rac1 (POR1), plenty of SH3s (POSH), and CDC42-binding protein kinase alpha (CDC42BPA). To affect microtubule orientation and cell-to-cell adhesion, Rac1 binds to the actin-binding protein IQGAP1. The binding of IQGAP1 to the microtubule tip protein Clip170 captures growing microtubules at the leading edge of migrating fibroblasts, which results in cell polarisation [33, 63].

Therefore, Rac1 is essential for normal cell function; however, when improperly activated, it contributes to tumour cell growth, invasion, and angiogenesis [59]. Based on the culmination of evidence, the treatment of high-grade glioma should focus on targeting Rac1 [9].

7. NDV-Rac1 Interaction for Proliferation and Invasion Inhibition of GBM

A recent study reported that NDV is preferentially replicated in Rac1-activated cells [36], and a growing list of studies have directly or indirectly pointed to the Rac1 protein as a key factor in NDV infection of cancerous cells [7, 10]. This direction mainly discriminates the proliferation and invasive behaviour of normal and cancerous cells that are regulated by Rac1 protein signalling [33].

The involvement of Rac1 in NDV infection of GBM is the focus of this subtopic. To begin, the direct involvement of Rac1 in NDV-GBM cell tropism is discussed via two platforms: endocytosis viral entry and NDV-induced cell-to-cell fusion, called syncytium formation.

The paramyxovirus family, including NDV, primarily gain their entry into the infected cell when the HN viral protein recognises and binds cellular receptors at the plasma membrane, after which F protein triggers the merging of the viral envelope and plasma membrane, driving the introduction of the viral nucleocapsid into the cell. However, in a high viral concentration, NDV can enter the infected cell via caveolae-mediated endocytosis [64].

Caveolae are small, flask-shaped invaginations in the plasma membrane that contain high levels of cholesterol and glycosphingolipids as well as caveolins, structural proteins that form the caveolae [64]. Endocytosis is a cellular

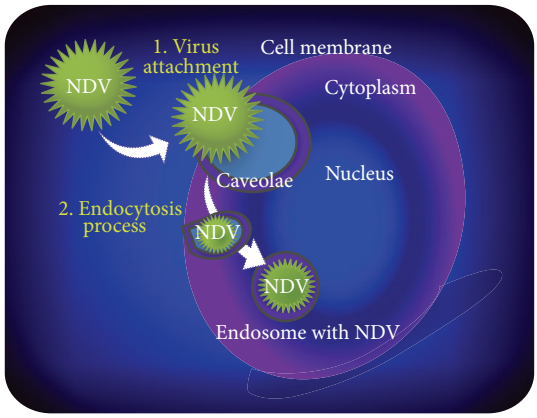

Figure 3: Schematic illustration of viral internalisation via caveolae-mediated endocytosis. Viral particles enter the cell through an endocytic pathway after viral-cell membrane fusion in a caveolae pocket that finally carries the virus into the cell endosome.

absorption process of large molecules that is primarily used for the nonselective internalisation of fluid and protein into the cell. The mechanism also drives the uptake of foreign particles, including viruses. Caveolae-mediated endocytosis has a strong connection with the actin cytoskeleton and involves the cholesterol-rich lipid raft domains at the plasma membrane [65], as well as a complex signalling pathway involving tyrosine kinases and phosphatases [66].

Therefore, some viruses are potentially contained within small invaginations in the plasma membranes of host cell that form the caveosome, which delivers virus particles to early endosomes (Figure 3) within the infected cells [66]. Cantín et al. [64] described the colocalization of NDV with caveolin and with the early endosome marker EEA1, leading to the suggestion that a certain percentage of the virus manages to penetrate the cell through caveolin-dependent endocytic pathways [67]. In that particular study, after 30 minutes of NDV infection, a strong colocalization of NDV HN protein and EEA1 was found, thus confirming that HN is targeted to early endosomes. EEA1 is an early endosomal antigen 1 marker protein used for localization of the virus in the intracellular structures. Endocytosis in paramyxovirus suggests that Rho GTPase Rac1 protein signalling has a role in the initial steps in the viral life cycle [68]. This suggestion is corroborated by a study on dynamic Rac1 and caveolin interaction that reported a direct interconnection of Rac1 as upstream of caveolin, where Rac1 activity promotes caveolin accumulation at Rac1-positive peripheral adhesions of the cell [69]. Thus, it seems probable that Rac1 activity interacts with caveolar regulation.

Remarkably, Rac1 protein is also involved in the phospholipase-D (PLD) regulation of phosphatidylcholine hydrolysis to yield phosphatidic acid and choline. Phosphatidic acid is a subsequent messenger involved in membrane remodelling events that are critical to cell growth, as well as vesicle trafficking into the cell and secretion [60, 70].

Furthermore, NDV infection is known to induce syncytium formation as a result of cell-to-cell fusion [10]. Our screening via live cell imaging of the GBM cell line showed that uninfected cells exhibit a migratory behaviour without intercell aggregation. In contrast, most migration GBM cell lines commonly fused with each other to form a giant syncytium cell with multiple nuclei (Figure 4(d)) after being treated with lentogenic NDV strain V4UPM, compared to untreated cells (Figure 4(a)). The syncytium cell also displayed the characteristic of actin reorganisation to form new borders surrounding the multiple nuclei, as indicated in Figures 4(b), 4(c), and 4(d).

According to Mansour et al. [10], enhanced fusogenicity has been shown to improve the oncolytic activity of NDV and vesicular stomatitis virus (VSV). In NDV-infected cells, syncytia are formed by the accumulation of newly synthesised viral HN and F glycoproteins, causing fusion with neighbouring cells. Thus, it can be postulated that apoptosis resistance may delay the apoptosis of NDV-infected cells, allowing fusion with an increased number of neighbouring cells and enhanced syncytium formation. As a benefit, the process helps to prolong the survival of cancer cells and allows the virus to replicate freely in the absence of an antiviral response [10].

Despite the extensive data [62, 71] regarding the mechanism of glioma cell migration, there is little information on the mechanism of cell-to-cell fusion. Taylor et al. [61] reported that in order to establish infection and promote cell fusion, the physical barrier imposed by the cortical actin meshwork in infected cells must be overcome. This process often requires the reprogramming of the actin cytoskeleton, thus explaining the reorganisation of the actin cytoskeleton network of NDV-infected glioma cells (Figures 4(c) and 4(d)).

NDV budding-out from the infected cell occurs with the involvement of a lipid raft on the cell membrane. Membrane lipid rafts are defined as cholesterol- and sphingolipid-rich microdomains in the exoplasmic leaflet of the cellular plasma membrane [72]. Lipid rafts associated with the actin cytoskeleton are thought to be sites of viral protein assembly in paramyxovirus budding-out and are released from the infected cell upon replication of the virus. This notion was first proposed after the detection of large quantities of actin in purified preparations of paramyxoviruses, including NDV [73].

The involvement of NDV in the regulation of or interaction with the cellular actin cytoskeleton has been crucial in its establishment of infection. This proposition is supported by a study that showed that cells infected by other paramyxoviruses, such as Hendra virus and simian virus 5, often display actin reorganisation, which suggests that Rac1 has a role in the early steps of the viral life cycle [68].

Thus, the role of Rac1 as a pleiotropic regulator of multiple cellular functions, including actin cytoskeletal reorganisation, gene transcription, and cell migration [74], needs to be elucidated further to explain the mechanism of the NDV-Rac1 interaction in human cancer cells. Puhlmann et al. [36] showed that Rac1 overexpression led to a significant increase in NDV replication in the cell pool, accompanied by increased oncolysis, thus identifying Rac1 as an oncogenic protein that is essential for NDV sensitisation and replication in tumorigenic cells.

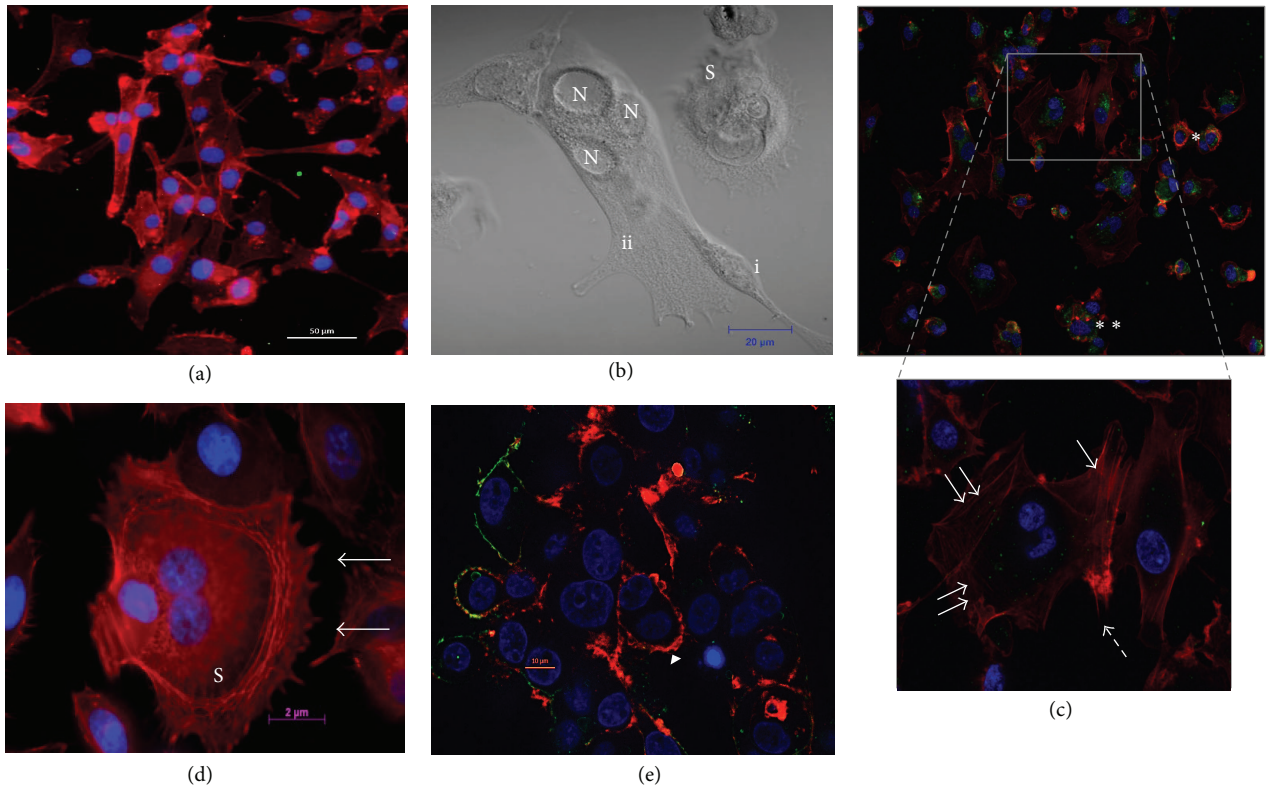

Figure 4: (a) Singular cells of untreated GBM with actin cytoskeleton staining (red colour). (b) Phase contrast microphotograph of NDV-infected GBM cells; (i) single-cell fusion process into the syncytium cells (ii) that is characterised by multiple nuclei (N). (c) Actin cytoskeleton staining of syncytium process in infected cells, showing actin cytoskeleton reorganisation (arrows in higher magnification microphotograph). (d) Completed actin reorganisation of three cells to become one syncytium cell (S). The asterisk (∗) and apoptotic syncytium (arrow head) in (c) and (e) represent actin cytoskeleton denaturation and cell death in a singular cell and a syncytium cell, respectively. The nucleus is stained blue and the NDV is stained green.

In glioma cells, depletion of Rac1 expression by siRNA strongly inhibits lamellipodia formation and results in a decrease in cell migration and invasion. Moreover, inhibition of Rac1 activity via a dominant negative form of Rac1 induces apoptosis in primary and glioma cell lines, but not in normal adult astrocytes [14].

This is particularly interesting, as our experience with live cell imaging also showed the repressed mobility of infected cells at approximately 12 hours after infection. In the live cell movie, initial recording showed active cellular migration of the cells all over the microscopic view in both untreated and NDV V4UPM-treated GBM cells. However, the cellular migration was repressed as both singular and syncytium infected cells appeared to struggle locally and finally underwent cytolysis (video supplement). In contrast, the mobility behaviour continued in the untreated cells.

Ultimately, both singular and syncytium NDV-infected cells undergo apoptosis as showed in bottom-left quadrant of the video and Figure 4(e) [4, 75]. However, the live cell video supplement also shows that the syncytium formation induced temporary death resistance compared to the singular infected cells, indicating that NDV possibly infects glioma cells and exploits the cellular cytoskeleton for cell fusion to extend the infected cell's survival time and allow its replication.

Therefore, the fact that NDV replication requires Rac1 for tropism in human cancer cells [36], as well as the role of Rac1 in cell migration [60] and actin reorganisation [76], the rearrangement of actin cytoskeletons in syncytium cells (Figure 4(d)) and the repressed mobility of NDV-treated GBM cells observed in the live cell video have placed Rac1 in NDV tropism in GBM. In our previous work [7], Rac1 gene expression in NDV-treated GBM at 24-hour intervals showed significant Rac1 gene downregulation. Guided by the acute cytolytic effects observed in live cells, Rac1 protein expression was screened at 3, 6, 9, and 12 hours. The results indicated that the Rac1 protein was linearly upregulated at 3, 6, and 9 hours after infection, followed by significant downregulation at 12 hours after infection.

Ibrahim [77] reported that lentogenic NDV strain V4UPM infection of a GBM cell line induced cell cycle arrest at the S phase. In breast cancer cell lines, siRNA treatment against Rac1 suppressed the protein and its downstream NFKB, leading to S phase cell cycle arrest and apoptosis [59]. These interactions have indirectly placed the NDV

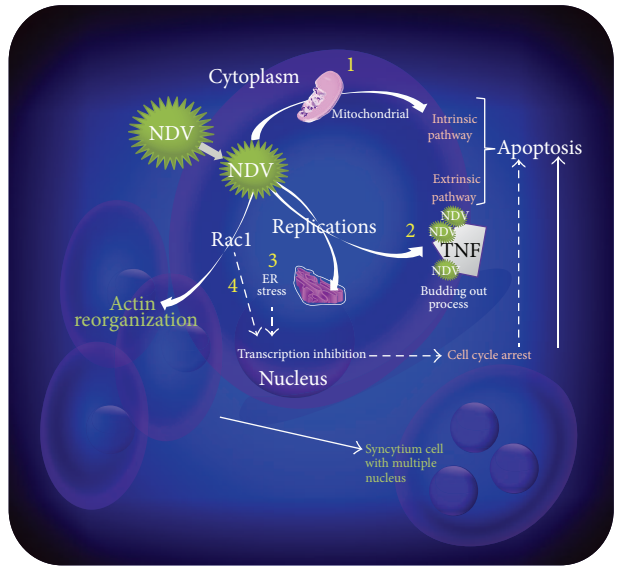

Figure 5: Multiple signalling reported in NDV induces cell death pathways in a cancerous cell. NDV infection of cancerous cells potentially induces direct apoptosis via intrinsic (1) or extrinsic (2) pathways. The NDV replication activity also induces ER stress (3), which triggers the transcription inhibition that leads to cell cycle arrest. NDV interactions with Rac1 (4) protein to induce syncytium formation also potentially induces cell cycle arrest, while cellular actin reorganisation in syncytium cells also induces denaturing of the actin cytoskeleton, which leads to cell death.

interaction in the proliferation and invasion of the GBM cell via Rac1 protein.

8. NDV-Induced Apoptosis Pathways

The NDV-Rac1 interaction is not the only mechanism, as many other pathways have been discovered. Figure 5 summarises the NDV-GBM interactions that lead to cell death. Elankumaran et al. [4] reported that NDV primarily initiates apoptosis via the intrinsic pathway. NDV infection induces mitochondrial permeability, leading to the release of cytochrome C. It further binds to procaspase 9 to form an apoptosome, which further activates Caspase-9 and Caspase-3, subsequently leading to apoptosis [4, 75].

NDV infections of cancerous cells also induce cell death via extrinsic apoptosis signalling, rather than via an intrinsic pathway. The pathway is triggered by death ligands such as tumours necrosis factor (TNF), which induces TNF-related apoptosis-inducing ligand (TRAIL) and subsequently promotes cell death via Caspase-8. Proteolytic Caspase-8 cleaves and activates executioner Caspase-3, leading to further cell death [4].

Knowledge of asynchronous apoptosis signalling between the intrinsic and extrinsic pathways of cells infected by NDV is limited. The interference of NDV with the cellular actin cytoskeleton to sustain syncytium cell viability for their replication might be a cause. The NDV viral proteins line up on the actin cytoskeleton of infected cells for the budding-out to produce new virion progeny, which might suggest secondary apoptosis induction via the extrinsic pathway. Janmey [78] described that during apoptosis, major cytoskeleton filaments, including actin, cytokeratin, and microtubules, are degraded. The degradation of actin causes the cell to collapse and induces mechanical tension, cell detachment, and subsequent cell death.

9. Conclusion

In summary, a growing body of data has shown that the aberrant Rac1 oncogene is among the major regulators of GBM proliferation and invasion [58] and that NDV tropism in cancerous cells is connected with Rac1 protein signalling [36]. This finding is supported by the fact that cells infected with paramyxovirus often display actin reorganization, suggesting that Rac1 has a role in the early steps of the viral life cycle [68]. NDV has also been known to infect the GBM cell line and induce actin rearrangement in syncytium cells, leading to syncytium cell death. These findings indicate that lentogenic NDV is a promising bullet targeted at inhibiting GBM proliferation and invasion via its interaction with Rac1.

Conflict of Interests

The authors declare no conflict of interests.

Acknowledgment

The authors would like to thank Majlis Kanser Nasional (MAKNA) for its financial grant and continuous support for this study.

References

[1] C. Biederer, S. Ries, C. H. Brandts, and F. McCormick, "Replication-selective viruses for cancer therapy," *Journal of Molecular Medicine*, vol. 80, no. 3, pp. 163–175, 2002.

[2] F. J. Zemp, J. C. Corredor, X. Lun, D. A. Muruve, and P. A. Forsyth, "Oncolytic viruses as experimental treatments for malignant gliomas: using a scourge to treat a devil," *Cytokine and Growth Factor Reviews*, vol. 21, no. 2-3, pp. 103–117, 2010.

[3] S. J. Russell, "RNA viruses as virotherapy agents," *Cancer Gene Therapy*, vol. 9, no. 12, pp. 961–966, 2002.

[4] S. Elankumaran, D. Rockemann, and S. K. Samal, "Newcastle disease virus exerts oncolysis by both intrinsic and extrinsic caspase-dependent pathways of cell death," *Journal of Virology*, vol. 80, no. 15, pp. 7522–7534, 2006.

[5] R. Martinez and M. Esteller, "The DNA methylome of glioblastoma multiforme," *Neurobiology of Disease*, vol. 39, no. 1, pp. 40–46, 2010.

[6] O. O. Kanu, B. Hughes, C. Di et al., "Glioblastoma multiforme oncogenomics and signaling pathways," *Clinical Medicine: Oncology*, vol. 3, pp. 39–52, 2009.

[7] Z. Mustafa, H. S. Shamsuddin, A. Ideris et al., "Viability reduction and rac1 gene downregulation of heterogeneous Ex-Vivo glioma acute slice infected by the oncolytic newcastle disease virus strain V4UPM," *BioMed Research International*, vol. 2013, Article ID 248507, 8 pages, 2013.

[8] E. A. Maher, F. B. Furnari, R. M. Bachoo et al., "Malignant glioma: genetics and biology of a grave matter," *Genes and Development*, vol. 15, no. 11, pp. 1311–1333, 2001.

[9] G. M. O'Neill, J. Zhong, A. Paul, and S. J. Kellie, "Mesenchymal migration as a therapeutic target in glioblastoma," *Journal of Oncology*, vol. 2010, Article ID 430142, 17 pages, 2010.

[10] M. Mansour, P. Palese, and D. Zamarin, "Oncolytic specificity of newcastle disease virus is mediated by selectivity for apoptosis-resistant cells," *Journal of Virology*, vol. 85, no. 12, pp. 6015–6023, 2011.

[11] D. Zamarin and P. Palese, "Oncolytic Newcastle disease virus for cancer therapy: old challenges and new directions," *Future Microbiology*, vol. 7, no. 3, pp. 347–367, 2012.

[12] M. M. Zulkifli, R. Ibrahim, A. M. Ali et al., "Newcastle diseases virus strain V4UPM displayed oncolytic ability against experimental human malignant glioma," *Neurological Research*, vol. 31, no. 1, pp. 3–10, 2009.

[13] P. A. McKinney, "Brain tumours: incidence, survival, and aetiology," *Journal of Neurology, Neurosurgery & Psychiatry*, vol. 75, no. 2, pp. ii12–ii17, 2004.

[14] M. Nakada, D. Kita, T. Watanabe et al., "Aberrant signaling pathways in Glioma," *Cancers*, vol. 3, no. 3, pp. 3242–3278, 2011.

[15] E. C. Holland, "Glioblastoma multiforme: the terminator," *Proceedings of the National Academy of Sciences of the United States of America*, vol. 97, no. 12, pp. 6242–6244, 2000.

[16] A. Zanotto-Filho, E. Braganhol, R. Schröder et al., "NFκB inhibitors induce cell death in glioblastomas," *Biochemical Pharmacology*, vol. 81, no. 3, pp. 412–424, 2011.

[17] M. Nakada, S. Nakada, T. Demuth, N. L. Tran, D. B. Hoelzinger, and M. E. Berens, "Molecular targets of glioma invasion," *Cellular and Molecular Life Sciences*, vol. 64, no. 4, pp. 458–478, 2007.

[18] A. Haseley, C. Alvarez-Breckenridge, A. R. Chaudhury, and B. Kaur, "Advances in oncolytic virus therapy for glioma," *Recent Patents on CNS Drug Discovery*, vol. 4, no. 1, pp. 1–13, 2009.

[19] V. Nagesh, T. L. Chenevert, C. I. Tsien et al., "Quantitative characterization of hemodynamic properties and vasculature dysfunction of high-grade gliomas," *NMR in Biomedicine*, vol. 20, no. 6, pp. 566–577, 2007.

[20] X. Lun, D. L. Senger, T. Alain et al., "Effects of intravenously administered recombinant vesicular stomatitis virus (VSVΔM51) on multifocal and invasive gliomas," *Journal of the National Cancer Institute*, vol. 98, no. 21, pp. 1546–1557, 2006.

[21] A. Jemal, R. Siegel, E. Ward, Y. Hao, J. Xu, and M. J. Thun, "Cancer statistics, 2009," *CA: A Cancer Journal for Clinicians*, vol. 59, no. 4, pp. 225–249, 2009.

[22] Z. A. Omar, M. Z. Ali, and N. S. I. Tamin, *Malaysian Cancer Statistics—Data and Figure Peninsular Malaysia 2006*, National Cancer Registry, Ministry of Health, Putrajaya, Malaysia, 2006.

[23] M. Farooqui, M. A. Hassali, A. Knight et al., "A qualitative exploration of Malaysian cancer patients'perceptions of cancer screening," *BMC Public Health*, vol. 13, article 48, 2013.

[24] D. N. Louis, E. C. Holland, and J. G. Cairncross, "Glioma classification: a molecular reappraisal," *The American Journal of Pathology*, vol. 159, no. 3, pp. 779–786, 2001.

[25] N. A. Butowski and S. M. Chang, "Glial tumors: the current state of scientific knowledge," *Clinical Neurosurgery*, vol. 53, pp. 106–113, 2006.

[26] M. C. Chamberlain, "Bevacizumab for the treatment of recurrent glioblastoma," *Clinical Medicine Insights: Oncology*, vol. 5, pp. 117–129, 2011.

[27] G. Karpel-Massler and M. E. Halatsch, "The molecular basis of resistance to the antiproliferative effect of EGFR inhibition in human glioblastoma multiforme cell lines," in *Brain Tumors—Current and Emerging Therapeutic Strategies*, A. L. Abujamra, Ed., pp. 245–252, InTech, Vienna, Austria, 2011.

[28] M. Bredel, D. M. Scholtens, A. K. Yadav et al., "NFKBIA deletion in glioblastomas," *The New England Journal of Medicine*, vol. 364, no. 7, pp. 627–637, 2011.

[29] P. Villalonga, R. M. Guasch, K. Riento, and A. J. Ridley, "RhoE inhibits cell cycle progression and Ras-induced transformation," *Molecular and Cellular Biology*, vol. 24, no. 18, pp. 7829–7840, 2004.

[30] B. Everts and H. G. Van Der Poel, "Replication-selective oncolytic viruses in the treatment of cancer," *Cancer Gene Therapy*, vol. 12, no. 2, pp. 141–161, 2005.

[31] D. Joyce, B. Bouzahzah, M. Fu et al., "Integration of Rac-dependent regulation of cyclin D1 transcription through a nuclear factor-κB-dependent pathway," *The Journal of Biological Chemistry*, vol. 274, no. 36, pp. 25245–25249, 1999.

[32] L. Boyer, S. Travaglione, L. Falzano et al., "Rac GTPase instructs nuclear factor- kappaB activation by conveying the SCF complex and IkBalpha to the ruffling membranes," *Molecular Biology of the Cell*, vol. 15, no. 3, pp. 1124–1133, 2004.

[33] D. Sun, D. Xu, and B. Zhang, "Rac signaling in tumorigenesis and as target for anticancer drug development," *Drug Resistance Updates*, vol. 9, no. 6, pp. 274–287, 2006.

[34] M. A. Garcia, P. Gallego, M. Campagna et al., "Activation of NF-κB pathway by virus infection requires Rb expression," *PLoS ONE*, vol. 4, no. 7, Article ID e6422, 2009.

[35] L. A. Selznick, M. F. Shamji, P. Fecci, M. Gromeier, A. H. Friedman, and J. Sampson, "Molecular strategies for the treatment of malignant glioma—genes, viruses, and vaccines," *Neurosurgical Review*, vol. 31, no. 2, pp. 141–155, 2008.

[36] J. Puhlmann, F. Puehler, D. Mumberg, P. Boukamp, and R. Beier, "Rac1 is required for oncolytic NDV replication in human cancer cells and establishes a link between tumorigenesis and sensitivity to oncolytic virus," *Oncogene*, vol. 29, no. 15, pp. 2205–2216, 2010.

[37] B. S. Seal, D. J. King, and H. S. Sellers, "The avian response to Newcastle disease virus," *Developmental and Comparative Immunology*, vol. 24, no. 2-3, pp. 257–268, 2000.

[38] D. Nidzworski, L. Rabalski, and B. Gromadzka, "Detection and differentiation of virulent and avirulent strains of Newcastle disease virus by real-time PCR," *Journal of Virological Methods*, vol. 173, no. 1, pp. 144–149, 2011.

[39] J. C. Dortmans, G. Koch, P. J. Rottier, and B. P. Peeters, "Virulence of newcastle disease virus: what is known so far?" *Veterinary Research*, vol. 42, no. 1, article 122, 2011.

[40] V. Schirrmacher and P. Fournier, "Newcastle disease virus: a promising vector for viral therapy, immune therapy, and gene therapy of cancer," *Methods in Molecular Biology*, vol. 542, pp. 565–605, 2009.

[41] J. G. Sinkovics and J. C. Horvath, "Newcastle disease virus (NDV): brief history of its oncolytic strains," *Journal of Clinical Virology*, vol. 16, no. 1, pp. 1–15, 2000.

[42] A. I. Freeman, Z. Zakay-Rones, J. M. Gomori et al., "Phase I/II trial of intravenous NDV-HUJ oncolytic virus in recurrent glioblastoma multiforme," *Molecular Therapy*, vol. 13, no. 1, pp. 221–228, 2006.

[43] A. M. Alabsi, S. A. A. Bakar, R. Ali et al., "Effects of Newcastle disease virus strains AF2240 and V4-UPM on cytolysis and apoptosis of leukemia cell lines," *International Journal of Molecular Sciences*, vol. 12, no. 12, pp. 8645–8660, 2011.

[44] K. A. Parato, D. Senger, P. A. J. Forsyth, and J. C. Bell, "Recent progress in the battle between oncolytic viruses and tumours," *Nature Reviews Cancer*, vol. 5, no. 12, pp. 965–976, 2005.

[45] R. J. Prestwich, F. Errington, K. J. Harrington, H. S. Pandha, P. Selby, and A. Melcher, "Oncolytic viruses: do they have a role in anti-cancer therapy?" *Clinical Medicine. Oncology*, vol. 2, pp. 83–96, 2008.

[46] S. Krishnamurthy, T. Takimoto, R. A. Scroggs, and A. Portner, "Differentially regulated interferon response determines the outcome of newcastle disease virus infection in normal and tumor cell lines," *Journal of Virology*, vol. 80, no. 11, pp. 5145–5155, 2006.

[47] J. Miyakoshi, K. D. Dobler, J. Allalunis-Turner et al., "Absence of IFNA and IFNB genes from human malignant glioma cell lines and lack of correlation with cellular sensitivity to interferons," *Cancer Research*, vol. 50, no. 2, pp. 278–283, 1990.

[48] B. Yaacov, E. Elihaoo, I. Lazar et al., "Selective oncolytic effect of an attenuated Newcastle disease virus (NDV-HUJ) in lung tumors," *Cancer Gene Therapy*, vol. 15, no. 12, pp. 795–807, 2008.

[49] I. Lazar, B. Yaacov, T. Shiloach et al., "The oncolytic activity of Newcastle disease virus NDV-HUJ on chemoresistant primary melanoma cells is dependent on the proapoptotic activity of the inhibitor of apoptosis protein livin," *Journal of Virology*, vol. 84, no. 1, pp. 639–646, 2010.

[50] R. M. Lorence, B. B. Katubig, K. W. Reichard et al., "Complete regression of human fibrosarcoma xenografts after local Newcastle disease virus therapy," *Cancer Research*, vol. 54, no. 23, pp. 6017–6021, 1994.

[51] J. G. Sinkovics and J. C. Horvath, "Natural and genetically engineered viral agents for oncolysis and gene therapy of human cancers," *Archivum Immunologiae et Therapiae Experimentalis*, vol. 56, supplement 1, pp. 3s–59s, 2008.

[52] M. Aghi and E. A. Chiocca, "Gene therapy for glioblastoma," *Neurosurgical Focus*, vol. 20, no. 4, article E18, 2006.

[53] D. Kirn, R. L. Martuza, and J. Zwiebel, "Replication-selective virotherapy for cancer: biological principles, risk management and future directions," *Nature Medicine*, vol. 7, no. 7, pp. 781–787, 2001.

[54] D. L. Senger, C. Tudan, M. Guiot et al., "Suppression of Rac activity induces apoptosis of human glioma cells but not normal human astrocytes," *Cancer Research*, vol. 62, no. 7, pp. 2131–2140, 2002.

[55] O. Gjoerup, J. Lukas, J. Bartek, and B. M. Willumsen, "Rac and Cdc42 are potent stimulators of E2F-dependent transcription capable of promoting retinoblastoma susceptibility gene product hyperphosphorylation," *The Journal of Biological Chemistry*, vol. 273, no. 30, pp. 18812–18818, 1998.

[56] D. Michaelson, W. Abidi, D. Guardavaccaro et al., "Rac1 accumulates in the nucleus during the G2 phase of the cell cycle and promotes cell division," *Journal of Cell Biology*, vol. 181, no. 3, pp. 485–496, 2008.

[57] M. Auer, B. Hausott, and L. Klimaschewski, "Rho GTPases as regulators of morphological neuroplasticity," *Annals of Anatomy*, vol. 193, no. 4, pp. 259–266, 2011.

[58] C. Krakstad and M. Chekenya, "Survival signalling and apoptosis resistance in glioblastomas: opportunities for targeted therapeutics," *Molecular Cancer*, vol. 9, article 135, 2010.

[59] T. Yoshida, Y. Zhang, L. A. R. Rosado et al., "Blockade of Rac1 activity induces G1 cell cycle arrest or apoptosis in breast cancer cells through downregulation of cyclin D1, survivin, and X-linked inhibitor of apoptosis protein," *Molecular Cancer Therapeutics*, vol. 9, no. 6, pp. 1657–1668, 2010.

[60] A. Y. Chan, S. J. Coniglio, Y. Chuang et al., "Roles of the Rac1 and Rac3 GTPases in human tumor cell invasion," *Oncogene*, vol. 24, no. 53, pp. 7821–7829, 2005.

[61] M. P. Taylor, O. O. Koyuncu, and L. W. Enquist, "Subversion of the actin cytoskeleton during viral infection," *Nature Reviews Microbiology*, vol. 9, no. 6, pp. 427–439, 2011.

[62] X. Li, J. W. Law, and A. Y. Lee, "Semaphorin 5A and plexin-B3 regulate human glioma cell motility and morphology through Rac1 and the actin cytoskeleton," *Oncogene*, vol. 31, no. 5, pp. 595–610, 2012.

[63] J. Szczepanowska, "Involvement of Rac/Cdc42/PAK pathway in cytoskeletal rearrangements," *Acta Biochimica Polonica*, vol. 56, no. 2, pp. 225–234, 2009.

[64] C. Cantín, J. Holguera, L. Ferrerira, E. Villar, and I. Muñoz-Barroso, "Newcastle disease virus may enter cells by caveolae-mediated endocytosis," *Journal of General Virology*, vol. 88, part 2, pp. 559–569, 2007.

[65] N. Branza-Nichita, A. Macovei, and C. Lazar, "Caveolae-dependent endocytosis in viral infection," in *Molecular Regulation of Endocytosis*, B. Ceresa, Ed., p. 31, InTech, 2012.

[66] J. Mercer, M. Schelhaas, and A. Helenius, "Virus entry by endocytosis," *Annual Review of Biochemistry*, vol. 79, pp. 803–833, 2010.

[67] J. J. Martín, J. Holguera, L. Sánchez-Felipe, E. Villar, and I. Muñoz-Barroso, "Cholesterol dependence of Newcastle Disease Virus entry," *Biochimica et Biophysica Acta—Biomembranes*, vol. 1818, no. 3, pp. 753–761, 2012.

[68] R. M. Schowalter, M. A. Wurth, H. C. Aguilar et al., "Rho GTPase activity modulates paramyxovirus fusion protein-mediated cell-cell fusion," *Virology*, vol. 350, no. 2, pp. 323–334, 2006.

[69] M. Nethe, E. C. Anthony, M. Fernandez-Borja et al., "Focal-adhesion targeting links caveolin-1 to a Rac1-degradation pathway," *Journal of Cell Science*, vol. 123, no. 11, pp. 1948–1958, 2010.

[70] M. H. Park, B. Ahn, Y. Hong, and D. S. Min, "Overexpression of phospholipase D enhances matrix metalloproteinase-2 expression and glioma cell invasion via protein kinase C

and protein kinase A/NF-κB/Sp1-mediated signaling pathways," *Carcinogenesis*, vol. 30, no. 2, pp. 356–365, 2009.

[71] V. M. Paulino, Z. Yang, J. Kloss et al., "TROY (TNFRSF19) is overexpressed in advanced glial tumors and promotes glioblastoma cell invasion via Pyk2-Rac1 signaling," *Molecular Cancer Research*, vol. 8, no. 11, pp. 1558–1567, 2010.

[72] J. P. Laliberte, L. W. McGinnes, M. E. Peeples, and T. G. Morrison, "Integrity of membrane lipid rafts is necessary for the ordered assembly and release of infectious Newcastle disease virus particles," *Journal of Virology*, vol. 80, no. 21, pp. 10652–10662, 2006.

[73] M. S. Harrison, T. Sakaguchi, and A. P. Schmitt, "Paramyxovirus assembly and budding: building particles that transmit infections," *International Journal of Biochemistry and Cell Biology*, vol. 42, no. 9, pp. 1416–1429, 2010.

[74] E. E. Bosco, J. C. Mulloy, and Y. Zheng, "Rac1 GTPase: a "Rac" of all trades," *Cellular and Molecular Life Sciences*, vol. 66, no. 3, pp. 370–374, 2009.

[75] Z. Fábián, C. M. Csatary, J. Szeberényi, and L. K. Csatary, "p53-independent endoplasmic reticulum stress-mediated cytotoxicity of a Newcastle disease virus strain in tumor cell lines," *Journal of Virology*, vol. 81, no. 6, pp. 2817–2830, 2007.

[76] C. Albertinazzi, A. Cattelino, and I. de Curtis, "Rac GTPases localize at sites of actin reorganization during dynamic remodeling of the cytoskeleton of normal embryonic fibroblasts," *Journal of Cell Science*, vol. 112, no. 21, pp. 3821–3831, 1999.

[77] R. Ibrahim, *Local V4UPM strain newcastle viruses induce cell death of brain tumor cell lines [M.S. thesis]*, Universiti Putra Malaysia, Serdang, Malaysia, 2011.

[78] P. A. Janmey, "The cytoskeleton and cell signaling: component localization and mechanical coupling," *Physiological Reviews*, vol. 78, no. 3, pp. 763–781, 1998.

Hindawi Publishing Corporation
BioMed Research International
Volume 2014, Article ID 484261, 9 pages
http://dx.doi.org/10.1155/2014/484261

Clinical Study

Intraoperative Cerebral Glioma Characterization with Contrast Enhanced Ultrasound

Francesco Prada,[1] Luca Mattei,[1,2] Massimiliano Del Bene,[1] Luca Aiani,[3] Marco Saini,[1] Cecilia Casali,[1] Assunta Filippini,[1,2] Federico Giuseppe Legnani,[1] Alessandro Perin,[1] Andrea Saladino,[1] Ignazio Gaspare Vetrano,[1,2] Luigi Solbiati,[4] Alberto Martegani,[3] and Francesco DiMeco[1,5]

[1] *Department of Neurosurgery, Fondazione IRCCS Istituto Neurologico "C. Besta", 20133 Milan, Italy*
[2] *Università degli Studi di Milano, 20122 Milan, Italy*
[3] *Department of Radiology, Ospedale Valduce, 22100 Como, Italy*
[4] *Department of Radiology, Ospedale di Circolo, 21052 Busto Arsizio, Italy*
[5] *Department of Neurosurgery, Johns Hopkins Medical School, Baltimore, MD 21218, USA*

Correspondence should be addressed to Francesco Prada; francesco.prada@istituto-besta.it

Received 13 February 2014; Accepted 1 May 2014; Published 12 June 2014

Academic Editor: Gustavo Pradilla

Background. Contrast enhanced ultrasound (CEUS) is a dynamic and continuous modality providing real-time view of vascularization and flow distribution patterns of different organs and tumors. Nevertheless its intraoperative use for brain tumors visualization has been performed few times, and a thorough characterization of cerebral glioma had never been performed before. *Aim*. To perform the first characterization of cerebral glioma using CEUS and to possibly achieve an intraoperative differentiation of different gliomas. *Methods*. We performed CEUS in an off-label setting in 69 patients undergoing surgery for cerebral glioma. An intraoperative qualitative analysis was performed comparing iCEUS with B-mode imaging. A postprocedural semiquantitative analysis was then performed for each case, according to EFSUMB criteria. Results were related to histopathology. *Results*. We observed different CE patterns: LGG show a mild, dotted CE with diffuse appearance and slower, delayed arterial and venous phase. HGG have a high CE with a more nodular, nonhomogeneous appearance and fast perfusion patterns. *Conclusion*. Our study characterizes for the first time human brain glioma with CEUS, providing further insight regarding these tumors' biology. CEUS is a fast, safe, dynamic, real-time, and economic tool that might be helpful during surgery in differentiating malignant and benign gliomas and refining surgical strategy.

1. Background

Cerebral gliomas, both HGG and LGG, are a daunting challenge. Complete tumor resection remains the best treatment option as long as it can be achieved without neurological sequelae. The role of imaging techniques in surgical resection of brain lesions is crucial in every step of surgery: they help planning surgical strategy, provide orientation during surgery, and indicate tumor boundaries and relationships with eloquent areas and vital structures, thus enhancing precision, accuracy, and safety for the patients while maximizing resection [1–4]. In recent years we are witnessing an increased use of ultrasounds (US) in neurosurgery, as their reliability as an intraoperative tool for tumor detection has been shown in multiple studies [5–9]. US obviates the need for high costs and specialized surgical instruments. However, although standard US B-mode imaging is excellent for tumor localization, little information is provided regarding microcirculation and perfusion dynamics, even when integrated with Doppler sonography [10–13].

The use of contrast agents in medical imaging is aimed at enhancing differences and characteristics of various organs, vessels, and cavities, making their visualization more simple and efficient, and US are routinely used in diagnostic

radiology. Contrast enhanced ultrasound (CEUS) is nowadays an established technique for many organs, as it allows, among other things, better detecting neoplastic lesions [14]. Furthermore, for their ability to highlight microcirculation, contrast agents are used in oncology in order to quantify the flow characteristics through an organ or tumor which differ according to the type of lesion and the organ involved [15–19]. The main clinically recognized application is the characterization of focal liver lesions [20]: CEUS with low-transmit power insonation allows real-time assessment of contrast enhancement and vascularity of focal lesions during the different dynamic phases, after injection of an intravenous contrast agent. Contrast agents containing microbubbles have been found to give the highest contrast with ultrasound scanning [21, 22]. The microbubbles consist of air or inert gas encapsulated in a layer of protein or polymers. Microbubbles are typically 5 micrometers in diameter, a similar size to red blood cells, and can therefore be transported into the smallest capillaries and across the lungs, thus allowing the visualization of the arterial system after venous injection. The pharmacokinetics of the microbubbles is quite different from that of contrast agents used for CT and MRI which generally diffuse in the interstitial space [15, 16, 23]. Second generation US contrast agents are clinically safe and well tolerated [24].

Given these technical features, it seems worthwhile and a promising effort to test this method for brain gliomas characterization and for its role in maximizing surgical resection, as already carried out by the radiological community for other organs. In fact, CEUS could provide us with further insight into glioma biology: being a dynamic and continuous modality it offers a real-time direct view of the degree of vascularization, microcirculation, flow distribution patterns, and tissue resistances of the different type of gliomas, adding all these pieces of information to the anatomical ones obtained with standard B-mode imaging.

Nonetheless its use in cerebral surgery has only been attempted few times so far [25–27], and there are no guidelines provided on this regard.

In this paper the authors describe, for the first time, the different patterns of cerebral gliomas enhancement using the CEUS technique, as compared with the lesion characterization achieved by using preliminary baseline US.

2. Material and Methods

2.1. Study Design and Patient Population. We performed intraoperative CEUS in an off-label setting in patients with supratentorial cerebral gliomas (both HGG and LGG) confirmed on preoperative MRI, undergoing craniotomy for tumor removal.

We included patients with no cardiopathy (New York Heart Association, NYHA I-II) and a good general status (ASA I-III).

All patients underwent preoperative assessment consisting of a thorough neurological and general conditions evaluation.

All patients were fully informed regarding their treatment and procedure and a written informed consent was obtained. The principles of the Declaration of Helsinki and the European Federation of Societies for Ultrasound in Medicine and Biology (EFSUMB) recommendations on CEUS [18, 28] had been followed.

2.2. Equipment and Contrast Agent. We used a last generation ultrasound device (MyLab, Esaote, Italy) with a 3–11 MHz linear probe.

The US system is equipped with Virtual Navigator software (MedCom, Germany) that permits fusion imaging between preoperative MRI and real-time intraoperative ultrasound imaging, allowing for neuronavigation.

As a contrast agent we used sulphur-hexafluoride, a second-generation ultrasound contrast agent (SonoVue, Bracco, Italy).

CEUS scanning is performed using contrast-tuned imaging (CnTI) technology that allows for real-time angiosonography, using second generation ultrasound contrast agents. Contrast-tuned imaging permits a selective synchronization of the US system to the signal produced by the microbubbles after transmission of a single-frequency pulse at the sulfur hexafluoride resonance frequency. The standard US imaging had been improved by CPI (combined pulsed imaging), a sophisticated algorithm based on a mix of high and low frequencies that improves B-mode penetration and resolution.

2.3. Procedure and Data Analysis. We perform a preoperative MRI based surgical planning. The craniotomy is performed with neuronavigation using standard preoperative MRI and coupled US using Virtual Navigator (Esaote, Italy).

The ultrasound apparatus is brought in and the 3–11 MHz intraoperative linear US probe (LA 332, Esaote, Italy) is placed in a transparent plastic surgical sterile sheath (Civco, USA), provided with US specific transducing gel.

After bone flap removal the US navigated probe is placed on the dura mater for scanning and standard B-mode imaging is acquired. All lesions are initially evaluated with B-mode imaging: they are defined as highly, mildly hyper-, iso-, and hypoechoic compared to normal brain parenchyma. Other lesion characteristics taken into account are diffuse or circumscribed appearance, homogeneous versus heterogeneous lesions, and presence of cystic/necrotic areas. The lesion is then identified on the two axes and measured. The lesion is also localized with neuronavigation on the corresponding coupled MRI.

Intraoperative CEUS is performed with the linear probe using low-power insonation and the obtained harmonic signals transduced with CnTI algorithm that allows for real-time and continuous imaging. Before microbubble contrast agent injection the focus is positioned below the level of the lesion. The contrast agent (SonoVue, Bracco, Italy) is injected intravenously by the anesthesiologist, as a bolus of 2.4 mL (5 mg/mL), followed by a flush of 10 cc. saline. The timer is started after UCA injection and perfusion dynamics is described starting from UCA arrival in major vessels; digital cine clips are registered continuously during baseline US scanning and during the different vascular phases.

Table 1: Summarizing CEUS features of different grades of human cerebral gliomas.

Brain Lesion	Number of pts.	Echogenicity	Appearance	Cystic areas and/or necrosis	Arterial phase	CEUS peak	Venous phase	CE
Low-grade glioma	22	Iso/hyperechoic	Diffuse; homogeneous	Small/microcysts	15″	20″	30″	Mild
Anaplastic glioma	11	Iso/hyperechoic	Diffuse; homogeneous	Small/microcysts	10″	15″	20–25″	Mild/high
Glioblastoma	36	Hyperechoic	Diffuse/circumscribed; heterogeneous	Large necrotic areas	2-3″	5″	10″	High

After UCA injection, a first intraoperative qualitative analysis was performed, aimed at determining whether a contrast enhancement was detectable for every lesion and at its afferent and efferent vessels visualization. Data were also stored in the US device for offline analysis.

An offline data analysis of the CEUS cine clips was performed using a semiquantitative assessment, following the EFSUMB guidelines. Gliomas patterns of contrast enhancement (CE) were evaluated following the EFSUMB guidelines: timing (arterial and venous phase (time is given as range)), degree of CE (low, mild, and high; comparison with brain parenchyma), and contrast distribution (centripetal/centrifugal pattern, visibility of afferent/efferent vessels, intralesional vessels, and cystic/necrotic areas).

All data obtained by online and offline analysis were correlated with histopathology.

3. Results

Our population consisted of 69 patients (mean age 49 years; age range 12–71 years) who underwent surgery for supratentorial cerebral glioma. Histopathological data showed 47 HGG and 22 LGG. We further divided the two groups in two other subgroups: HGG group was composed of 36 glioblastomas (GBM) and 11 anaplastic astrocytomas (ANA). LGG group had 18 astrocytomas (ASTRO) and 4 oligodendrogliomas (OLIGO). Ultrasound findings were correlated with histopathology.

On standard US B-mode imaging glioblastoma (n – 47) appeared all hyperechoic compared to brain parenchyma, with a heterogeneous appearance composed of multiple well-defined nodular areas and others with diffuse margins. Size ranged from 3 to 7 cm of maximal diameter. All but three lesions had cystic/necrotic areas. Anaplastic astrocytoma (n – 11) ranged from 4 to 7 cm in diameter. All three appeared hyperechoic with a diffuse, dense texture, with some areas more hyperechoic compared to the rest of the lesion. No cystic/necrotic areas were noted. The brain/tumor interface was not everywhere clearly visible.

In the LGG group all lesions (n – 22) appeared mildly hyperechoic compared to brain parenchyma. Size ranged from 3 to 9 cm in maximum diameter. All lesions had a homogenous texture with blurred margins at the brain/tumor interface except one oligoastrocytoma which had a discrete appearance with clear border. Microcysts were visible in 5 cases only.

After ultrasound contrast agent (UCA) injection different patterns were observed (Figures 1 and 2). All data are summarized in Table 1.

In the HGG group we further divided CE pattern into the two histological subgroups.

GBMs (n – 47) have rapid arterial and venous phase with a very fast arterial phase (2-3 seconds), chaotic transit of microbubbles within the lesion, and a CE peak at 5 seconds. CEUS transit time is very fast with a venous phase at 10 seconds. The major arterial supply was clearly visible, as well as the venous drainage system, almost invariably towards the periventricular zone. GBMs appear all hyperenhanced compared to normal brain parenchyma and have a very strong and intense contrast enhancement with a persistent parenchymal phase. They have an irregular and heterogeneous CE pattern with an alternation of nodular high contrast dense pattern with ring-like enhancement surrounding hypoperfused necrotic or nonperfused cystic areas. Many intralesional vessels are noted. We did not observe hypoperfused areas in only 6 cases, while 5 other cases only had small scattered hypoperfused areas. Tumor borders are better defined after CE than in standard B-mode imaging. GBMs showed a rapid refilling (around 3-4 seconds) after rapid sonication at high mechanical index sonication.

ANAs appeared to have a slower arterial phase compared to GBMs (10 sec), with a CE peak at around 15 seconds after UCA arrival. The transit of the microbubbles is slower and less chaotic and the venous phase is delayed as well (20–25 seconds), determining a lesion transit time of 5–10 seconds. Arterial supply and venous drainage are less identifiable than in GBMs. ANAs appear to have a diffuse hyperechoic pattern compared to brain parenchyma but have an initial mild and more homogeneous CE compared to GBMs, which is then reinforced during the parenchymal phase. We found a diffuse and persistent CE pattern in all cases, with scattered areas of higher CE in one case, the brain tumor interface. Few small hypoperfused areas were observed. Few intralesional vessels were observed. The border of the tumor is less identifiable than in GBMs. After high mechanical index sonication the replenishing kinetics is around 10 seconds.

In the LGG group, CEUS patterns for ASTRO were similar to ANAs. Nevertheless the vascular phases were slower, with an arterial phase at 15 seconds and a CE peak at around 20 seconds. The transit of the microbubbles appears even more steady (15–20 sec) with a venous phase after 30 seconds. Arterial supply is not always clear, as well as the venous drainage. ASTRO are mildly hyperechoic after UCA compared to brain parenchyma, and the tumor parenchymal phase is steady and uniform. Its CE pattern is dotted and

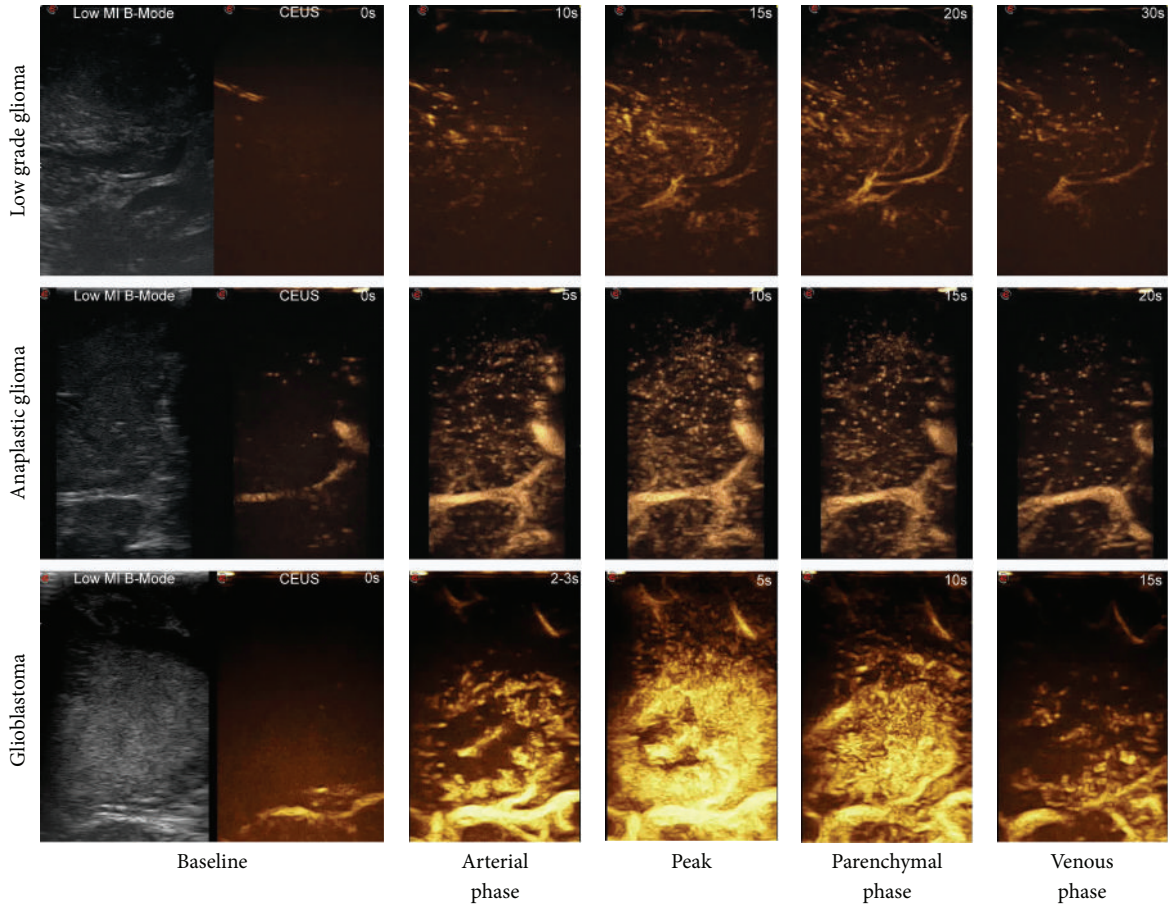

Figure 1: Time frame of how different grades of glioma are visualized with CEUS. In the first column of each row low mechanical index US and baseline CEUS (CA arrival – t_0) are displayed; then different CEUS phases (time is displayed in the top right corner of each image) are displayed only. The image clearly shows the differences in terms of timing, degree of enhancement, and CEUS patterns for different types of glioma, with a continuous and dynamic modality.

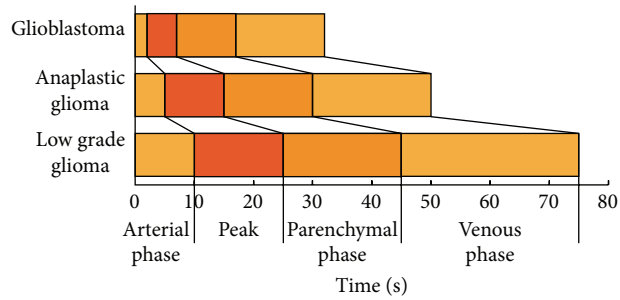

Figure 2: Schematic representation showing the differences in terms of timing and degree of enhancement (light orange: mild enhancement; dark orange: high enhancement) for different glioma grades.

homogeneous, with only two cases with microcystic areas. No intralesional vessels were noted. The replenishment kinetics is similar to the initial CE phase with a timing of around 10–15 seconds.

In OLIGOs we found similar features as in ANAs. In two cases the lesion was more well-defined, with faster arterial and venous phase, similar to GBMs, with an intralesion cyst.

4. Discussion

In this paper we performed the first intraoperative human cerebral gliomas characterization with the CEUS technique, as already had been performed for different lesions in other organs. The overall picture shows that in B-mode the main differences between lesions at different grades of malignancy are the degree of hyperechogenicity when compared to the surrounding parenchyma, the presence of cystic/necrotic areas, and a more or less defined brain/tumor interface. These findings account for the fact that the role of B-mode imaging is mainly limited in assisting tumor localization, providing only morphological information regarding the lesion, with little or no information about vascularization [7, 8]. Conversely, once enhanced, the tumor is highlighted and reveals other specific characteristics. These findings might possibly be related to their grade (Figure 3). For example, glioblastomas show rapid arterial and venous phase, a clearly visible arterial supply and venous drainage, and a very strong and intense contrast enhancement, with well-defined tumor borders. Lower grades were characterized by gradually less intense CE, less defined tumor borders, slower arterial and venous phases, poorly identifiable feeders

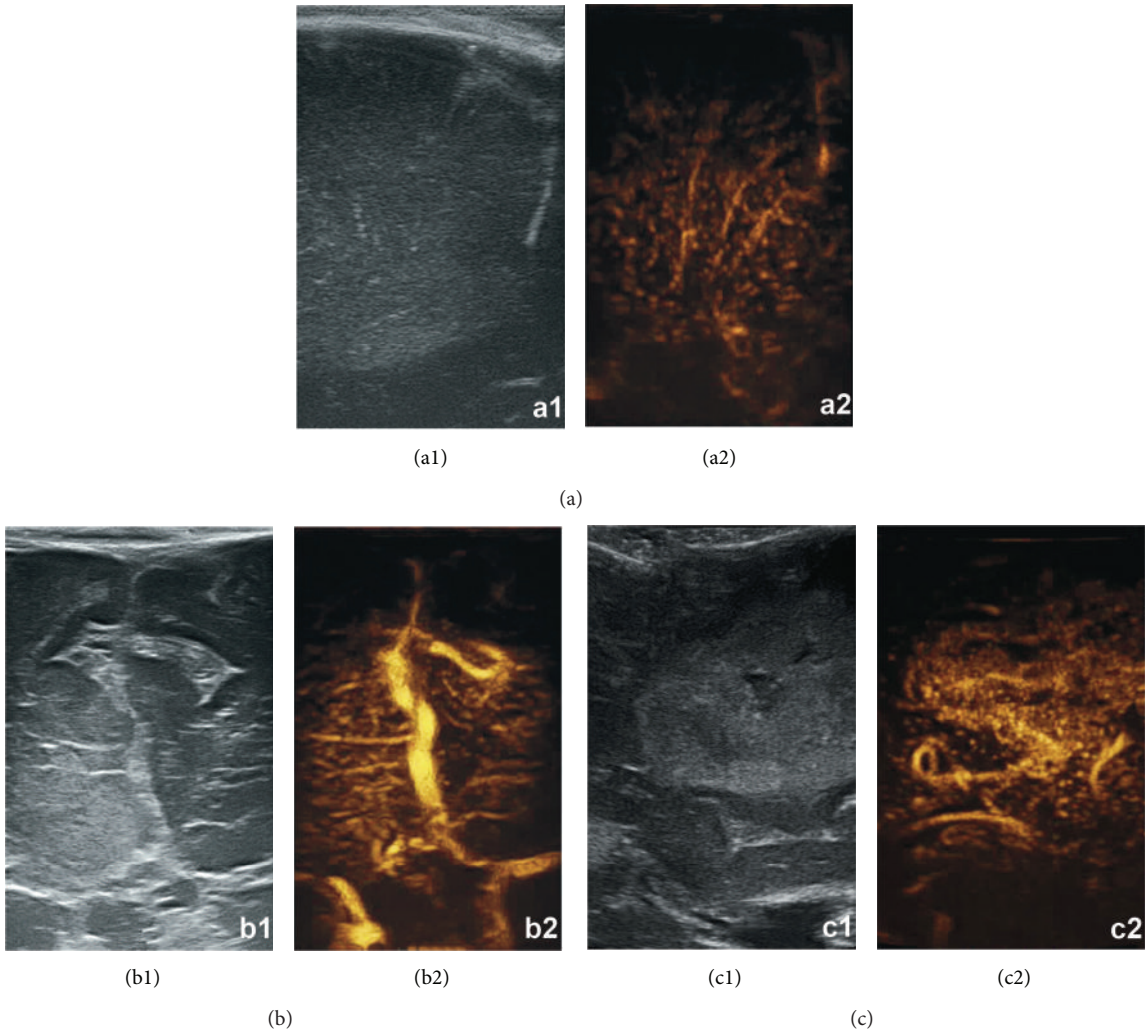

Figure 3: Comparison between standard gray-scale B-mode imaging and CEUS (resp., left and right picture in each panel) for different glioma grades (panel a: LGG, panel b: ANA, and panel c: GBM).

and drainage, and a CE pattern progressively more homogeneous, accounting for the absence of necrotic/cystic areas and a minor amount of neoangiogenesis. Surprisingly, we observed a slighter but well-defined CE in low grades too, where preoperative MRI did not show any enhancement. We have been able to directly visualize each of the 69 lesions both in B-mode and after contrast infusion, regardless of its histology, thus making the comparison between the two modalities always possible. We also observed different morphologic and dynamic CEUS patterns, showing a very good correlation with histopathology (Figures 1 and 2). This confirms once more the reliability of this technique in assisting tumor resection. For the semiquantitative description of the lesions which followed the EFSUMB guidelines [18], consider parameters such as timing, degree of contrast enhancement (low, mild, and high) compared to normal brain parenchyma, diffuse or circumscribed appearance, homogeneous versus heterogeneous lesions, presence of cystic/necrotic areas, the pattern of CE, the timing of the different phases of CE, and microbubbles transit time within the tumor. Also, the arterial supply and the venous drainage were described when identified.

Of course CEUS cannot be considered as an alternative to histological examination, which remains the gold standard for diagnosis. Nevertheless, some of our cases considered on preoperative MRI as being low-grade gliomas were later histologically evaluated as anaplastic tumors. In these cases we intraoperatively observed some areas of focal CEUS enhancement. Therefore this technique can be helpful in guiding the surgeon through the choice of the areas for biopsy, thus possibly improving the accuracy of the final histological diagnosis.

Another original aspect of our study is the unprecedented opportunity to conduct tumor resection under direct visualization and to highlight tumor boundaries and tumor remnants with CEUS during and after tumor resection. Performing CEUS prior to glioma resection will help differentiate tumor/edematous brain interface in HGG, and, as mentioned above, it will be able to show anaplastic areas within otherwise low-grade lesions (Figure 4).

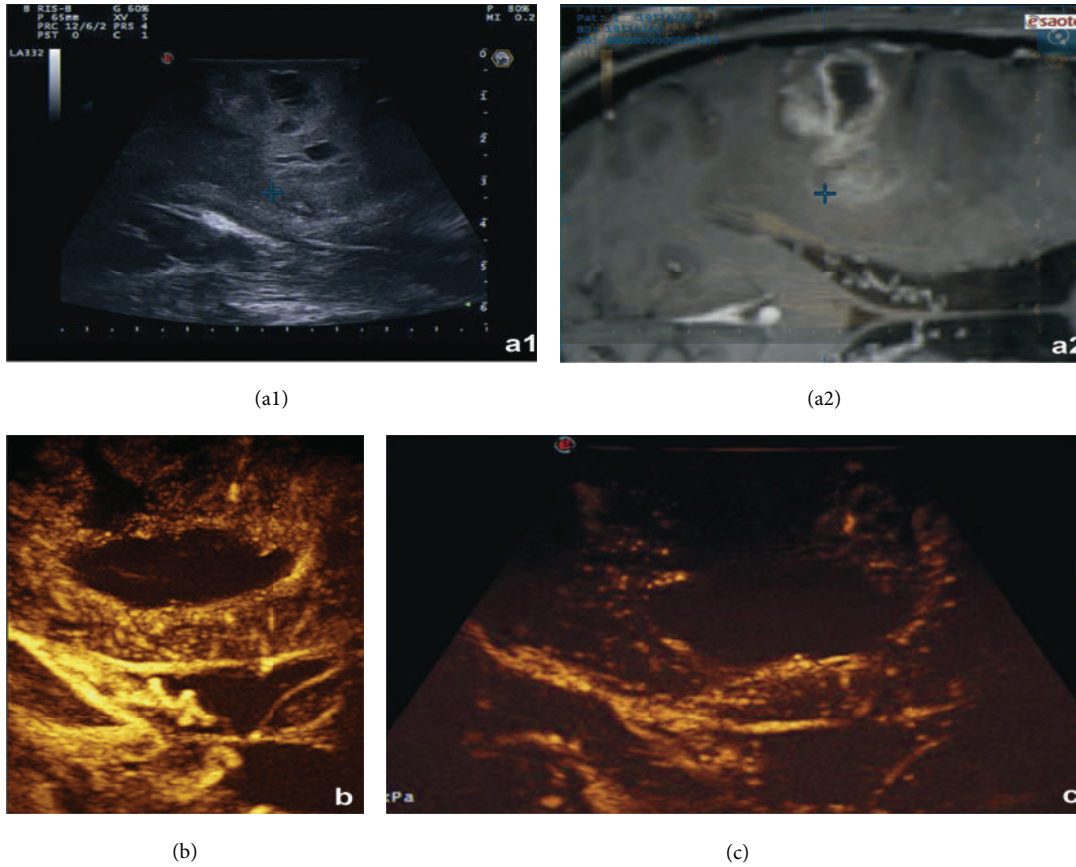

Figure 4: Intraoperative control of a right frontal GBM, using fusion imaging between intraoperative US (a1) and preoperative MRI (a2) linked via a navigated US probe with a virtual navigation system: (a1) shows a hyperechoic superficial lesion, with ill-defined borders and microcystic areas and in (a2) the corresponding MRI imaging is displayed. In panel (b) the B-mode imaging is enhanced with a contrast agent, showing a superficial nodular enhancement with a deeper ring enhancement delimitating a nonperfused necrotic central area. Medullary draining veins are also visible, draining towards the ependymal zone. In panel (c) the postresection control with CEUS shows the absence of the nodular ring enhancement, without contrast enhancement along the wall of the surgical cavity.

After tumor removal in 9 GBMs we performed CEUS in order to highlight tumor remnants, thus possibly maximizing resection. In 3 cases we visualized CE areas which led to further tissue removal, whereas in the other 6 cases CE was not detected. Among the latter cases we also observed, in 2 cases, hyperechogenic areas in B-mode, suggestive for tumor residual which did not show any clear enhancement after contrast injection: in these cases the surgeon is facing one of the following possible situations. Either the area identified is a parenchymal contusion, which is hyperechoic due to the presence of blood cloth and this can be better discerned by visual inspection, or the hyperechoic area might represent a devascularized tumoral area: in fact, one should always keep in mind that microbubble contrast agents are confined to the intravascular compartment, unlike those used for CT or MRI enhancing, which mainly diffuse in the interstitial space. Therefore the closure of a tumor feeding artery leads to a noncontrasted area even when tumor is present. For the same reason, tumors with a greater degree of vascularization (i.e., GBMs) will be more clearly distinguishable from the surrounding healthy parenchyma, presenting with more defined borders as compared to less vascularized ones.

The capacity of CEUS to almost invariably visualize, in higher grades, feeding arteries and venous drainage is helpful for the intraoperative management of the surgical strategy, for example, by discerning whether a vessel is an actual tumor feeder, being as such safely subject to closure by cauterization, or is a vessel which is just passing through the tumor, heading to a portion of healthy parenchyma. Of course an early identification of a true feeder helps in controlling any major bleeding and in keeping the operatory field clean, while recognizing and preserving a vessel which is not strictly related to the tumor can prevent unexpected complications.

In the literature few studies using bedside transcranial US have been performed to evaluate the role of iCEUS in depicting cerebral tumors [29–31]. Harrer et al. used bedside transcranial CEUS prior to surgery and had been capable of discriminating brain lesions from the brain parenchyma and of partially describing them. Vicenzini et al. performed time intensity/curves using dedicated software: indeed time-intensity curves should be performed on a large sample size in order to provide statistically relevant results [28]. However tumor visualization was somehow poor due to transcranial US performed through a temporal window:

despite being a well-established technique it suffers from limitations to tumor visualization due to the presence of the cranial vault in terms of both spatial resolution and tumor location. Intraoperative iCEUS permitting direct tumor visualization during surgery for brain tumor removal has been described only a few times [25–27]. Kanno and colleagues in 2005 evaluated that 40 brain tumors did not perform a continuous imaging because they used a first generation contrast agent. Engelhardt and colleagues in 2008 performed iCEUS during brain tumor removal, using a second generation contrast agent with specific algorithm on a very small and homogeneous cohort of patients (7 GBM patients). They also performed an offline analysis with time-intensity curves. He and colleagues evaluated 29 brain tumors using iCEUS but with some technical limitations: they used a phased array probe, with low frequency and a vast view-field, and the US imaging was performed in power Doppler modality instead of using a contrast specific algorithm, dramatically reducing both US spatial resolution and definition.

Of course, further studies are needed in order to assess CEUS role in tumor resection; the potentiality of this technique to maximize tumor resection has yet to be investigated and demonstrated. Comparison with other imaging modalities (such as MRI imaging T1 weighted GD) will be necessary for defining further advantages or limitations of this technique when compared with other imaging standards in actual practice. Moreover, further studies aimed at quantitative data analysis are mandatory for a rigorous validation of the method: these results will further improve CEUS characterization of cerebral gliomas and will also enhance knowledge of tumor biology, possibly leading to prediction of the responsiveness to therapy of a specific individual tumor, or to orientation during the choice of the best therapeutic option [32, 33].

In fact, one major limitation of this study is related to the semiquantitative nature of the analysis that has been performed on the data obtained by CEUS. Nondestructive US scanning, with specific algorithm performed with low acoustic power and sulfur hexafluoride, filled microbubble contrast agents, opens up to quantitative data analysis with dedicated software leading to real-time assessment and quantification of tumor contrast enhancement with microbubbles, measurement of organ transit time after microbubble injection, and analysis of tissue perfusion. Tissue perfusion may be quantified also by further evaluating the replenishment kinetics of the volume of microbubbles after their destruction in the imaged slice (using high mechanical index US), obtaining quantitative parameters related to local tissue perfusion [15, 19]. However, we believe that the first step, as already performed for other organs and in our previous study [34], is the qualitative and semiquantitative analysis; time-intensity curves providing quantitative data require very large cohorts of patients in order to achieve a statistical relevance, so we feel that a quantitative analysis would be of little value in this study [28, 29, 32, 33].

Finally, another limitation related to the technique might be that CEUS, as any method based on ultrasound imaging, is dependent on the experience of the examiner [35]. Moreover, in the neurosurgical community, few surgeons are accustomed to and specifically trained in the use of ultrasounds, and this is especially true for CEUS, since its use in neurosurgery is relatively new. Therefore, for a correct image interpretation a period of specific training is required.

5. Conclusions

In this paper we establish for the first time a CEUS characterization of cerebral gliomas.

By defining the paradigm of CEUS enhancement in gliomas, we add valuable biological information such as vascularization, microcirculation, and tissue perfusion dynamic and add these pieces of information to those obtained with standard B-mode imaging and might corroborate histological diagnosis.

Performing CEUS during glioma removal can be helpful for the surgeon to differentiate between tumor and edematous brain in HGG, while it will show anaplastic areas within otherwise considered low-grade lesions. After gross tumor removal CEUS might also be used in the future to highlight tumor remnants, thus maximizing resection avoiding neurological sequelae due to damaged healthy brain tissue. This may lead to reduction of hospitalization time and ameliorating prognosis, improving free survival rates and ameliorating the quality of life in glioma patients.

CEUS can be a fast, safe, dynamic, feasible and repeatable, relatively economic, precise, and accurate tool that helps in differentiating malignant and benign lesions and in maximizing tumor resection, thus improving free survival rates in glioma patients; we believe that CEUS is definitely a methodology to further understand and develop in glioma surgery and the expected results will certainly integrate scientific excellence possibly leading to better treatment for cerebral tumors bearing patients.

Abbreviations

CEUS: Contrast enhanced ultrasound
US: Ultrasound
CE: Contrast enhancement
MRI: Magnetic resonance imaging
WHO: World Health Organization
HGG: High grade glioma
LGG: Low grade glioma
GBM: Glioblastoma (WHO grade IV)
ANA: Anaplastic astrocytoma (WHO grade III)
ASTRO: Astrocytoma (WHO grade II)
OLIGO: Oligodendroglioma (WHO grade II)
UCA: Ultrasound contrast agent.

Conflict of Interests

The authors declare that they have no conflict of interests regarding the publication of this paper.

References

[1] P. W. A. Willems, M. J. B. Taphoorn, H. Burger, J. W. B. van der Sprenkel, and C. A. F. Tulleken, "Effectiveness of neuronavigation in resecting solitary intracerebral contrast-enhancing tumors: a randomized controlled trial," *Journal of Neurosurgery*, vol. 104, no. 3, pp. 360–368, 2006.

[2] H. Busse, A. Schmitgen, C. Trantakis, R. Schober, T. Kahn, and M. Moche, "Advanced approach for intraoperative MRI guidance and potential benefit for neurosurgical applications," *Journal of Magnetic Resonance Imaging*, vol. 24, no. 1, pp. 140–151, 2006.

[3] F. Lindseth, J. H. Kaspersen, S. Ommedal et al., "Multimodal image fusion in ultrasound-based neuronavigation: improving overview and interpretation by integrating preoperative MRI with intraoperative 3D ultrasound," *Computer Aided Surgery*, vol. 8, no. 2, pp. 49–69, 2003.

[4] W. Stummer, A. Novotny, H. Stepp, C. Goetz, K. Bise, and H. J. Reulen, "Fluorescence-guided resection of glioblastoma multiforme by using 5-aminolevulinic acid-induced porphyrins: a prospective study in 52 consecutive patients," *Journal of Neurosurgery*, vol. 93, no. 6, pp. 1003–1013, 2000.

[5] J. Sosna, M. M. Barth, J. B. Kruskal, and R. A. Kane, "Intraoperative sonography for neurosurgery," *Journal of Ultrasound in Medicine*, vol. 24, no. 12, pp. 1671–1682, 2005.

[6] G. Unsgaard, A. Gronningsaeter, S. Ommedal, and T. A. Nagelhus Hernes, "Brain operations guided by real-time two-dimensional ultrasound: new possibilities as a result of improved image quality," *Neurosurgery*, vol. 51, no. 2, pp. 402–412, 2002.

[7] T. Selbekk, A. S. Jakola, O. Solheim et al., "Ultrasound imaging in neurosurgery: approaches to minimize surgically induced image artefacts for improved resection control," *Acta Neurochirurgica*, vol. 155, no. 6, pp. 973–980, 2013.

[8] M. Woydt, A. Krone, G. Becker, K. Schmidt, W. Roggendorf, and K. Roosen, "Correlation of intra-operative ultrasound with histopathologic findings after tumour resection in supratentorial gliomas. A method to improve gross total tumour resection," *Acta Neurochirurgica*, vol. 138, no. 12, pp. 1391–1398, 1996.

[9] M. Woydt, G. H. Vince, J. Krauss, A. Krone, N. Soerensen, and K. Roosen, "New ultrasound techniques and their application in neurosurgical intra-operative sonography," *Neurological Research*, vol. 23, no. 7, pp. 697–705, 2001.

[10] F. Lindseth, L. Lovstakken, O. M. Rygh, G. A. Tangen, H. Torp, and G. Unsgaard, "Blood flow imaging: an angle-independent ultrasound modality for intraoperative assessment of flow dynamics in neurovascular surgery," *Neurosurgery*, vol. 65, no. 6, supplement, pp. 149–157, 2009.

[11] S. Mirzai and M. Samii, "Current status and future challenges in cerebral blood flow mapping in intracranial tumors," *Keio Journal of Medicine*, vol. 49, supplement 1, pp. A16–A24, 2000.

[12] G. Becker, J. Perez, A. Krone et al., "Transcranial color-coded real-time sonography in the evaluation of intracranial neoplasms and arteriovenous malformations," *Neurosurgery*, vol. 31, no. 3, pp. 420–428, 1992.

[13] J. Wang, X. Liu, W. H. Hou et al., "The relationship between intra-operative ultrasonography and pathological grade in cerebral glioma," *Journal of International Medical Research*, vol. 36, no. 6, pp. 1426–1434, 2008.

[14] J. M. Correas, L. Bridal, A. Lesavre, A. Méjean, M. Claudon, and O. Hélénon, "Ultrasound contrast agents: properties, principles of action, tolerance, and artifacts," *European Radiology*, vol. 11, no. 8, pp. 1316–1328, 2001.

[15] E. Quaia, "Assessment of tissue perfusion by contrast-enhanced ultrasound," *European Radiology*, vol. 21, no. 3, pp. 604–615, 2011.

[16] A. Martegani, L. Aiani, and C. Borghi, "The use of contrast-enhanced ultrasound in large vessels," *European Radiology*, vol. 14, supplement 8, pp. P73–P86, 2004.

[17] P. S. Sidhu, B. I. Choi, and M. B. Nielsen, "The EFSUMB guidelines on the non-hepatic clinical applications of contrast enhanced ultrasound (CEUS): a new dawn for the escalating use of this ubiquitous technique," *Ultraschall in der Medizin*, vol. 33, no. 1, pp. 5–7, 2012.

[18] F. Piscaglia, C. Nolsøe, C. F. Dietrich et al., "The EFSUMB guidelines and recommendations on the clinical practice of contrast enhanced ultrasound (CEUS): update 2011 on non-hepatic applications," *Ultraschall in der Medizin*, vol. 33, no. 1, pp. 33–59, 2012.

[19] E. Quaia, F. Calliada, M. Bertolotto et al., "Characterization of focal liver lesions with contrast-specific US modes and a sulfur hexafluoride-filled microbubble contrast agent: diagnostic performance and confidence," *Radiology*, vol. 232, no. 2, pp. 420–430, 2004.

[20] E. Quaia, "The real capabilities of contrast-enhanced ultrasound in the characterization of solid focal liver lesions," *European Radiology*, vol. 21, no. 3, pp. 457–462, 2011.

[21] M. Claudon, D. Cosgrove, T. Albrecht et al., "Guidelines and good clinical practice recommendations for contrast enhanced ultrasound (CEUS)—update 2008," *Ultraschall in der Medizin*, vol. 29, no. 1, pp. 28–44, 2008.

[22] G. Mostbeck, ""Hot topics" in contrast-enhanced ultrasound (CEUS)—introduction," *Ultraschall in der Medizin*, vol. 33, supplement 1, pp. S1–S2, 2012.

[23] V. Gibbs, D. Cole, and A. Sassano, *Ultrasound Physics and Technology*, Elsevier Health Sciences, 2009.

[24] F. Piscaglia, L. Bolondi, and Italian Society for Ultrasound in Medicine and Biology (SIUMB) Study Group on Ultrasound Contrast Agents, "The safety of Sonovue in abdominal applications: retrospective analysis of 23188 investigations," *Ultrasound in Medicine and Biology*, vol. 32, no. 9, pp. 1369–1375, 2006.

[25] H. Kanno, Y. Ozawa, K. Sakata et al., "Intraoperative power Doppler ultrasonography with a contrast-enhancing agent for intracranial tumors," *Journal of Neurosurgery*, vol. 102, no. 2, pp. 295–301, 2005.

[26] M. Engelhardt, C. Hansen, J. Eyding et al., "Feasibility of contrast-enhanced sonography during resection of cerebral tumours: initial results of a prospective study," *Ultrasound in Medicine and Biology*, vol. 33, no. 4, pp. 571–575, 2007.

[27] W. He, X.-Q. Jiang, S. Wang et al., "Intraoperative contrast-enhanced ultrasound for brain tumors," *Clinical Imaging*, vol. 32, no. 6, pp. 419–424, 2008.

[28] F. Giangregorio, A. Bertone, L. Fanigliulo et al., "Predictive value of time-intensity curves obtained with contrast-enhanced ultrasonography (CEUS) in the follow-up of 30 patients with Crohn's disease," *Journal of Ultrasound*, vol. 12, no. 4, pp. 151–159, 2009.

[29] E. Vicenzini, R. Delfini, F. Magri et al., "Semiquantitative human cerebral perfusion assessment with ultrasound in brain space-occupying lesions: preliminary data," *Journal of Ultrasound in Medicine*, vol. 27, no. 5, pp. 685–692, 2008.

[30] J. U. Harrer, W. Möller-Hartmann, M. F. Oertel, and C. Klötzsch, "Perfusion imaging of high-grade gliomas: a comparison between contrast harmonic and magnetic resonance imaging," *Journal of Neurosurgery*, vol. 101, no. 4, pp. 700–703, 2004.

[31] U. Bogdahn, T. Fröhlich, G. Becker et al., "Vascularization of primary central nervous system tumors: detection with contrast-enhanced transcranial color-coded real-time sonography," *Radiology*, vol. 192, no. 1, pp. 141–148, 1994.

[32] L. Chami, N. Lassau, M. Chebil, and C. Robert, "Imaging of melanoma: usefulness of ultrasonography before and after contrast injection for diagnosis and early evaluation of treatment," *Clinical, Cosmetic and Investigational Dermatology*, vol. 4, pp. 1–6, 2011.

[33] F. Knieling, M. J. Waldner, R. S. Goertz et al., "Early response to anti-tumoral treatment in hepatocellular carcinoma—can quantitative contrast-enhanced ultrasound predict outcome?" *Ultraschall in der Medizin*, vol. 34, no. 1, pp. 38–46, 2013.

[34] F. Prada, A. Perin, A. Martegani et al., "Intraoperative contrast enhanced ultra-sound (iCEUS) for brain surgery," *Neurosurgery*, vol. 74, no. 5, pp. 542–552, 2014.

[35] E. Quaia, V. Alaimo, E. Baratella et al., "Effect of observer experience in the differentiation between benign and malignant liver tumors after ultrasound contrast agent injection," *Journal of Ultrasound in Medicine*, vol. 29, no. 1, pp. 25–36, 2010.

Hindawi Publishing Corporation
BioMed Research International
Volume 2014, Article ID 393174, 8 pages
http://dx.doi.org/10.1155/2014/393174

Research Article

Progesterone Induces the Growth and Infiltration of Human Astrocytoma Cells Implanted in the Cerebral Cortex of the Rat

Liliana Germán-Castelán,[1] Joaquín Manjarrez-Marmolejo,[2] Aliesha González-Arenas,[1] María Genoveva González-Morán,[3] and Ignacio Camacho-Arroyo[1]

[1] *Facultad de Química, Departamento de Biología, Universidad Nacional Autónoma de México, Ciudad Universitaria, Coyoacán, 04510 Ciudad de México, DF, Mexico*
[2] *Laboratorio de Fisiología de la Formación Reticular, Unidad de Investigaciones Cerebrales, Instituto Nacional de Neurología y Neurocirugía MVS, 14269 Ciudad de México, DF, Mexico*
[3] *Facultad de Ciencias, Laboratorio de Biología de la Reproducción animal, Departamento de Biología Comparada, Universidad Nacional Autónoma de México, Ciudad Universitaria, Coyoacán, 04510 Ciudad de México, DF, Mexico*

Correspondence should be addressed to Ignacio Camacho-Arroyo; camachoarroyo@gmail.com

Received 11 February 2014; Accepted 7 May 2014; Published 22 May 2014

Academic Editor: Betty Tyler

Progesterone (P_4) promotes cell proliferation in several types of cancer, including brain tumors such as astrocytomas, the most common and aggressive primary intracerebral neoplasm in humans. In this work, we studied the effects of P_4 and its intracellular receptor antagonist, RU486, on growth and infiltration of U373 cells derived from a human astrocytoma grade III, implanted in the motor cortex of adult male rats, using two treatment schemes. In the first one, fifteen days after cells implantation, rats were daily subcutaneously treated with vehicle (propylene glycol, 160 μL), P_4 (1 mg), RU486 (5 mg), or P_4 + RU486 (1 mg and 5 mg, resp.) for 21 days. In the second one, treatments started 8 weeks after cells implantation and lasted for 14 days. In both schemes we found that P_4 significantly increased the tumor area as compared with the rest of the treatments, whereas RU486 blocked P_4 effects. All rats treated with P_4 showed tumor infiltration, while 28.6% and 42.9% of the animals treated with RU486 and P_4 + RU486, respectively, presented it. Our data suggest that P_4 promotes growth and migration of human astrocytoma cells implanted in the motor cortex of the rat through the interaction with its intracellular receptor.

1. Introduction

Astrocytomas are the most common and aggressive primary intracerebral tumors. They arise from astrocytes, glial progenitor cells, or cancer stem cells [1–5] and they are classified by the World Health Organization (WHO) in four grades (I–IV) according to their histological characteristics such as mitotic activity, nuclear atypia, cellularity, vascularity, and necrosis [6–8]. Anaplastic astrocytoma (WHO grade III) and glioblastoma (WHO grade IV) are the most frequent and malignant brain tumors in world population. They are characterized by high mitotic activity, nuclear atypia, and infiltrative lesions [9], and prognosis depends on multiple factors such as size, localization, and evolution time; however, generally, the survival of patients is very brief (24–36 months in anaplastic astrocytoma and less than 12 months in glioblastoma [10, 11]). Current medical treatments such as neurosurgery, radiotherapy, and chemotherapy achieve only a modest improvement in the length of survival and quality of life of patients [12–14].

Progesterone (P_4) is a steroid hormone derived from cholesterol that regulates several functions such as sexual behavior, pregnancy, and neuroprotection, and it has also been related to cancer progression [15–17]. P_4 exerts many of its effects through the interaction with its intracellular receptor (PR) which is a ligand-activated transcription factor [18, 19]. It has been reported that PR expression directly correlates with astrocytomas evolution grade, suggesting that PR-positive tumors present a high proliferative potential [20, 21].

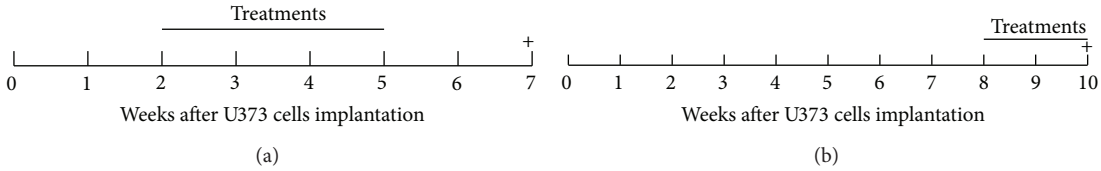

Figure 1: Scheme of treatments administered to the rats implanted with U373 cells in the motor cortex. (a) Short progression. (b) Long progression. + indicates the euthanasia.

It has been demonstrated that P_4 promotes astrocytomas growth [22–25] and that the administration of RU486 (PR antagonist) blocks P_4 effects [23, 26–28]. It has also been reported that RU486 improves the efficacy of chemoradiotherapy in glioblastoma xenografts in mice [29]. Previous studies about the role of P_4 in astrocytoma cell lines proliferation *in vitro* have shown that P_4 increases cell growth, as well as the expression of genes involved in cell cycle progression and metastasis such as cyclin D1, EGFR, and VEGF [30]; however, no *in vivo* studies have been performed. In this work, we studied the effects of P_4 on tumor progression of U373 cells derived from a human astrocytoma grade III implanted in the motor cortex of the rat.

2. Materials and Methods

2.1. Cell Line and Culture. U373 astrocytoma cell line derived from a human astrocytoma grade III (ATCC, Manassas, VA) was maintained in Dulbecco's modification of Eagle's medium (DMEM) supplemented with 10% fetal bovine serum, 1 mM pyruvate, 2 mM glutamine, and 0.1 mM nonessential amino acids, all from Gibco (Grand Island, NY), at 37°C in a humidified atmosphere with 95% air/5% CO_2. DMEM was changed every 48 hours until reaching 70–80% cellular confluence.

2.2. Implantation of Tumor Cells in the Rat Brain. The Wistar adult male rats (250–300 g) maintained on a 12 : 12 light/dark cycle with food and water ad libitum were intraperitoneally anesthetized with ketamine-xylazine (80/10 mg/kg resp.) and mounted in a stereotaxic apparatus. The head was cleaned and shaved, and the scalp was incised in the anteroposterior direction exposing the skull. Small holes were drilled in the left side of skull and a stainless-steel guide cannula (21-gauge) was inserted at the coordinates: Bregma AP = 1.6; L = 3.0, 2 mm above the injection site (motor cortex) according with the Paxinos and Watson atlas [31]. 120,000 U373 cells in a volume of 2 μL of DMEM were slowly injected during a 2 min period using an injection cannula (25-gauge) inserted into the guide cannula connected through a polyethylene tube. The injection cannula that protruded 2 mm of guide cannula was maintained in the injection site for 5 more minutes after the injection. The hole bone was sealed using bone wax, and rats were given a dose of enrofloxacin (10 mg/kg) during 48 hours. All animal procedures were performed as per the following guidelines: (i) the Neurology and Neurosurgery National Institute's Ethical Code for the care and use of laboratory animals and (ii) Mexican guidelines for the production, care, and use of laboratory animals (NOM-062-ZOO-1999). The animals were maintained in the vivarium conditions until they were used.

2.3. Treatments. Rats were randomly divided into four groups (7 rats/group), and each group was assigned to the following subcutaneous treatments (P_4 and RU486 were dissolved in propylene glycol): vehicle (160 μL of propylene glycol) (Baker Analyzed, Center Valley, PA); 1 mg of P_4 (RBI, Natick, MA); 5 mg of RU486 (SIGMA, St. Louis, MO); or 1 mg of P_4 + 5 mg of RU486. We performed two treatment schemes (Figure 1). In the first one (short progression), steroids were daily administered for 21 days, starting on day 15 after U373 cells implantation, and rats were euthanized 15 days after the last treatment. In the second scheme (long progression), we selected another 4 groups (2 rats/group) divided into the same way as described above, but the treatments started 8 weeks after U373 cells implantation; they lasted 14 days and the rats were euthanized one day after the last treatment.

2.4. Histology. Each rat was perfused with saline followed by 4% paraformaldehyde. Brains were removed and immersed in 4% paraformaldehyde at room temperature for 2 weeks. Afterwards, the brains were stored in sucrose gradient solutions (10%, 20%, and 30%) at room temperature for 24 hours each. Brain sections (10 μm thick) were cut in the coronal plane around the implant site using a cryostat Leica CM1850 (Hesse, Germany). Some sections were stained by the Nissl method and examined in an Olympus Bx43 microscope (Tokyo, Japan).

2.5. Immunofluorescence. Another set of brain sections was blocked in 10% normal goat serum/0.05% Tween-PBS (blocking buffer) 1 hour at room temperature and incubated at 4°C overnight with primary antibodies that identified glioma and proliferating cells, respectively: mouse Anti SOX2 (1 : 50) (sc-365964, Santa Cruz Biotechnology, Dallas, TX) and rabbit Anti-Ki-67 (1 : 400) (Ab9260, Chemicon International, Temecula, CA) in blocking buffer. The antibodies were removed and the sections were washed three times with 0.05% Tween-TBS for 10 minutes and then incubated 1 hour at room temperature with secondary antibodies: Alexa 594 A-21203 (1 : 500) (Life Technologies, Carlsbad, CA) and FITC sc-2078 (1 : 500) (Santa Cruz Biotechnology, Dallas, TX). Nuclei were stained with Hoestch 33342 (Thermo Scientific, Waltham, MA). Sections were covered from light, washed, mounted with Fluoro Care Anti-Fade Mountant (Biocare Medical, Concord, CA), and visualized in an Olympus Bx43

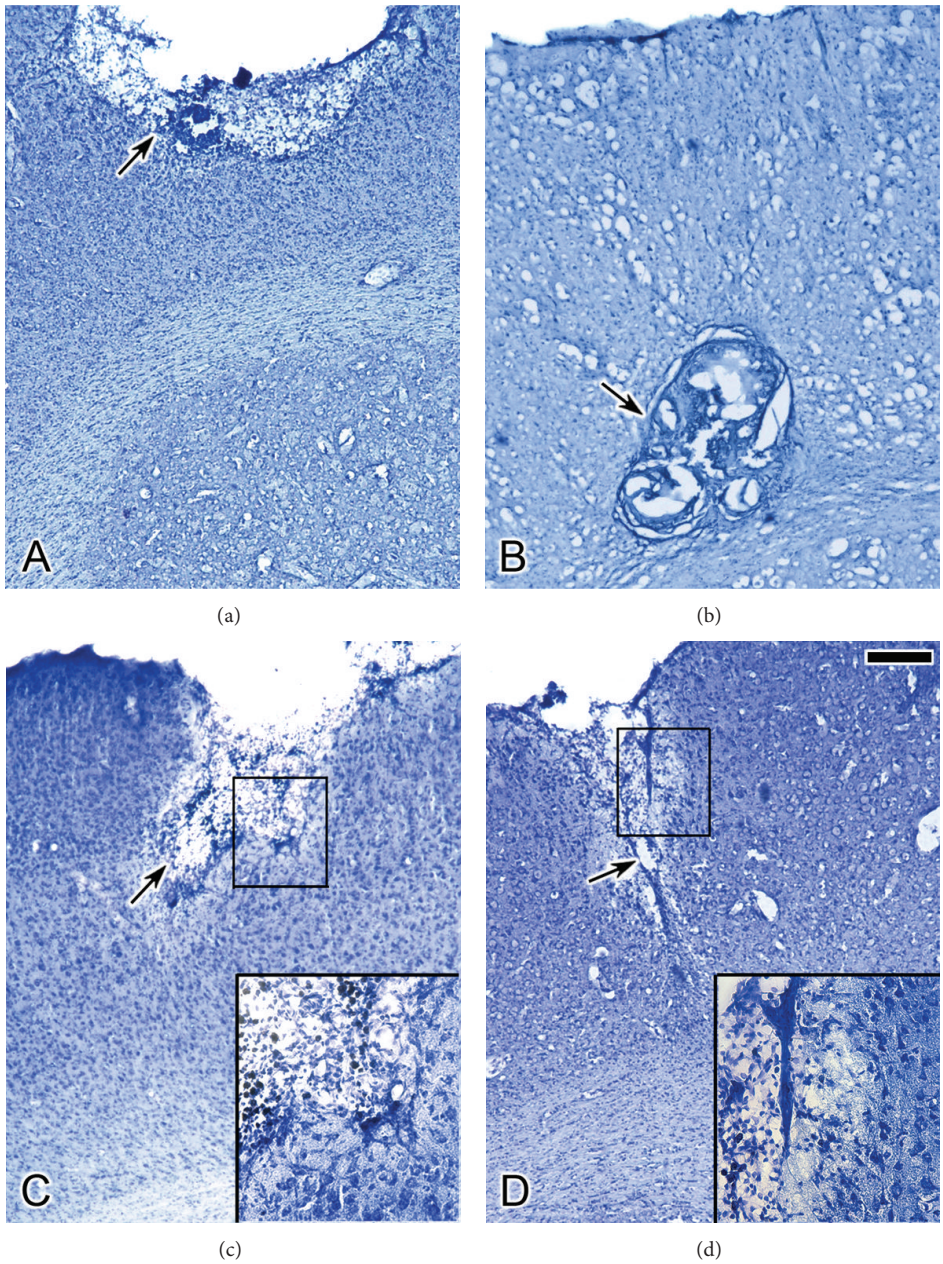

(a) (b)

(c) (d)

Figure 2: Effects of P_4 and RU486 on the growth and infiltration of U373 human astrocytoma cells implanted in the motor cerebral cortex of the rat. Vehicle (propylene glycol) (a); P_4 (b); RU486 (c); P_4 + RU486 (d). Tumor cells are marked with an arrow. Magnification is represented by 200 μm scale in (a)–(d) and by 100 μm scale in the inserts (c)-(d).

fluorescence microscope. The tumor area and its infiltration length were quantified by using the program Image-Pro Plus 7.0 Media Cybernetics (Rockville, MD). The considered tumor area was the largest one of all the sections obtained from each brain, and the infiltration length was measured from the implant site to the longest distance reached by astrocytoma cells.

2.6. Statistical Analysis. Data from tumor area were analyzed by using ANOVA followed by the Bonferroni test for the comparison between groups. Infiltration length data were analyzed by using chi-square test. Prism 5.0 (GraphPad, San Diego, CA) was used for calculating probability values.

3. Results

In this work, we studied the effects of P_4 and RU486 administration on the progression and infiltration of grade III human astrocytoma cells (U373) implanted in the motor cortex of the rat. In the Nissl stained brain sections from the short progression group, we observed that, in rats treated with

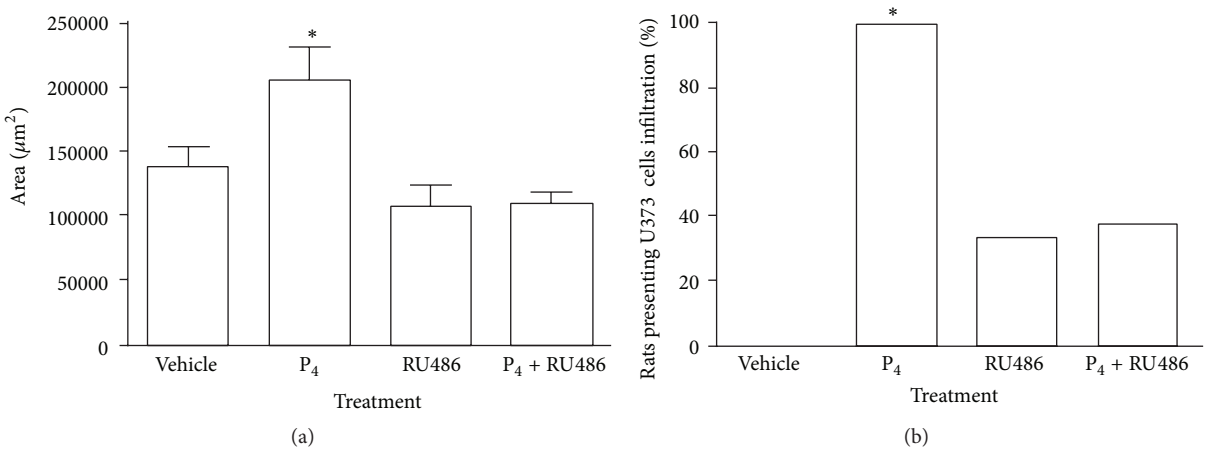

Figure 3: Effects of P_4 and RU486 on the growth and infiltration of U373 cells implanted in the motor cortex of the rat. (a) Tumor area. Data represent mean ± SEM. (b) Percentage of rats with astrocytoma cells infiltration in the brain after treatments. $n = 7$. $^*P < 0.01$ versus all groups.

vehicle, U373 cells stayed around the implantation area. In this group we did not find tumor infiltration (Figure 2(a)). In rats treated with P_4, we observed both significant tumor growth and infiltration to deeper structures of the brain. The average distance covered by U373 cells with this treatment was $1119 \pm 45.6\,\mu$m (mean ± SEM). At the level of the corpus callosum, tissue structure was lost and we could not identify individual tumor cells; only amorphous structures were noticed (Figure 2(b)). Rats treated with RU486 (Figure 2(c)) showed a restricted tumor growth around the implant site with slight infiltration ($82.2 \pm 35.4\,\mu$m). U373 cells were rounded or with elongated edges and they were smaller in comparison with normal astrocytic cells (insert Figure 2(c)). Figure 2(d) shows a representative brain section of a rat treated with P_4 + RU486. U373 cell morphology was diverse, showing variations in size and shape (insert Figure 2(d)). We observed that RU486 blocked P_4 effects on tumor growth and invasion. Tumor infiltration ($121.6 \pm 43.3\,\mu$m) was lower than that found in the rats treated with P_4 and slightly higher (nonsignificant) than in the treatment with RU486.

P_4 significantly increased both the tumor area of implanted U373 cells in the cerebral cortex of the rat (Figure 3(a)) and the infiltration length. Importantly, 100% of the rats treated with P_4 showed cell migration toward deeper structures in the brain, while 28.6% and 42.9% of the animals treated with RU486 and P_4 + RU486, respectively, showed it (Figure 3(b)). Although rats treated with vehicle presented a restricted tumor formation, they did not show tumor infiltration (Figure 3).

In the long progression group, despite the fact that we followed a different treatment scheme, the results of steroid administration were very similar to those of the short progression group (data not shown). Figure 4 shows immunofluorescence staining of SOX2 and Ki-67 markers on brain sections of the long progression group treated with vehicle, P_4, RU486, or P_4 + RU486. As we observed in short progression group with brain sections stained with the Nissl method, in animals treated with vehicle, U373 cells stayed around the implant area, whereas, with P_4 treatment, U373 cells migrated to deeper brain structures. In both treatments, Ki-67 and SOX2 were colocalized in 74% and 63% of the cells, respectively. Interestingly, we found that, in rats treated with RU486, there were just few cells positive to Ki-67 (18%) of the total cells that expressed SOX2, indicating the absence of proliferating glioma cells. Finally, in rats treated with both P_4 and RU486, we noticed a decrease in U373 cells infiltration compared to those treated with P_4, demonstrating that RU486 blocked P_4 effects. With this treatment, Ki-67 and SOX2 presented colocalization in 48% of the cells.

4. Discussion

In the present study, we analyzed the effects of P_4 and its antagonist RU486 on the growth and invasion of U373 cells implanted in the motor cortex of the rat. The increase in tumor growth after P_4 administration observed in our *in vivo* conditions is consistent with the results observed in *in vitro* experiments with U373 cells [23, 26]. Additionally, it has been reported that, in U373 cells, P_4 increases S-phase of the cell cycle [23] which could explain the increase in cell proliferation and therefore in tumor size. We also observed that RU486 blocked P_4 effects, since rats treated with P_4 + RU486 showed a significant decrease in tumor area in comparison with those treated with P_4. These data are also consistent with previous reports in astrocytoma cell cultures [23, 26] and suggest that P_4 effects on astrocytoma cell growth occur via the classic mechanism of action, through an interaction with PR.

P_4 treatment also increased astrocytoma cells migration as well as the number of animals that presented tumor infiltration. These results have not been reported in brain tumors; however, there are studies in breast cancer indicating that P_4 increases migration and invasion in MCF7 and T47D breast cancer cells and that RU486 treatment decreases migration [32]. It has been reported that progestins increase invasiveness in different cell lines of breast cancer. This

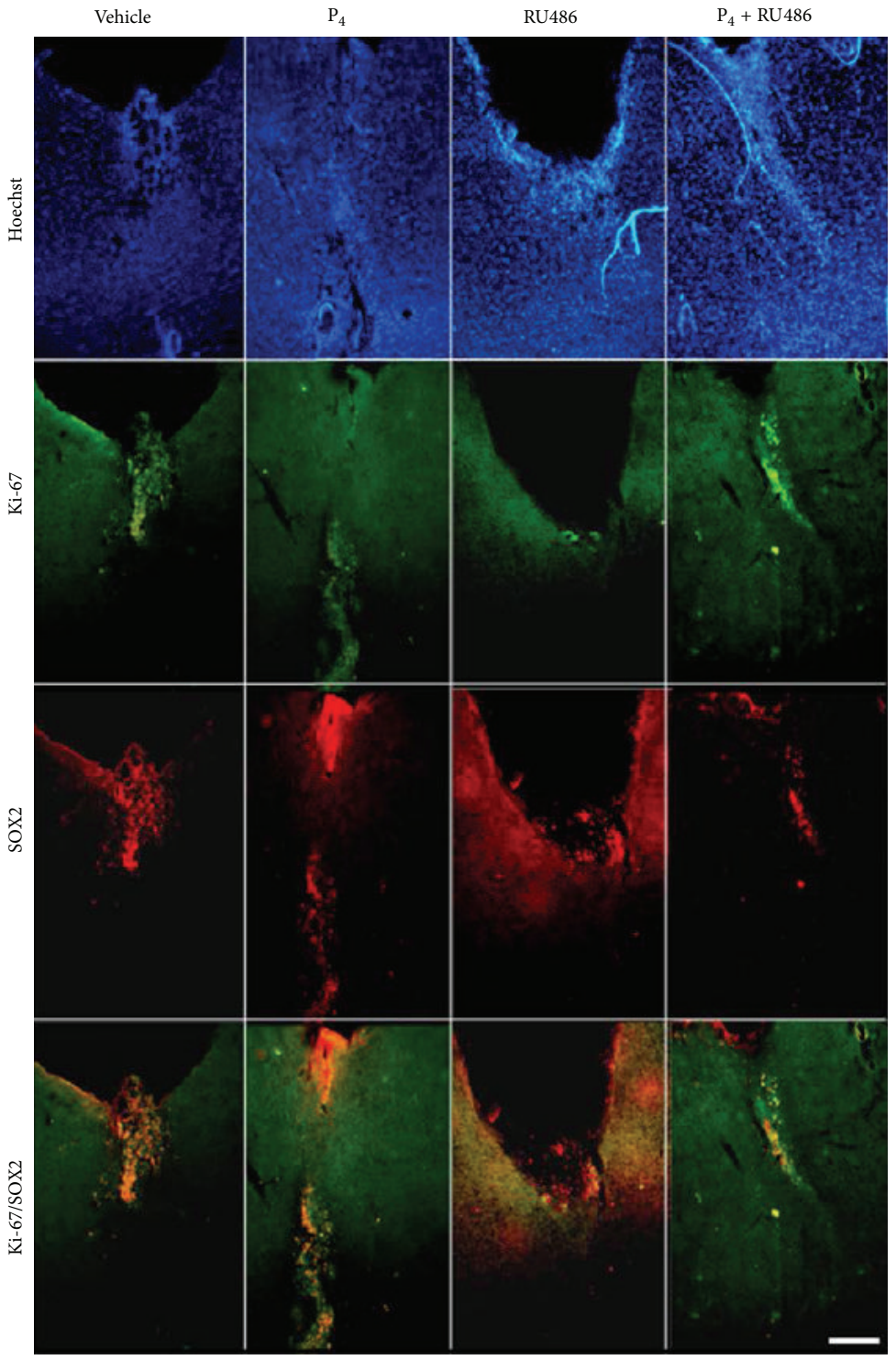

Figure 4: SOX2 and Ki-67 expression in U373 cells implanted in the motor cortex of rats under different treatments: vehicle, P_4, RU486, or P_4 + RU486. Each panel shows nuclei stained with Hoechst in blue, Ki-67 expression in bright green, SOX2 expression in red, and the colocalization of Ki-67 and SOX2 in orange. Magnification is represented by 100 μm scale in all photomicrographs.

effect can occur through various mechanisms, including overexpression of proteins such as superoxide dismutase, tissue factor, and protease-activated receptors [33–35]; the enhancing of matrix metalloproteinases and urokinase-type plasminogen activator activities [36]; the activating of the focal adhesion kinase [37], and the activation of rapid signaling cascades that leads to modifications in the actin cytoskeleton and the cell membrane [38, 39]. In other several cell lines, including glioma cells, it has been found that voltage-gated ion channels play a significant role in initiation

and progression of cancer [40, 41] and even some of them as the potassium voltage-gated channel are regulated by P_4 [42]. In our model, we observed that RU486 blocked P_4 effects on tumor infiltration, suggesting that, as in the case of tumor growth, P_4 effects occur through the interaction with PR; the precise mechanism involved in astrocytoma cells infiltration induced by P_4 needs further investigation. Interestingly, although rats treated with vehicle presented a restricted growth of astrocytoma tumor area, no infiltration was observed in any rat unlike the animals treated with RU486 in which approximately 30% presented it (Figure 3). This may be due to a progestational action of RU486 that depends on the formation of specific RP dimers. Human PR presents two isoforms, PR-A and PR-B (94 and 114 kDa, resp.) with different function, regulation, and expression pattern. At basal state, PR is associated with heat shock proteins (HSP70 and HSP90) and once the hormone enters the cell, it interacts with PR and induces conformational changes that allow the dissociation of the HSP complex followed by phosphorylation and dimerization of the receptor. The active receptor possesses high affinity for specific sequences in the DNA called P_4 response elements (PRE) that are found in the promoter region of P_4 target genes. Once bound to PRE, PR can regulate gene transcription through the recruitment of corregulator proteins and the interaction with the basal transcription machinery [43, 44]. RU486 is a type II antagonist, which promotes PR dimerization and allows binding of the dimers to the PRE. It has been shown that RU486-bound A:A dimers are transcriptionally silent, whereas RU486-bound B:B dimers can activate transcription. RU486-bound A:B dimers act to distinctly inhibit transcriptional activation, and it is the activity that is commonly observed in P_4 responsive cells [45, 46]. It is important to mention that PR-A and PR-B isoforms have been detected in human astrocytoma cell lines and biopsies, and their expression is directly related to the tumor evolution grade. Interestingly, PR-B content is three times higher than PR-A in U373 cells [23, 47] which could lead to an increased formation of B:B dimers and an activation of transcriptional activity upon RU486 treatment. However, the effects of this activation are significantly lower than those observed with P_4 treatment. It has also been reported that, in astrocytoma tumors implanted in the cerebral cortex, the direction of migration is ventral through cortical gray matter and into the corpus callosum [48], which is consistent with our results.

Regarding the observed change in morphology of the implanted astrocytoma cells treated with RU486 (alone or in combination with P_4), it has been reported that its administration induces alterations in the cellular structure of cancer cells of different origins (including glioblastoma cells). Such changes were associated with a redistribution of actin fibers that can form nonadhesive membrane ruffles, leading to a dysregulated cellular adhesion capacity and thereby altering the invasion capacity of these cells [49].

We observed that implanted cells expressed proliferation and glioma cells markers (Ki-67 and SOX2, resp.) and that, in many of them, both markers exhibited colocalization. These results demonstrated that the implanted U373 cells were present in the cerebral tissue of the rat and that they continued their proliferation. We also found that the percentage of Ki-67/SOX2 colocalization was higher in vehicle-treated rats that in those treated with P_4. This could be related to the progression of these tumors induced by P_4 leading to a dedifferentiation process where the resulting cells express less proliferation markers but overexpress invasion and/or migration markers. In the case of RU486 treatment, we observed very few cells positive to Ki-67 while those expressing SOX2 were found in a greater number. This indicates that there were glioma cells but they were not proliferating. It has been reported that RU486 induces G1-S blockage of the cell cycle in human ovarian cancer cells [50] and that RU486 reduces the activity of cdk2, enzyme that is involved in the regulation of the transcription factor E2F1 which modulates S-phase progression [51, 52].

5. Conclusions

P_4 induces proliferation and infiltration of a tumor caused by the implant of human astrocytoma cells in the motor cortex of the rat through the interaction with intracellular PR.

Conflict of Interests

The authors declare that there is no conflict of interests regarding the publication of this paper.

Acknowledgments

This work was supported by Programa de Apoyo a Proyectos de Investigación e Innovación Tecnológica (PAPIIT) IN212611, DGAPA, UNAM, México.

References

[1] D. Friedmann-Morvinski, E. A. Bushong, E. Ke et al., "Dedifferentiation of neurons and astrocytes by oncogenes can induce gliomas in mice," *Science*, vol. 338, pp. 1080–1084, 2012.

[2] S. Alcantara Llaguno, J. Chen, C.-H. Kwon et al., "Malignant astrocytomas originate from neural stem/progenitor cells in a somatic tumor suppressor mouse model," *Cancer Cell*, vol. 15, no. 1, pp. 45–56, 2009.

[3] L. Cheng, S. Bao, and J. N. Rich, "Potential therapeutic implications of cancer stem cells in glioblastoma," *Biochemical Pharmacology*, vol. 80, no. 5, pp. 654–665, 2010.

[4] D. L. Schonberg, D. Lubelski, T. E. Miller, and J. N. Rich, "Brain tumor stem cells: molecular characteristics and their impact on therapy," *Molecular Aspects of Medicine*, 2013.

[5] D. Y. Cho, S. Z. Lin, W. K. Yang et al., "Targeting cancer stem cells for treatment of glioblastoma multiforme," *Cell Transplant*, vol. 22, pp. 731–739, 2013.

[6] D. N. Louis, H. Ohgaki, O. D. Wiestler et al., "The 2007 WHO classification of tumours of the central nervous system," *Acta Neuropathologica*, vol. 114, no. 2, pp. 97–109, 2007.

[7] A. Rousseau, K. Mokhtari, and C. Duyckaerts, "The 2007 WHO classification of tumors of the central nervous system—what has changed?" *Current Opinion in Neurology*, vol. 21, no. 6, pp. 720–727, 2008.

[8] C. Daumas-Duport, B. Scheithauer, J. O'Fallon, and P. Kelly, "Grading of astrocytomas: a simple and reproducible method," *Cancer*, vol. 62, no. 10, pp. 2152–2165, 1988.

[9] T. Tihan and M. M. Bloomer, "Astrocytic neoplasms of the central nervous system and orbit: a morphologic perspective," *Seminars in Diagnostic Pathology*, vol. 27, no. 2, pp. 114–121, 2010.

[10] L. Arko, I. Katsyv, G. E. Park, W. P. Luan, and J. K. Park, "Experimental approaches for the treatment of malignant gliomas," *Pharmacology and Therapeutics*, vol. 128, no. 1, pp. 1–36, 2010.

[11] A. A. Brandes, A. Tosoni, E. Franceschi, M. Reni, G. Gatta, and C. Vecht, "Glioblastoma in adults," *Critical Reviews in Oncology/Hematology*, vol. 67, no. 2, pp. 139–152, 2008.

[12] D. Osoba, M. Brada, W. K. A. Yung, and M. D. Prados, "Health-related quality of life in patients with anaplastic astrocytoma during treatment with temozolomide," *European Journal of Cancer*, vol. 36, no. 14, pp. 1788–1795, 2000.

[13] S. Sahebjam, M. McNamara, and W. P. Mason, "Management of glioblastoma in the elderly," *Clinical Advances in Hematology and Oncology*, vol. 10, pp. 379–386, 2012.

[14] K. Anton, J. M. Baehring, and T. Mayer, "Glioblastoma multiforme: overview of current treatment and future perspectives," *Hematology/Oncology Clinics of North America*, vol. 26, pp. 825–853, 2012.

[15] R. D. Brinton, R. F. Thompson, M. R. Foy et al., "Progesterone receptors: form and function in brain," *Frontiers in Neuroendocrinology*, vol. 29, no. 2, pp. 313–339, 2008.

[16] I. Camacho-Arroyo and J. M. Montor, "Beyond reproductive effects of sex steroids," *Mini Reviews in Medicinal Chemistry*, vol. 12, pp. 1037–1039, 2012.

[17] J. D. Graham and C. L. Clarke, "Physiological action of progesterone in target tissues," *Endocrine Reviews*, vol. 18, pp. 502–519, 1997.

[18] J. E. Levine, P. E. Chappell, J. S. Schneider, N. C. Sleiter, and M. Szabo, "Progesterone receptors as neuroendocrine integrators," *Frontiers in Neuroendocrinology*, vol. 22, no. 2, pp. 69–106, 2001.

[19] M. Schumacher and R. Guennoun, "Progesterone: synthesis, metabolism, mechanisms of action, and effects in the nervous system. An overview," in *Hormones, Brain and Behavior*, D. W. Pfaff, A. P. Arnold, A. M. Etgen, S. E. Fahrbach, and R. T. Rubin, Eds., vol. 3, pp. 1505–1560, 2009.

[20] E. Cabrera-Muñoz, A. González-Arenas, M. Saqui-Salces et al., "Regulation of progesterone receptor isoforms content in human astrocytoma cell lines," *Journal of Steroid Biochemistry and Molecular Biology*, vol. 113, no. 1-2, pp. 80–84, 2009.

[21] H. Khalid, S. Shibata, M. Kishikawa, A. Yasunaga, M. Iseki, and T. Hiura, "Immunohistochemical analysis of progesterone receptor and Ki-67 labeling index in astrocytic tumors," *Cancer*, vol. 80, pp. 2133–2140, 1997.

[22] M. J. Riemenschneider and G. Reifenberger, "Astrocytic tumors," *Recent Results in Cancer Research*, vol. 171, pp. 3–24, 2009.

[23] G. González-Agüero, A. A. Gutiérrez, D. González-Espinosa et al., "Progesterone effects on cell growth of U373 and D54 human astrocytoma cell lines," *Endocrine*, vol. 32, pp. 129–135, 2007.

[24] G. González-Agüero, R. Ondarza, A. Gamboa-Domínguez, M. A. Cerbón, and I. Camacho-Arroyo, "Progesterone receptor isoforms expression pattern in human astrocytomas," *Brain Research Bulletin*, vol. 56, pp. 43–48, 2001.

[25] R. S. Carroll, J. Zhang, K. Dashner, M. Sar, P. M. Black, and C. Raffel, "Steroid hormone receptors in astrocytic neoplasms," *Neurosurgery*, vol. 37, no. 3, pp. 496–504, 1995.

[26] E. Cabrera-Muñoz, O. T. Hernández-Hernández, and I. Camacho-Arroyo, "Role of progesterone in human astrocytomas growth," *Current Topics in Medicinal Chemistry*, vol. 11, pp. 1663–1667, 2011.

[27] R. Ramaswamy, K. Ashton, R. Lea et al., "Study of effectiveness of mifepristone for glioma cell line growth suppression," *British Journal of Neurosurgery*, vol. 26, pp. 336–339, 2012.

[28] J. Pinski, G. Halmos, Y. Shirahige, J. L. Wittliff, and A. V. Schally, "Inhibition of growth of the human malignant glioma cell line (U87MG) by the steroid hormone antagonist RU486," *Journal of Clinical Endocrinology and Metabolism*, vol. 77, no. 5, pp. 1388–1392, 1993.

[29] M. Llaguno-Munive, L. A. Medina, R. Jurado, M. Romero-Piña, and P. Garcia-Lopez, "Mifepristone improves chemo-radiation response in glioblastoma xenografts," *Cancer Cell International*, vol. 13, article 29, 2013.

[30] O. T. Hernández-Hernández, T. K. González-García, and I. Camacho-Arroyo, "Progesterone receptor and SRC-1 participate in the regulation of VEGF, EGFR and Cyclin D1 expression in human astrocytoma cell lines," *The Journal of Steroid Biochemistry and Molecular Biology*, vol. 132, pp. 127–134, 2012.

[31] G. Paxinos and C. Watson, *The Rat Brain in Stereotaxic Coordinates*, Academic Press, New York, NY, USA, 4th edition, 1998.

[32] G. Epstein Shochet, S. Tartakover Matalon, L. Drucker et al., "Hormone-dependent placental manipulation of breast cancer cell migration," *Human Reproduction*, vol. 27, no. 1, pp. 73–88, 2012.

[33] A. K. Holley, K. K. Kiningham, D. R. Spitz, D. P. Edwards, J. T. Jenkins, and M. R. Moore, "Progestin stimulation of manganese superoxide dismutase and invasive properties in T47D human breast cancer cells," *Journal of Steroid Biochemistry and Molecular Biology*, vol. 117, no. 1-3, pp. 23–30, 2009.

[34] S. Kato, M. Pinto, A. Carvajal et al., "Progesterone increases tissue factor gene expression, procoagulant activity, and invasion in the breast cancer cell line ZR-75-1," *Journal of Clinical Endocrinology and Metabolism*, vol. 90, no. 2, pp. 1181–1188, 2005.

[35] J. Diaz, E. Aranda, S. P. Henriquez et al., "Progesterone promotes focal adhesion formation and migration in breast cancer cells through induction of protease-activated receptor 1," *Journal of Endocrinology*, vol. 214, no. 2, pp. 165–175, 2012.

[36] R. P. Carnevale, C. J. Proietti, M. Salatino et al., "Progestin effects on breast cancer cell proliferation, proteases activation, and in vivo development of metastatic phenotype all depend on progesterone receptor capacity to activate cytoplasmic signaling pathways," *Molecular Endocrinology*, vol. 21, no. 6, pp. 1335–1358, 2007.

[37] X.-D. Fu, L. Goglia, A. M. Sanchez et al., "Progesterone receptor enhances breast cancer cell motility and invasion via extranuclear activation of focal adhesion kinase," *Endocrine-Related Cancer*, vol. 17, no. 2, pp. 431–443, 2010.

[38] X.-D. Fu, M. Flamini, A. M. Sanchez et al., "Progestogens regulate endothelial actin cytoskeleton and cell movement via the actin-binding protein moesin," *Molecular Human Reproduction*, vol. 14, no. 4, pp. 225–234, 2008.

[39] X.-D. Fu, M. S. Giretti, L. Goglia et al., "Comparative actions of progesterone, medroxyprogesterone acetate, drospirenone and nestorone on breast cancer cell migration and invasion," *BMC Cancer*, vol. 8, article 166, 2008.

[40] S. P. Fraser, I. Ozerlat-Gunduz, W. J. Brackenbury et al., "Regulation of voltage-gated sodium channel expression in cancer:

hormones, growth factors and auto-regulation," *Philosophical Transactions of the Royal Society of London B: Biological Sciences*, vol. 369, no. 1638, 2014.

[41] S. Wang and B. Jiao, "The inhibition of tamoxifen on sodium channel in SHG-44 glioma cell-line," *Chinese Journal of Applied Physiology*, vol. 25, pp. 207–210, 2009.

[42] A. Ramírez, L. M. Hinojosa, J. D. J. Gonzales et al., "KCNH1 potassium channels are expressed in cervical cytologies from pregnant patients and are regulated by progesterone," *Reproduction*, vol. 146, pp. 615–623, 2013.

[43] B. M. Jacobsen and K. B. Horwitz, "Progesterone receptors, their isoforms and progesterone regulated transcription," *Molecular and Cellular Endocrinology*, vol. 357, no. 1-2, pp. 18–29, 2012.

[44] D. P. Edwards, S. E. Wardell, and V. Boonyaratanakornkit, "Progesterone receptor interacting coregulatory proteins and cross talk with cell signaling pathways," *Journal of Steroid Biochemistry and Molecular Biology*, vol. 83, no. 1–5, pp. 173–186, 2002.

[45] J. Chen, J. Wang, J. Shao, and Y. Gao, "The unique pharmacological characteristics of mifepristone (RU486): from terminating pregnancy to preventing cancer metastasis," *Medicinal Research Reviews*, pp. 1–22, 2014.

[46] C. A. Sartorius, S. D. Groshong, L. A. Miller et al., "New T47D breast cancer cell lines for the independent study of progesterone B- and A-receptors: only antiprogestin-occupied B-receptors are switched to transcriptional agonists by cAMP," *Cancer Research*, vol. 54, no. 14, pp. 3868–3877, 1994.

[47] V. Hansberg-Pastor, A. González-Arenas, M. A. Peña-Ortiz, E. García-Gómez, M. Rodríguez-Dorantes, and I. Camacho-Arroyo, "The role of DNA methylation and histone acetylation in the regulation of progesterone receptor isoforms expression in human astrocytoma cell lines," *Steroids*, vol. 78, no. 5, pp. 500–507, 2013.

[48] E. R. Laws Jr., W. J. Goldberg, and J. J. Bernstein, "Migration of human malignant astrocytoma cells in the mammalian brain: scherer revisited," *International Journal of Developmental Neuroscience*, vol. 11, no. 5, pp. 691–697, 1993.

[49] B. N. Brandhagen, C. R. Tieszen, T. M. Ulmer, M. S. Tracy, A. A. Goyeneche, and C. M. Telleria, "Cytostasis and morphological changes induced by mifepristone in human metastatic cancer cells involve cytoskeletal filamentous actin reorganization and impairment of cell adhesion dynamics," *BMC Cancer*, vol. 13, article 35, 2013.

[50] A. A. Goyeneche, R. W. Carón, and C. M. Telleria, "Mifepristone inhibits ovarian cancer cell growth in vitro and in vivo," *Clinical Cancer Research*, vol. 13, no. 11, pp. 3370–3379, 2007.

[51] C. R. Tieszen, A. A. Goyeneche, B. N. Brandhagen, C. T. Ortbahn, and C. M. Telleria, "Antiprogestin mifepristone inhibits the growth of cancer cells of reproductive and non-reproductive origin regardless of progesterone receptor expression," *BMC Cancer*, vol. 11, article 207, 2011.

[52] E. A. Musgrove, C. S. Lee, A. L. Cornish, A. Swarbrick, and R. L. Sutherland, "Antiprogestin inhibition of cell cycle progression in T-47D breast cancer cells is accompanied by induction of the cyclin-dependent kinase inhibitor p21," *Molecular Endocrinology*, vol. 11, pp. 54–66, 1997.

Hindawi Publishing Corporation
BioMed Research International
Volume 2014, Article ID 207974, 6 pages
http://dx.doi.org/10.1155/2014/207974

Clinical Study

Fluorescence-Guided Surgery and Biopsy in Gliomas with an Exoscope System

José Piquer,[1] Jose L. Llácer,[1] Vicente Rovira,[1] Pedro Riesgo,[1] Ruben Rodriguez,[1] and Antonio Cremades[2]

[1] *Department of Neurosurgery, Hospital de la Ribera, Carretera Corbera km1, 46600 Alzira, Valencia, Spain*
[2] *Department of Pathology, Hospital de la Ribera, Alzira, Spain*

Correspondence should be addressed to José Piquer; jose.piquer@telefonica.net

Received 13 February 2014; Revised 16 April 2014; Accepted 4 May 2014; Published 21 May 2014

Academic Editor: Francesco DiMeco

Background. The introduction of fluorescence-guided resection allows a better identification of tumor tissue and its more radical resection. We describe our experience with a modified exoscope to detect 5 ALA-induced fluorescence in neuronavigation-guided brain surgery or biopsy of malignant brain tumors. *Methods*. Thirty-eight patients with a suspected preoperative diagnosis of high-grade astrocytoma were included. We used a neuronavigation device and a high-definition exoscope system with a built-in filter to detect 5-ALA fluorescence in all cases. Thirty patients underwent craniotomy with tumor resection and 8 underwent frameless stereotactic brain biopsy. *Results*. Histopathological diagnosis confirmed the presence of high-grade gliomas in 34 patients. Total resection was achieved in 23 cases and subtotal in 7. No relevant complications related to the administration of 5-ALA were detected. *Conclusions*. The use of the exoscope in 5-ALA fluorescence-guided tumor surgery has twofold implications: during brain tumor surgery it can be considered a valuable tool to achieve a more radical resection of the lesion, and when applied to a biopsy of a suspected brain high-grade glioma, it decreases the possibility of a negative biopsy.

1. Introduction

High-grade gliomas represent the majority of adult malignant brain tumors and include grade III anaplastic astrocytoma (AA), anaplastic oligodendroglioma (AO), mixed anaplastic oligoastrocytoma (AOA), and grade IV glioblastoma multiforme (GBM) [1]. The best treatment of these tumors is extensive surgical resection, when it is possible, accompanied by chemotherapy and radiotherapy [2–4]. However, there are also cases in which biopsy is the best option [5].

Because of the infiltrative nature of these tumors, complete resection is a complex neurosurgical procedure, regardless of the location of the lesion. Several methods have been introduced to help achieve the maximum cytoreductive treatment. Recent developments, including brain mapping, neuronavigation, intraoperative ultrasound, magnetic resonance imaging, and fluorescence techniques [6, 7], now allow multimodal approaches. Under the suspicious of a high-grade lesion, when a brain biopsy is indicated, the stereotactic frame biopsy is still considered the gold standard technique for its precise localization [8], specially in cases of deep seated tumors. However, technological development in the neurosurgical practice has increased the number of centers in which brain biopsies are usually obtained by frameless magnetic resonance imaging- (MRI-) guided neuronavigation. Either way, the percentage of biopsies with inconclusive pathologic diagnosis varies between 7 and 15% in relation to nontumor or necrotic areas. Thus, even if a pathologist is available to study the sample at the time of the surgery, it is difficult to ensure that it will be useful for diagnosis [9].

It has been described that 5-ALA fluorescence helps to visualize tumor tissue in real-time during surgery, and most of the studies have been performed using fluorescence microscopy [10–13] or, much less frequently, an endoscope [14]. Both neurosurgical microscopes and neuroendoscopes may be modified to detect 5-ALA-induced fluorescence.

This can be achieved by implementing a system to switch between white and blue light and installing an observation filter (440 nm) between the surgical field and microscope/endoscope. This can be done with an exoscope as well, which is a system that consists of a tubular telescope connected to a camera and a high definition monitor.

In this report we describe our experience in the treatment of high-grade gliomas using 5-ALA fluorescence-guided exoscopy, as an alternative or complement to the use of another optical device, in order to obtain the highest level of tumor resection or to confirm the adequacy of the specimen obtained during biopsy procedures.

2. Methods

The present study, approved by the Ethics Committee for Clinical Research of our institution, included 38 patients with preoperative suspicion of brain high-grade astrocytoma in neuroimaging techniques. Thirty patients underwent tumor resection and 8 underwent frameless stereotactic biopsy at the Department of Neurosurgery at Hospital Universitario de la Ribera (Alzira, Spain) between December 2012 and January 2014.

All patients received an oral dose of 20 mgr/Kg of body weight of 5-ALA 5-6 hours prior to the surgical procedure and were submitted to the standard protocols for low exposure to sunlight or artificial light. In all cases, clinical data were collected from electronic and paper medical records, including the suspected clinical diagnosis, the definitive histopathological diagnosis, and any systemic or neurological morbidity (progression of neurological deficit).

2.1. Preoperative Procedures. A brain 1.5-T MRI was performed as conventional preoperative study of the lesion in all cases. For those patients harboring tumors in proximity to eloquent areas (specially primary motor and sensory cortices, and primary language areas), a functional MRI was also performed. A Contrast T1-weighted MRI sequence in combination with a StealthStation Surgical Navigation System (Medtronic, Inc., Minneapolis, MI, USA) was used for preoperative planning and intraoperative neuronavigation of tumor resection or frameless stereotactic biopsy. All lesions were topographically classified according to Shinoda et al. [15]. Neurophysiologic monitoring by transcranial or cortical stimulation for motor-evoked potentials was performed in tumor resection cases in which the tumor was close to primary motor areas, and when necessary, the central groove was located by median nerve somatosensory-evoked potentials.

2.2. Surgical Procedure. When tumor resection was the goal, the routine procedure consisted of a tailored craniotomy according to the location of the lesion, followed with maximal tumor resection by using neuronavigation, 5-ALA fluorescence, and the appropriate fluorescence filter mounted in an exoscopy system. In those areas, where the tumor tissue looked red or pink under fluorescence, resection was carried out by alternating white and blue light in the exoscope. In patients with tumors close to eloquent areas, the resection stopped according to anatomical and neuronavigation limits, together with changes in neurophysiological monitoring indicating that an eloquent area could be compromised, even though remaining of some fluorescence tumor tissue was encountered. But in those with tumors not related to a particular eloquent area, the resection stopped when 5-ALA fluorescence was not visible, in conjunction to neuronavigation guidance of tumor limits. During surgery, several samples exhibiting different fluorescence intensities were obtained for tissue analysis. Fluorescence intensity was subjectively graded during surgery by both the surgeon and the assistant using a scale from 1 to 5 (5 being the highest intensity). In order to assess the extent of the resection, postoperative control MRI was performed in all craniotomy cases within the first 72 hours after surgery. Complete resection was considered when no enhancement was seen at the tumor cavity on T1-weighted imaging.

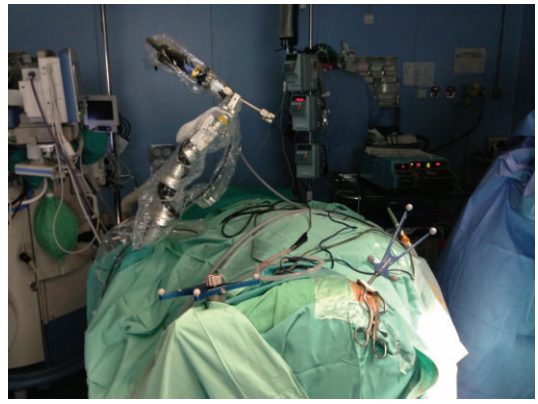

Figure 1: View of high-definition exoscope-assisted system in neuronavigation-guided biopsy.

In frameless stereotactic biopsy cases we used the Navigus System (Medtronic), in combination with 5-ALA fluorescence and the exoscopy system. The biopsy was performed under general anesthesia and with the head fixed with the three-point Mayfield device. Automatic burr-hole insertion of 11 mm diameter was performed in the selected entry area, and, after assembling the biopsy system, a referenced needle of 1.2 mm diameter was introduced to reach the target. From 5 to 7 tumor samples of 1 to 2 mm size were obtained from each of the patients; the presence or absence of fluorescence was observed, and the samples were sent to histopathological examination.

2.3. Exoscope Description. For fluorescence detection, a high-definition exoscope system (HD-Xoscope, HDXO-SCOPE, Karl Storz Endoscopy, Tuttlingen, Germany) was used, including a specially developed autoclavable rigid lens telescope and a fiber optic light source channel (Figure 1). This system implements a 5-ALA filter blocking the excitation light while the fluorescence signal from the 5-ALA (380–450 nm) could pass through, along with normal white light. Upon excitation with blue light (lambda = 400–410 nm),

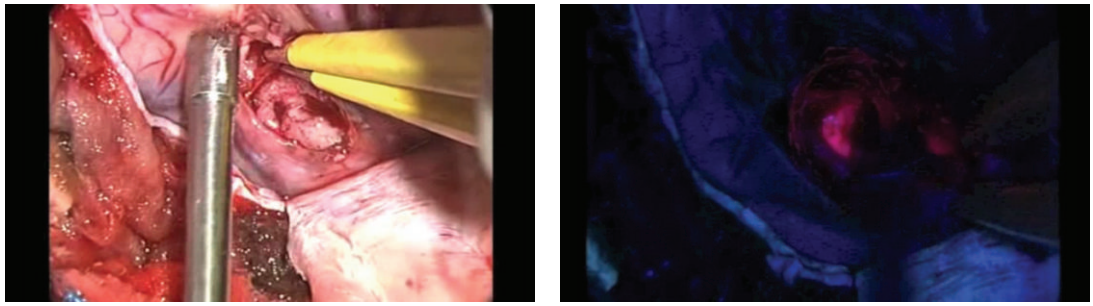

(a) (b)

Figure 2: Glioblastoma multiforme surgical view. (a) Tumor and infiltration area without fluorescence. (b) Tumor and infiltration area under 5-ALA fluorescence.

protoporphyrin IX, the 5-ALA metabolite accumulated in tumor cells, is strongly fluorescent (peak kappa = 635 nm) and can be viewed in a specifically prepared neurosurgical optical system. Fluorescence emission may be classified as intense (solid) red fluorescence, corresponding to tumor tissue, or appear blue in the case of normal tissue not accumulating protoporphyrin IX, which reflects blue-violet light. The telescope is held in position by a pneumatic endoscope holder and the system is complemented with a 3-chip sterilizable high-definition digital camera, with optical zoom and focus features, and a video display with a medical grade 23" high-definition video monitor.

3. Results

The age of patients who underwent craniotomy (Table 1) was between 21 and 78 years with a mean age of 52 years. Eleven patients were women and 19 were men. The age range in patients who underwent biopsy (Table 2) was between 44 and 76 years with a mean age of 62.6 years. Four of these patients were men and 4 women.

In the craniotomy group, MRI evaluation indicated that total resection was achieved in 23 cases and subtotal resection in 7 patients. Progression of hemiparesis was observed in three patients after surgery, with subsequent partial recovery in two of them and transient dysphasia in one patient. Perioperative mortality occurred in a 79-year-old patient due to liver failure. In the biopsy group, no complications were seen. Minor adverse events related to the administration of 5-ALA were observed: a slight increase in serum GGT in one case and thrombocytopenia in two cases. However, no serious complications were registered in any of the groups.

Histopathological results in the craniotomy group reported three patients with metastases and 27 with high-grade gliomas: 23 with glioblastoma multiforme and two with oligodendroglioma and anaplastic astrocytoma in the remaining two of them. The mean fluorescence intensity, according to the subjective assessment of the surgeon and the assistant on a 1–5 scale, was 3.9 in the GBM group (IQR = 3.5–4.5), 3 (IQR = 2.5–3.5) in the cases of anaplastic astrocytoma, and 4 (IQR = 3.5–4.5) for the oligodendrogliomas. Of the three metastases, one showed a level 4 of fluorescence. On the other hand, histopathological results in the biopsy group revealed Glioblastoma Multiforme in 6 cases, one case with a central nervous system lymphoma and another one with an anaplastic astrocytoma. In this group, 5 to 7 samples were taken from each patient, with clear variations in the fluorescence intensity in relation to the tissue area obtained (either tumor cells or necrosis or peritumoral area). The intraoperative biopsy showed no fluorescence at all in the patient with central nervous system lymphoma.

When analyzing the tissue samples of both groups the most fluorescent areas observed intraoperatively corresponded to tumor, according to the histological results. Thus, when positive fluorescence was observed at the surgical site or in the frameless biopsy sample, the existence of tumor was confirmed in all cases (100%). The first 14 surgeries were performed without the 5-ALA filter blocked to the exoscope. In five of the craniotomy rest cases and in three biopsy cases, operated with the 5-ALA blocked filter, the histological findings of presence or absence of tumor with the presence or absence of fluorescence (red or blue) is correlated. Tumor tissue or infiltration areas were easily identified by their bright red or pink color, while nontumor area reflected the blue light. In those patients where no fluorescence was observed (blue), the absence of tumor was confirmed in 62% of them (5 patients); necrosis was observed in other two, and only in one (12%) was the existence of brain tissue with a small infiltrative tumor area revealed. Although the sample is very small, this would result in a sensitivity of 73% and a specificity of 100%, or, what is the same, in a negative predictive value of only 63% but a positive predictive value of 100%.

4. Discussion

Various authors have described that fluorescence-guided tumor resection increases the rate of complete excision of high-grade gliomas, without significantly increasing morbidity [4, 12, 16–22]. 5-ALA fluorescence allows for tumor "visualization" in real-time during surgery, including diffuse infiltration areas in which tumor cells are mixed with normal parenchyma, so the malignant tissue can be easily identified [23, 24] (Figures 2(a) and 2(b)). The study performed by Stummer et al. [13] validated the use of 5-ALA fluorescence to guide the resection of high-grade gliomas using

Table 1: Clinical characteristics of tumor resection cases.

Case	Age	HPD	ALA I	L	Lobe	Resection grade	PND	Systemic CPL
1	40	AA	4	B-1-1	Left frontal	Subtotal	No	PTE
2	50	GBM	4	B-0-1	Left frontal	Total	No	No
3	61	GBM	5	A-0-0	Right parietotemporal	Total	No	TCP
4	43	GBM	4	A-0-0	Right temporal	Total	No	No
5	59	GBM	5	B-1-1	Left frontal	Subtotal	No	No
6	79	GBM	2	A-1-0	Right temporal	Total	No	TCP
7	28	OLG GIII	1	A-1-0	Right frontal	Total	No	No
8	45	OLG GIII	3	A-1-0	Right frontal	Total	No	No
9	50	AA	2	B-1-1	Left temporal	Subtotal	No	No
10	66	GBM	2	A-0-0	Right temporal	Total	No	No
11	44	GBM	4	B-1-1	Left temporal	Total	No	No
12	55	GBM	4	B-1-1	Left temporal	Subtotal	No	GGT
13	56	GBM	5	A-1-0	Right parietotemporal	Total	No	PTE
14	76	MET	5	B-1-1	Left temporal	Total	No	No
15	63	GBM	1	A-0-0	Right parietal	Total	No	PTE
16	68	MET	5	B-1-1	Left frontal	Total	HEM P	No
17	20	GBM	4	A-0-1	Left parietooccipital	Total	No	No
18	49	GBM	5	A-1-0	Right frontotemporal	Subtotal	HEM P	No
19	58	MET	4	A-1-0	Right frontal	Total	HEM P	No
20	66	GBM	1	A-1-0	Right temporal	Total	No	No
21	72	GBM	5	A-0-1	Right occipital	Subtotal	No	No
22	66	GBM	4	A-0-0	Right parietal	Total	No	No
23	64	GBM	4	A-0-0	Right parietal	Total	No	No
24	57	GBM	5	A-0-0	Right parietal	Subtotal	No	No
25	21	GBM	4	A-0-1	Left parietooccipital	Total	No	No
26	70	GBM	4	A-1-0	Right temporal	Total	No	No
27	23	GBM	5	B-1-1	Left frontal	Total	No	No
28	44	GBM	5	B-1-1	Left parietal	Total	No	No
29	34	GBM	4	A-1-0	Right frontal	Total	No	No
30	59	GBM	4	A-1-0	Right parietotemporal	Total	No	No

HPD: histopathological diagnosis; AA: anaplastic astrocytoma; GBM: glioblastoma multiforme; OLG: oligodendroglioma; G: grade, MET: metastasis; L: tumor location (Shinoda); location-size-eloquence of adjacent parenchyma; PND: postoperative neurological deficit; HEM P: hemiparesis progression; CPL: complications; PTE: pulmonary thromboembolism; TCP: thrombocytopenia; GGT: gamma glutamyl transferase.

a microscope, describing complete resection in 65% of patients treated with 5-ALA compared to 36% without 5-ALA, with a 6-month disease-free survival rate and common adverse effects between both groups.

In our study, of the 27 high-grade gliomas (23 GBM and 4 anaplastic gliomas) in the craniotomy group, total resection was accomplished in 79.3% of the cases, with clinical morbidity in three patients, these results being very similar to those observed in larger series.

Analogous to the microscope, our high-definition exoscope has been adapted to detect 5-ALA-induced fluorescence. The filter combination/specification is exactly the same as the one found in surgical microscopes from other manufacturers, sharing similar image properties. The exoscope obtains high quality images with a wide field and a target distance of 200 mm. This wide range allows it to be set far from the surgical field, and the instruments can be used with fluoroscopy, which is impossible with traditional neuroendoscopes. The exoscope is also helpful for visualizing deeply located lesions. On the other hand the exoscope is less heavy and expensive when compared with a microscope. It also allows both the surgeon and the assistant to adopt an ergonomic position, making it possible to perform surgery with "four hands," or to switch continuously from a microscopic to a macroscopic view during microsurgery, while the whole team has access to the same images [25]. Furthermore, allocating a microscope to detect fluorescence in the samples of guided biopsy involves using a disproportionate remedy and prevents using it at the same time in other open surgical procedure where it is most needed.

In frameless stereotactic biopsy, despite the high accuracy of neuronavigation systems in relation to the target point chosen, the samples obtained are not always useful for pathological diagnosis. Biopsies can be nondiagnostic in 2–15% of cases. Several causes for this result have been described, such as small lesion size, deep location, presence of necrosis, poorly differentiated tumors, lack of contrast enhancement, and deep tumor location [9]. This means that in many

Table 2: Clinical characteristics of tumor biopsy cases.

Case	Age	HPD	ALA I	L	Lobe	PND	Systemic CPL
1	76	GBM	3	C-0-0	Basal ganglia	No	No
2	44	GBM	4	C-1-0	Corpus callosum	No	No
3	70	GBM	4	B-0-1	Left temporal	No	No
4	60	GBM	5	B-0-1	Left temporal	No	No
5	50	GBM	4	A-1-1	Right frontoparietal	No	No
6	62	LINFOMA	1	C-1-1	Bilateral hemispheric	No	No
7	70	GBM	4	B-0-1	Left frontal rolandic area	No	No
8	69	GBM	3	A-0-1	Right parietofrontal	No	No

HPD: histopathological diagnosis; GBM: glioblastoma multiforme; L: tumor location (Shinoda); location-size-eloquence of adjacent parenchyma; PND: postoperative neurological deficit; CPL: complications.

centers biopsies should be examined intraoperatively by the pathologist, verifying that the sample contains tumor areas, with a consequent increase in operative time and the need for the presence of staff who can examine them. However, Shooman et al. [5] question the utility of intraoperative neuropathological assessment. They observe that intraoperative neuropathology rarely influences the procedures that are being performed. Furthermore, false-positive results left open the possibility that biopsy might be ceased prematurely despite an ultimately negative sample. In addition, a false-negative result may necessitate continuation of an ultimately fruitless procedure despite the acquisition of ample material. Since 5-ALA is a safe medication (there are few reported adverse reactions) and easy to administer, and as a result of the experience obtained from fluorescence-guided tumor resection, we think that its use would increase the diagnostic yield of brain biopsies. Panciani et al. [26] assessed the reliability of a multimodal strategy based on 5-ALA and neuronavigation and the combined approach represented the best sensitivity to tumor tissue. In the present series, all the fluorescent samples obtained within the tumor boundaries, and according to the neuronavigation, were positive for high-grade glioma in the pathological examination. 5-ALA-induced fluorescence showed high sensitivity for the assessment of malignant glioma and, interestingly, in cases of confirmed metastasis a high intraoperative fluorescence level was appreciated in the samples, even though they usually exhibit an inhomogeneous fluorescence pattern, as reported by other authors [27]. Inflammatory cells and reactive astrocytes in the peritumoral area may appear fluorescent. In contrast, necrotic areas can appear negative despite being intratumoral. Despite our limited series of patients, during biopsy procedures in high-grade gliomas, when relying on neuronavigation accuracy for identification of the tumor target, combined with positive fluorescence in the samples collected, the possibility that they would not be adequate for histopathological examination is minimal (Figures 3 and 4).

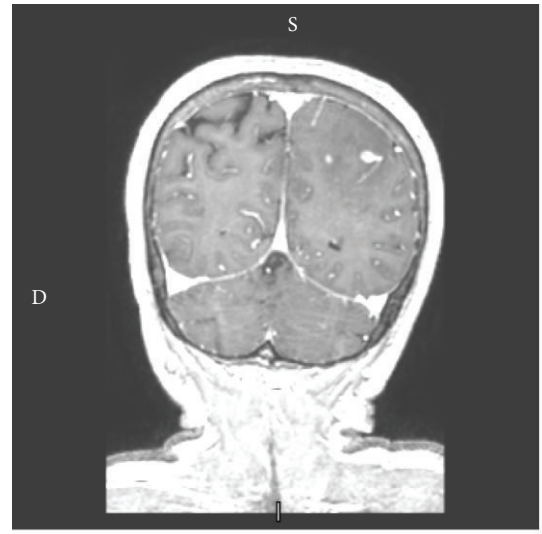

Figure 3: Coronal T1-weighted MR image with gadolinium showing a partially enhancing lesion.

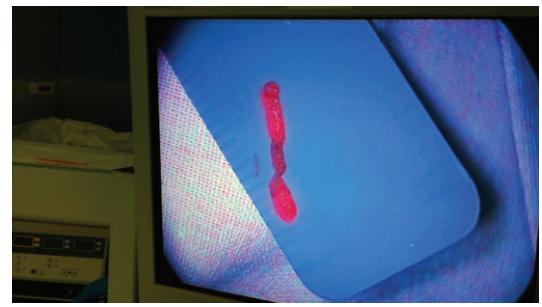

Figure 4: Sample obtained from tumor area in a neuronavigation-guided biopsy.

5. Conclusion

The high-definition exoscope system, modified to detect 5-ALA-induced fluorescence, is useful both for guided surgery of suspected high-grade gliomas and frameless MRI stereotactic biopsies, acting as a valuable tool to achieve more radical resections in brain tumor surgeries and decreasing the chances of negative biopsies. Further advantages, compared to other systems, include a lower cost and simple and manageable mobilization and transportation, as well as allowing

the surgeon to perform his act in a more ergonomic position and lessening the surgeon's fatigue.

Conflict of Interests

The authors declare that they have no conflict of interests regarding to the publication of this paper.

References

[1] D. N. Louis, H. Ohgaki, O. D. Wiestler et al., "The 2007 WHO classification of tumours of the central nervous system," *Acta Neuropathologica*, vol. 114, no. 2, pp. 97–109, 2007.

[2] E. E. Philip-Ephraim, K. I. Eyong, U. E. Williams, and R. P. Ephraim, "The role of radiotherapy and chemotherapy in the treatment of primary adult high grade gliomas: assessment of patients for these treatment approaches and the common immediate side effects," *ISRN Oncology*, vol. 2012, Article ID 902178, 6 pages, 2012.

[3] U. Pichlmeier, A. Bink, G. Schackert, and W. Stummer, "Resection and survival in glioblastoma multiforme: an RTOG recursive partitioning analysis of ALA study patients," *Neuro-Oncology*, vol. 10, no. 6, pp. 1025–1034, 2008.

[4] W. Stummer, H.-J. Reulen, T. Meinel et al., "Extent of resection and survival in glioblastoma multiforme: identification of and adjustment for bias," *Neurosurgery*, vol. 62, no. 3, pp. 564–574, 2008.

[5] D. Shooman, A. Belli, and P. L. Grundy, "Image-guided frameless stereotactic biopsy without intraoperative neuropathological examination: clinical article," *Journal of Neurosurgery*, vol. 113, no. 2, pp. 170–178, 2010.

[6] N. Sanai and M. S. Berger, "Recent surgical management of gliomas," *Advances in Experimental Medicine and Biology*, vol. 746, pp. 12–25, 2012.

[7] Y. Wang and T. Jiang, "Understanding high grade glioma: molecular mechanism, therapy and comprehensive management," *Cancer Letters*, vol. 331, no. 2, pp. 139–146, 2013.

[8] J. S. Smith, A. Quiñones-Hinojosa, N. M. Barbaro, and M. W. McDermott, "Frame-based stereotactic biopsy remains an important diagnostic tool with distinct advantages over frameless stereotactic biopsy," *Journal of Neuro-Oncology*, vol. 73, no. 2, pp. 173–179, 2005.

[9] E. L. Air, R. E. Warnick, and C. M. McPherson, "Management strategies after nondiagnostic results with frameless stereotactic needle biopsy: retrospective review of 28 patients," *Surgical Neurology International*, vol. 3, supplement 4, pp. S315–S319, 2012.

[10] L. M. Bernal-García, J. M. Cabezudo-Artero, M. Ortega-Martínez et al., "Fluorescence-guided resection with 5-aminolevulinic acid of an intramedullary tumor," *Neurocirugia*, vol. 21, no. 4, pp. 312–315, 2010.

[11] R. Díez Valle, S. Tejada Solis, M. A. Idoate Gastearena, R. García de Eulate, P. Domínguez Echávarri, and J. Aristu Mendiroz, "Surgery guided by 5-aminolevulinic fluorescence in glioblastoma: volumetric analysis of extent of resection in single-center experience," *Journal of Neuro-Oncology*, vol. 102, no. 1, pp. 105–113, 2011.

[12] P. P. Panciani, M. Fontanella, B. Schatlo et al., "Fluorescence and image guided resection in high grade glioma," *Clinical Neurology and Neurosurgery*, vol. 114, no. 1, pp. 37–41, 2012.

[13] W. Stummer, U. Pichlmeier, T. Meinel, O. D. Wiestler, F. Zanella, and H.-J. Reulen, "Fluorescence-guided surgery with 5-aminolevulinic acid for resection of malignant glioma: a randomised controlled multicentre phase III trial," *The Lancet Oncology*, vol. 7, no. 5, pp. 392–401, 2006.

[14] A. A. Potapov, D. J. Usachev, V. A. Loshakov et al., "First experience in 5-ALA fluorescence-guided and endoscopically assisted microsurgery of brain tumors," *Medical Laser Application*, vol. 23, no. 4, pp. 202–208, 2008.

[15] J. Shinoda, N. Sakai, S. Murase, H. Yano, T. Matsuhisa, and T. Funakoshi, "Selection of eligible patients with supratentorial glioblastoma multiforme for gross total resection," *Journal of Neuro-Oncology*, vol. 52, no. 2, pp. 161–171, 2001.

[16] M. J. Colditz and R. L. Jeffree, "Aminolevulinic acid (ALA)-protoporphyrin IX fluorescence guided tumour resection—part 1: clinical, radiological and pathological studies," *Journal of Clinical Neuroscience*, vol. 19, pp. 1471–1474, 2012.

[17] S. Cortnum and R. J. Laursen, "Fluorescence-guided resection of gliomas," *Danish Medical Journal*, vol. 59, no. 8, p. A4460, 2012.

[18] M. S. Eljamel, "Fluorescence image-guided surgery of brain tumors: explained step-by-step," *Photodiagnosis and Photodynamic Therapy*, vol. 5, no. 4, pp. 260–263, 2008.

[19] A. Nabavi, H. Thurm, B. Zountsas et al., "Five-aminolevulinic acid for fluorescence-guided resection of recurrent malignant gliomas: a phase II study," *Neurosurgery*, vol. 65, no. 6, pp. 1070–1076, 2009.

[20] D. W. Roberts, P. A. Valdes, B. T. Harris et al., "Adjuncts for maximizing resection: 5-aminolevuinic acid," *Clinical Neurosurgery*, vol. 59, pp. 75–78, 2012.

[21] K. Roessler, A. Becherer, M. Donat, M. Cejna, and I. Zachenhofer, "Intraoperative tissue fluorescence using 5- aminolevolinic acid (5-ALA) is more sensitive than contrast MRI or amino acid positron emission tomography (18F-FET PET) in glioblastoma surgery," *Neurological Research*, vol. 34, no. 3, pp. 314–317, 2012.

[22] T. Tykocki, R. Michalik, W. Bonicki, and P. Nauman, "Fluorescence-guided resection of primary and recurrent malignant gliomas with 5-aminolevulinic acid. Preliminary results," *Neurologia i Neurochirurgia Polska*, vol. 46, no. 1, pp. 47–51, 2012.

[23] G. von Campe, M. Moschopulos, and M. Hefti, "5-aminolevulinic acid-induced protoporphyrin IX fluorescence as immediate intraoperative indicator to improve the safety of malignant or high-grade brain tumor diagnosis in frameless stereotactic biopsies," *Acta Neurochirurgica*, vol. 154, no. 4, pp. 585–588, 2012.

[24] M. A. Kamp, P. Grosser, J. Felsberg et al., "5-aminolevulinic acid (5-ALA)-induced fluorescence in intracerebral metastases: a retrospective study," *Acta Neurochirurgica*, vol. 154, no. 2, pp. 223–228, 2012.

[25] A. N. Mamelak, T. Nobuto, and G. Berci, "Initial clinical experience with a high-definition exoscope system for microneurosurgery," *Neurosurgery*, vol. 67, no. 2, pp. 476–483, 2010.

[26] P. P. Panciani, M. Fontanella, D. Garbossa, A. Agnoletti, A. Ducati, and M. Lanotte, "aminolevulinic acid and neuronavigation in high-grade glioma surgery: results of a combined approach," *Neurocirugia*, vol. 23, pp. 23–28, 2012.

[27] G. Widhalm, G. Minchev, A. Woehrer et al., "Strong 5-aminolevulinic acid-induced fluorescence is a novel intraoperative marker for representative tissue samples in stereotactic brain tumor biopsies," *Neurosurgical Review*, vol. 35, pp. 381–391, 2012.

Hindawi Publishing Corporation
BioMed Research International
Volume 2014, Article ID 725921, 7 pages
http://dx.doi.org/10.1155/2014/725921

Research Article

Stem Cell Niches in Glioblastoma: A Neuropathological View

Davide Schiffer,[1] Marta Mellai,[1] Laura Annovazzi,[1] Valentina Caldera,[1] Angela Piazzi,[1] Tetyana Denysenko,[1,2] and Antonio Melcarne[2]

[1] *Neuro-Bio-Oncology Center, Policlinico di Monza Foundation (Vercelli)/Consorzio di Neuroscienze, University of Pavia, Via Pietro Micca 29, 13100 Vercelli, Italy*
[2] *Department of Neurosurgery, CTO Hospital, Via G. Zuretti 29, 10126 Turin, Italy*

Correspondence should be addressed to Davide Schiffer; davide.schiffer@unito.it

Received 20 January 2014; Revised 22 March 2014; Accepted 24 March 2014; Published 15 April 2014

Academic Editor: Francesco DiMeco

Glioblastoma (GBM) stem cells (GSCs), responsible for tumor growth, recurrence, and resistance to therapies, are considered the real therapeutic target, if they had no molecular mechanisms of resistance, in comparison with the mass of more differentiated cells which are insensitive to therapies just because of being differentiated and nonproliferating. GSCs occur in tumor niches where both stemness status and angiogenesis are conditioned by the microenvironment. In both perivascular and perinecrotic niches, hypoxia plays a fundamental role. Fifteen glioblastomas have been studied by immunohistochemistry and immunofluorescence for stemness and differentiation antigens. It has been found that circumscribed necroses develop inside hyperproliferating areas that are characterized by high expression of stemness antigens. Necrosis developed inside them because of the imbalance between the proliferation of tumor cells and endothelial cells; it reduces the number of GSCs to a thin ring around the former hyperproliferating area. The perinecrotic GSCs are nothing else that the survivors remnants of those populating hyperproliferating areas. In the tumor, GSCs coincide with malignant areas so that the need to detect where they are located is not so urgent.

1. Introduction

Glioblastoma (GBM) stem cells (GSCs), responsible for tumor growth, recurrence, and resistance to therapies, are considered the real therapeutic target in comparison with the mass of insensitive and differentiated tumor cells [1]. To know where they are located in the tumor and to detect them *in vivo* could be an important therapeutic achievement. Independently of their origin, by transformation from normal neural stem cells (NSCs) [2] or from progenitors [3] or from dedifferentiation of mature glia cells with the acquisition of stemness properties [4, 5], they occur in niches, corresponding to the niche of normal NSCs in the subventricular zone (SVZ) where the NSCs and progenitors are in close contact with the vasculature [6, 7]. They show self-renewing, proliferation, differentiation capacity, and high motility and express stemness antigens and an immature genetic signature [8]. Their stemness status and their relationship with angiogenesis are under specific molecular signaling [9].

GSCs occur in perivascular or perinecrotic niches, express stemness antigens, and show the same genetic alterations of primary tumors. Perivascular niches go from simple forms represented by endothelial cells associated with Nestin+ and CD133+ cells, which condition angiogenesis and tumor growth [10], to more complicated niches that include astrocytes, fibroblasts, macrophages, pericytes, non-stem tumor cells, and microglia [9] with a complicated cross-talk [11]. Perinecrotic niches have been described around circumscribed necroses where a central role is played by hypoxia and hypoxia-inducible factors 1/2 (HIF-1/2) [11] and an intrinsic and extrinsic regulation occurs [9, 11].

CD133 [12] or specific stemness proteins [13] have been used to recognize perivascular, dispersed, or perinecrotic GSCs [14]. The association of GSCs with endothelial cells and hypoxia by HIF-1/2 maintains cell stemness and favors invasion and angiogenesis.

Nestin is not a specific marker of stemness; however, from a neuropathological point of view, as deduced from its distribution complementary to that of GFAP in gliomas

Table 1: List of primary antibodies used.

Antibody	Source	Dilution	Code	Company
Ki-67/MIB.1	Mouse	1 : 100	M7240	Dako
GFAP	Mouse	1 : 200	M0761	Dako
Nestin	Mouse	1 : 200	MAB5326	Millipore
SOX2	Mouse	1 : 100	MAB2018	R&D Systems
REST	Rabbit	1 : 150	IHC-00141	Bethyl Laboratories
HIF-1	Mouse	1 : 100	NB100-105	Novus Biological
CD34	Mouse	Prediluted	790-2927	Ventana
α-Sm-actin	Mouse	Prediluted	760-2833	Ventana
GFAP*	Rabbit	1 : 200	Z0334	Dako
Nestin*	Rabbit	1 : 200	AB5922	Millipore
CD133/1 (AC133)*	Mouse	1 : 20	130-090-422	Miltenyi Biotec
Musashi.1*	Rabbit	1 : 200	AB5977	Millipore

*Tested by IF.

[15], it marks immature glia cells, including GSCs [16]. The problem is how far the concepts elaborated on niches can find corresponding aspects in human neuropathology, knowing that sometimes observations made in experimental conditions or in animal models are not confirmed [17]. In the present study, we wanted to verify in a series of human GBMs whether alternative interpretations exist to perinecrotic niches.

2. Materials and Methods

The study was performed on 15 GBMs operated at the Neurosurgical Unit of CTO Hospital, Turin. Surgical samples were split in two fragments. One was formalin fixed, paraffin embedded, and cut in 5 μm thick sections that were stained with haematoxylin and eosin (H&E) and by immunohistochemistry (IHC).

IHC was performed with the primary antibodies listed in Table 1 on a Ventana Full BenchMark automatic immunostainer (Ventana Medical Systems, Tucson, AZ, USA). Heat-induced epitope retrieval (HIER) was performed in Tris-EDTA, pH 8 (Ventana) and the ultraView Universal DAB Detection Kit (Ventana) was used as detection system.

The second fragment of the sample was frozen and 7 μm thick cryostat sections were cut, fixed with paraformaldehyde, and used for immunofluorescence (IF). Primary antibodies used are listed in Table 1; secondary antibodies were goat anti-rabbit fluorescein isothiocyanate (FITC-) conjugated IgG and rabbit anti-mouse tetramethylrhodamine isothiocyanate (TRITC-) conjugated IgG antibodies (Dako, Carpinteria, CA, USA). Negative controls were obtained by omitting the primary antibody. Observations were carried out on a Zeiss Axioskop Fluorescence Microscope (Karl Zeiss, Oberkochen, Germany) equipped with an AxioCam5MR5c and coupled to an imaging system (AxioVision Release 4.5, Zeiss).

Apoptosis was revealed by *in situ* terminal deoxynucleotidyl transferase-mediated dUTP-biotin nick end labelling (TUNEL) assay, using the *in situ* cell death detection kit, Fluorescein (Roche, Diagnostic Corporation Indianapolis, IN, USA) according to the manufacturer's protocols.

Cell density was evaluated as the mean number of cells counted in 5 microscopic fields, 1000x.

The labelling index (LI) of Ki-67/MIB.1 was calculated as the mean percentage of positive nuclei in comparison with the total number of nuclei in 5 microscopic fields, 1000x.

3. Results

In proliferating areas with very high cell density and Ki-67/MIB.1 labelling LI, hyperchromatic nuclei, and scanty cytoplasm, it was common to find Nestin+ cells around capillaries or larger vessels, prevailing on GFAP+ cells (Figures 1(a)–1(c)). In perivascular cell cuffings, Nestin still prevailed upon GFAP in the inner cell layer (Figures 1(d) and 1(e)). Hypercellular areas around circumscribed necroses (Figure 2(b)) showed a high Ki-67/MIB.1 LI (Figure 2(e)) and expressed much more Nestin than GFAP (Figures 1(f)–1(i)). These areas were frequently devoid of CD34+ small vessels or capillaries (Figure 2(a)). Circumscribed necroses developed in hyperproliferating areas and showed a necrotic centre with TUNEL-positive nuclear fragments and an internal slope with TUNEL-positive apoptotic nuclei. The palisades, crowded with Nestin+ cells and mitoses, flew into areas with lower cell density where GFAP+ cells progressively prevailed upon Nestin+ cells.

The hyperproliferating areas and the palisades strongly expressed SOX2 and REST (Figures 2(c) and 2(d)). HIF-1+ nuclei were mainly found in the palisade bordering the necrosis, but also scattered in the tissue (Figure 2(f)). Microvascular proliferations (MVP) could be variably surrounded by various cell types such as tumor cells, fibroblasts, macrophages, reactive astrocytes, and mainly alpha smooth muscle actin (α-sm-actin-) positive pericytes. By IF, the respective distribution of GFAP+ and Nestin+ cells was clearly evident (Figures 3(a)–3(c)). CD133+ and Musashi.1+ cells were found in small groups or scattered in the hyperproliferating areas and in the palisades (Figures 3(d)–3(f)).

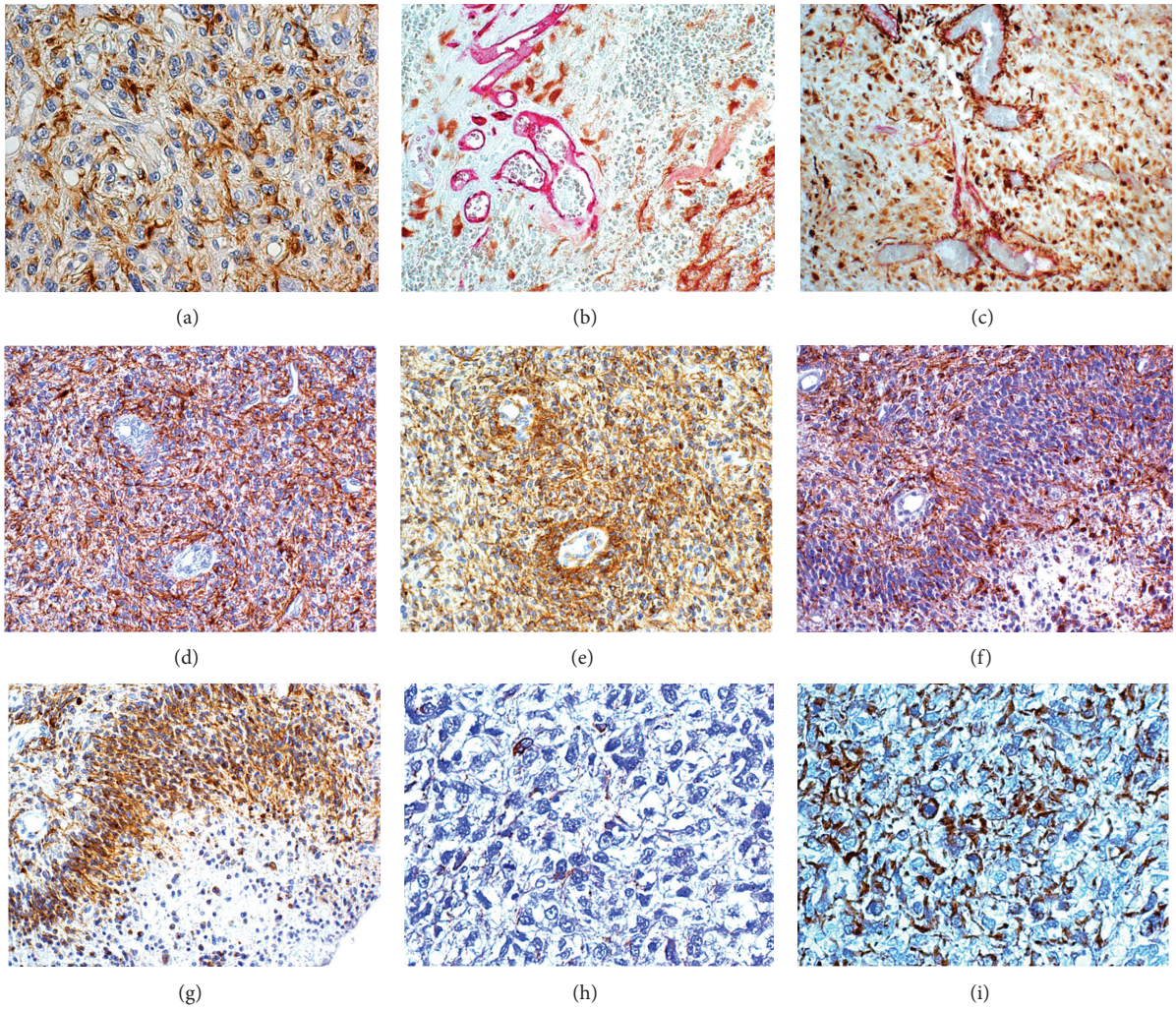

Figure 1: (a) Infiltration area with many positive cells on vessels of different size, Nestin, DAB, 200x. (b) Transition area: medium size vessels with no cell around, GFAP, DAB, 100x. (c) Same area with many positive cells around vessels, Nestin, DAB, 100x. (d) Proliferation area: cuffing of tumor cells around vessels; GFAP+ cells are in an external position, DAB, 200x. (e) *Id* Nestin+ cells prevail and are located in the inner layer of the cuffing, DAB, 200x. (f) Hyperproliferating area with a circumscribed necrosis: most cells do not express GFAP, DAB, 100x. (g) The same area: the cells strongly express Nestin, DAB, 100x. (h) *Id* for GFAP, DAB, 400x, and (i) Nestin, DAB, 400x.

4. Discussion

The close contact between Nestin+ cells and capillaries [10] and the perivascular position of tumor stem cells recognizable by CD133 positivity or expression of specific stem cell antigens [13] correspond, from the neuropathological point of view, to the distribution of Nestin in gliomas that is less extensive than that of GFAP, but it includes more immature tumor cells, stem cells, and progenitors [15]. As a matter of fact, in the cytogenesis, Nestin is the first antigen to be expressed and it persists in the following stages, for example, in radial glia which is the only glia expressing the three antigens Nestin, Vimentin, and GFAP at the same time. In the course of differentiation, GFAP expression progressively increases as that of Nestin decreases [15]. The perivascular position of stem cells observed by Nestin, CD133, or other stemness antigens corresponds to that of Nestin+ cells which, if not a specific marker of stem cells, marks immature cells [15]. Nestin is strongly expressed in hyperproliferating areas, where often GFAP is lacking, demonstrating that they contain more immature cells, that is, stem cells or progenitors, and this corresponds to what has been shown with CD133 or other stemness antigens [12, 13].

In the association of GSCs/progenitors with endothelial cells in perivascular positions, the latter maintain the stemness of the former and, on the other side, the former favor angiogenesis. This reciprocity is easily comprehensible when there is a direct contact between Nestin+ cells and endothelial cells, as it happens in capillaries or small vessels; it is more difficult when Nestin+ cells crowd around vessels with a thicker wall. Anyway, the association has been considered as instrumental to tumor diffusion and expansion, which are realized through the epithelial-mesenchymal transition [18].

The perivascular stem cell niche consists of distinct cell types and matrices that regulate proliferation, fate specification, and protection of normal neural stem cells

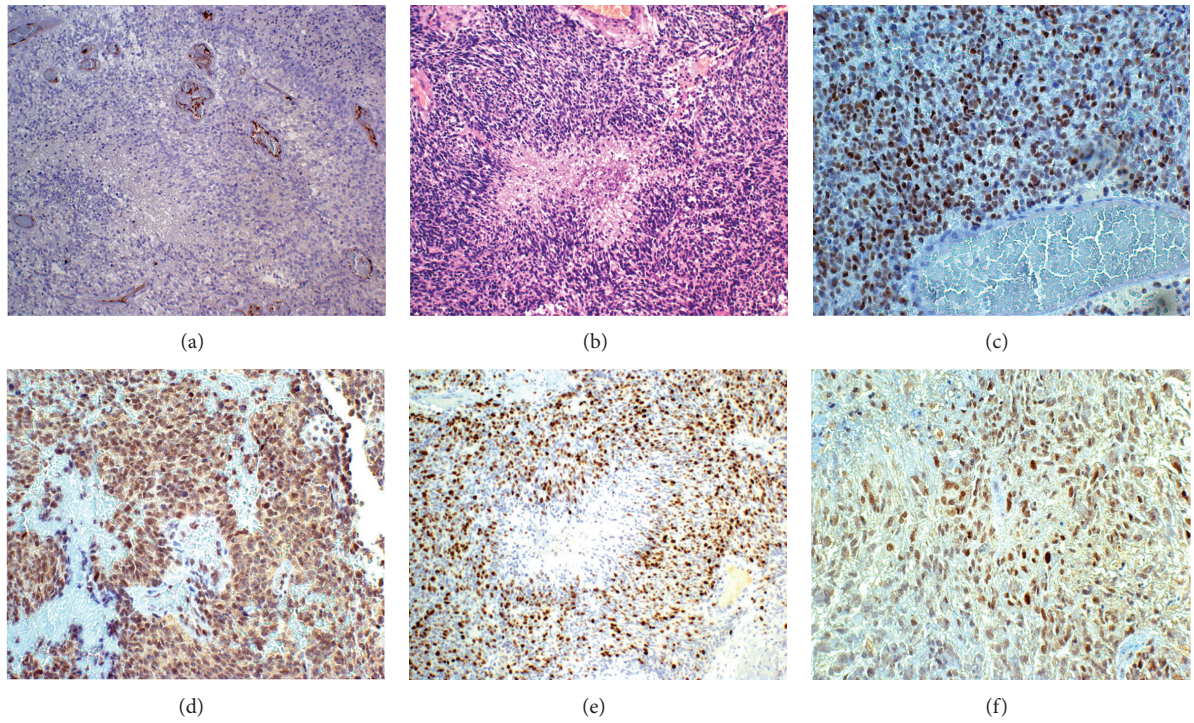

Figure 2: (a) Hyperproliferating area with a circumscribed necrosis devoid of vessels, CD34, DAB, 100x. (b) Circumscribed necrosis in a hypercellular area, H&E, 100x. (c) Hyperproliferating area strongly positive for SOX2, DAB, 100x. (d) *Id* for REST, DAB, 100x. (e) *Id* in a hyperproliferating area with high Ki-67/MIB.1 LI, DAB, 100x. (f) HIF-1-positive cells near a circumscribed necrosis, DAB, 200x.

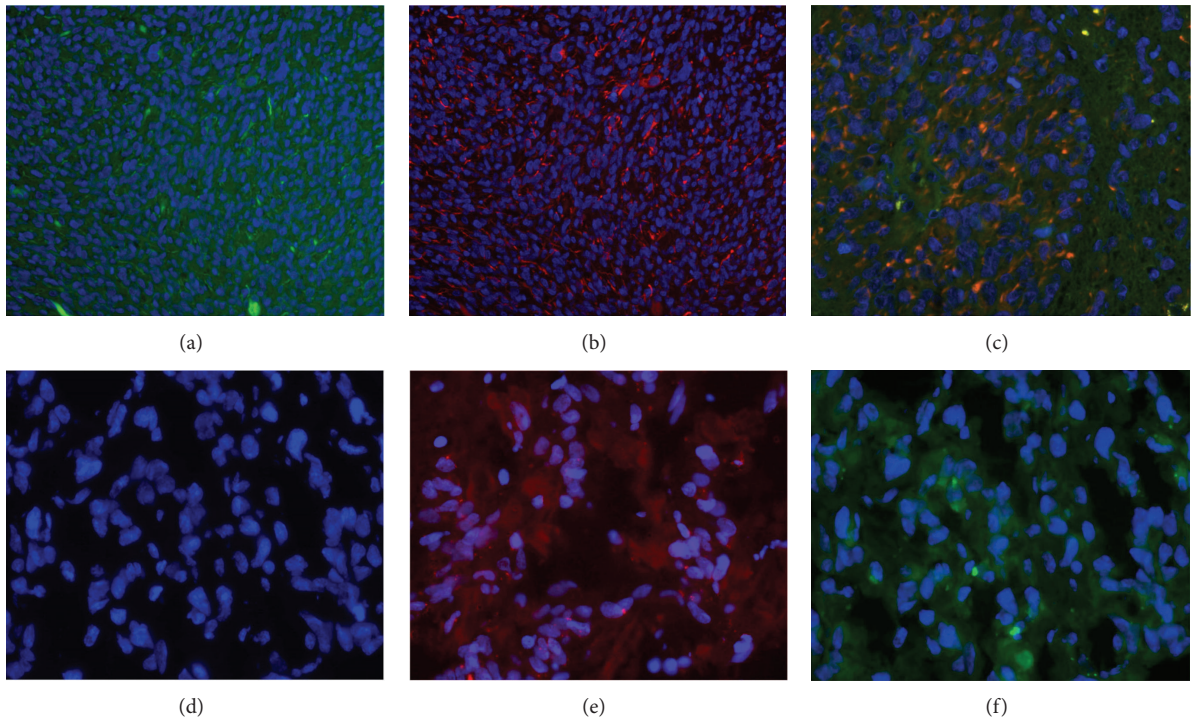

Figure 3: (a) Hyperproliferating area with few cells expressing GFAP, IF, 200x. (b) *Id* with many cells expressing Nestin, 200x. (c) Merge. (d) Hyperproliferating areas with omission of CD133 antibody, 400x. (e) Hyperproliferating area with CD133 antibody. (f) *Id* with Musashi.1, 400x.

(NSCs). The intimate association between normal NSCs and endothelial cells has been reported to regulate self-renewal and differentiation of normal NSCs. There would be a bidirectional communication between endothelial cells and tumor initiating cells (TICs) [19]. The composition of perivascular niche (PVN) has been carefully described, with also the inclusion of extra-cellular matrix, integrins, cell adhesion signaling, cadherin family, and so forth [20]. In GBMs, strong evidence for the existence of the epithelial-to-mesenchymal transition (EMT) process is still lacking, but this process is increasingly reported as instrumental to growth and diffusion of the tumor [21, 22]. EMT is a process letting differentiated epithelial cells establish stable contacts with neighbor cells, assume a mesenchymal cell phenotype with loss of cell-cell interactions, reduced cellular adhesion, active production of ECM proteases, increased cytoskeletal dynamics, and changes in transcription factor expression, and assume the acquisition of a stem cell program; all of them lead to increased migration and invasion ability.

The three major groups of transcription factors, the SNAI, TWIST, and Zinc-finger enhancer binding (ZEB) family members have been reported to be altered in GBM. Their overexpression follows the activation of WNT/β-catenin pathway and results in increased *in vitro* cell migration and invasion [23, 24]. It is likely that the high expression of mesenchymal genes in the mesenchymal subset of human GBMs [25] can be considered to be reminiscent of the EMT program [26] or that the aberrant activation of EMT factors during gliomagenesis can trigger the mesenchymal shift in GBM [27].

In the hyperproliferating zones of GBM there are areas devoid of vessels. Neoangiogenesis in gliomas is realized through a complex molecular mechanism focused on vascular endothelial growth factor (VEGF), angiopoietin-1 (Ang-1), angiopoietin-2 (Ang-2), hypoxia, and so forth [28]; that does not exclude the possibility that bone marrow-derived endothelial progenitor cells [29, 30] or mesenchymal stem cells [31] participate in the process. Angiogenesis starting from the vessels of the host produces, on the one side, a thick net of small neoformed vessels capable of nourishing a large population of tumors cells and, on the other side, multilayered bumpy vessels, usually derived from the penetrating meningeal vessels assailed by the invading tumor cells, inadequate to feed the multitude of invading cells [32, 33]. On the vessel walls, there is a crowding of pericytes, recruited by PDGFR expressed by endothelial cells, but also macrophages, fibroblasts, tumor or reactive astrocytes [11]. Pericytes are critical for the structural stability of the vascular niche, for survival of tumor endothelial cells [34], and, in general, for the establishment of the neovascular tree [35].

Perinecrotic niches represent an even more complicated matter. The perinecrotic GSCs are believed to be induced by hypoxia; the hypothesis is that HIF-1/2 activates key stem cell genes such as Nanog, Oct4, and c-Myc [35]. Circumscribed necroses have been carefully described and codified [28, 36, 37] as due to an ischemic process following a vascular occlusion or a pathology of the endothelium; the consequent hypoxia would stimulate angiogenesis, through HIF-1 and VEGF. According to our observations, another interpretation can be given. Necroses develop in hyperproliferating areas, with a high Ki-67/MIB.1 LI and a high Nestin expression in comparison with GFAP, due to the focal insufficiency of neoangiogenesis to feed a very large number of tumor cells, because of the imbalance between the high tumor cell proliferation capacity and the low one of endothelial cells [32, 38, 39]. This observation does not exclude that inside necroses regressive pathological vessels occur [37]. The palisades, as well as hypercellular areas, are composed of Nestin+, SOX2+, and REST+ cells, which can be considered as stemness markers [40, 41] with a high proliferation index, and contain CD133+ cells, as already observed [12]. It is likely that GSCs represent the quota of GSCs, that populated the hyperproliferating areas, remained after necrosis development. Similarly the palisades themselves are the remnants of the part of hyperproliferating areas spared by necrosis. This interpretation would not be in contrast with that of a vascular pathology as the first step of necrosis [37].

The real origin of GSCs is still debated. They are supposed to derive from the transformation of NSCs [42, 43], from mature astrocytes through dedifferentiation [4, 5], from precursor oligodendrocytes, or NG2 [44–47] or they represent a simple functional status [48–50]. The latter can be regulated in the microenvironment of the niches, considering the entire hyperproliferating area as a niche. The stem-like status could be reached by the most malignant cells, that is, dedifferentiated tumor cells, which acquire stemness properties. On the other hand, GSCs have been considered at the top of a hierarchy of tumor cells as for phenotypic and genotypic stemness expression [51, 52] corresponding to stemness hierarchy [50] which is at its maximum height in the most malignant phenotype of the tumor. Our observation that the capacity to generate neurospheres in culture varies according to the site of the sample [50], in agreement [53, 54] or in contrast [55] with other observations, is in line with the present results.

No possibility has been found till now to detect GSCs *in vivo* by MRI techniques. With 5-ALA, it was shown that TICs from the fluorescent mass are different from those of nonfluorescent margins which are tumorigenic *in vivo* but not self-renewing *in vitro* [54]. On the other hand, the results of this work demonstrate that the detection of GSCs *in vivo* is not so urgent, because they probably correspond more or less to the most malignant areas of GBM. This does not exclude that their annihilation by pharmacological means continues to be a therapeutic target.

5. Conclusions

Therapies directed to the elimination of GSCs in glioblastoma remain fundamental. They would require the *in vivo* detection of GSCs. GSCs, as expression of a functional status, roughly correspond to the most malignant tumor phenotype.

Conflict of Interests

The authors declare that there is no conflict of interests regarding the publication of this paper.

Acknowledgment

This work was supported by Grant no. 4011 SD/cv 2011-0438 from Compagnia di San Paolo, Turin, Italy.

References

[1] T. Reya, S. J. Morrison, M. F. Clarke, and I. L. Weissman, "Stem cells, cancer, and cancer stem cells," *Nature*, vol. 414, no. 6859, pp. 105–111, 2001.

[2] E. C. Holland, "Progenitor cells and glioma formation," *Current Opinion in Neurology*, vol. 14, no. 6, pp. 683–688, 2001.

[3] R. Galli, "The neurosphere assay applied to neural stem cells and cancer stem cells," *Methods in Molecular Biology*, vol. 986, pp. 267–277, 2013.

[4] N. Sanai, A. Alvarez-Buylla, and M. S. Berger, "Mechanisms of disease: neural stem cells and the origin of gliomas," *The New England Journal of Medicine*, vol. 353, no. 8, pp. 811–822, 2005.

[5] M. Assanah, R. Lochhead, A. Ogden, J. Bruce, J. Goldman, and P. Canoll, "Glial progenitors in adult white matter are driven to form malignant gliomas by platelet-derived growth factor-expressing retroviruses," *The Journal of Neuroscience*, vol. 26, no. 25, pp. 6781–6790, 2006.

[6] Q. Shen, S. K. Goderie, L. Jin et al., "Endothelial cells stimulate self-renewal and expand neurogenesis of neural stem cells," *Science*, vol. 304, no. 5675, pp. 1338–1340, 2004.

[7] T. D. Palmer, A. R. Willhoite, and F. H. Gage, "Vascular niche for adult hippocampal neurogenesis," *The Journal of Comparative Neurology*, vol. 425, no. 4, pp. 479–494, 2000.

[8] H. Sanai, A. D. Tramontin, A. Quiñones-Hinojosa et al., "Unique astrocyte ribbon in adult human brain contains neural stem cells but lacks chain migration," *Nature*, vol. 427, no. 6976, pp. 740–744, 2004.

[9] N. A. Charles, E. C. Holland, R. Gilbertson, R. Glass, and H. Kettenmann, "The brain tumor microenvironment," *Glia*, vol. 59, no. 8, pp. 1169–1180, 2011.

[10] C. Calabrese, H. Poppleton, M. Kocak et al., "A perivascular niche for brain tumor stem cells," *Cancer Cell*, vol. 11, no. 1, pp. 69–82, 2007.

[11] A. Filatova, T. Acker, and B. K. Garvalov, "The cancer stem cell niche(s): the crosstalk between glioma stem cells and their microenvironment," *Biochimica et Biophysica Acta*, vol. 1830, no. 2, pp. 2496–2508, 2013.

[12] K. Christensen, H. D. Schrøder, and B. W. Kristensen, "CD133 identifies perivascular niches in grade II-IV astrocytomas," *Journal of Neuro-Oncology*, vol. 90, no. 2, pp. 157–170, 2008.

[13] S. Seidel, B. K. Garvalov, V. Wirta et al., "A hypoxic niche regulates glioblastoma stem cells through hypoxia inducible factor 2α," *Brain*, vol. 133, part 4, pp. 983–995, 2010.

[14] H. He, M. W. Li, and C. S. Niu, "The pathological characteristics of glioma stem cell niches," *Journal of Clinical Neuroscience*, vol. 19, no. 1, pp. 121–127, 2012, Erratum in: *Journal of Clinical Neuroscience*, vol. 19, no. 6, p. e1, 2012.

[15] D. Schiffer, A. Manazza, and I. Tamagno, "Nestin expression in neuroepithelial tumors," *Neuroscience Letters*, vol. 400, no. 1-2, pp. 80–85, 2006.

[16] D. Schiffer, V. Caldera, M. Mellai et al., "Antigenic and genotypic similarity between primary glioblastomas and their derived neurospheres," *Journal of Oncology*, Article ID 314962, 2011.

[17] F. J. Rodriguez, B. A. Orr, K. L. Ligon, and C. G. Eberhart, "Neoplastic cells are a rare component in human glioblastoma microvasculature," *Oncotarget*, vol. 3, no. 1, pp. 98–106, 2012.

[18] J. P. Thiery, "Epithelial-mesenchymal transitions in tumour progression," *Nature Reviews Cancer*, vol. 2, no. 6, pp. 442–454, 2002.

[19] R. J. Gilbertson and J. N. Rich, "Making a tumour's bed: glioblastoma stem cells and the vascular niche," *Nature Reviews Cancer*, vol. 7, no. 10, pp. 733–736, 2007.

[20] M. D. Brooks, R. Sengupia, S. C. Snyder, and J. B. Rubin, "Hitting them where they live. Targeting the glioblastoma perivascular stem cell niche," *Current Pathobiology Reports*, vol. 1, no. 2, pp. 101–110, 2013.

[21] A. Pala, G. Karpel-Massler, C. R. Wirtz, and M. E. Halatsch, "Epithelial to mesenchymal transition and progression of glioblastoma," in *Clinical Management and Evolving Novel Therapeutic Strategies For Patients With Brain Tumors*, T. Lichtor, Ed., pp. 277–289, InTech, Rjieka, Croatia, 2013.

[22] B. Ortensi, M. Setti, D. Osti, and G. Pelicci, "Cancer stem cell contribution to glioblastoma invasiveness," *Stem Cell Research and Therapy*, vol. 4, no. 1, pp. 18–29, 2013.

[23] X. Jin, H. Y. Jeon, K. M. Joo et al., "Frizzled 4 regulates stemness and invasiveness of migrating glioma cells established by serial intracranial transplantation," *Cancer Research*, vol. 71, no. 8, pp. 3066–3075, 2011.

[24] U. D. Kahlert, D. Maciaczyk, S. Doostkam et al., "Activation of canonical WNT/beta-catenin signaling enhances in vitro motility of glioblastoma cells by activation of ZEB1 and other activators of epithelial-to-mesenchymal transition," *Cancer Letters*, vol. 325, no. 1, pp. 42–53, 2012.

[25] H. S. Phillips, S. Kharbanda, R. Chen et al., "Molecular subclasses of high-grade glioma predict prognosis, delineate a pattern of disease progression, and resemble stages in neurogenesis," *Cancer Cell*, vol. 9, no. 3, pp. 157–173, 2006.

[26] R. G. W. Verhaak, K. A. Hoadley, E. Purdom et al., "Integrated genomic analysis identifies clinically relevant subtypes of glioblastoma characterized by abnormalities in PDGFRA," *Cancer Cell*, vol. 17, no. 1, pp. 98–110, 2010.

[27] K. P. L. Bhat, K. L. Salazar, V. Balasubramaniyan et al., "The transcriptional coactivator TAZ regulates mesenchymal differentiation in malignant glioma," *Genes and Development*, vol. 25, no. 24, pp. 2594–2609, 2011.

[28] M. E. Hardee and D. Zagzag, "Mechanisms of glioma-associated neovascularization," *The American Journal of Pathology*, vol. 181, no. 4, pp. 1126–1141, 2012.

[29] D. Lyden, K. Hattori, S. Dias et al., "Impaired recruitment of bone-marrow-derived endothelial and hematopoietic precursor cells blocks tumor angiogenesis and growth," *Nature Medicine*, vol. 7, no. 11, pp. 1194–1201, 2001.

[30] D. Gao, D. J. Nolan, A. S. Mellick, K. Bambino, K. McDonnell, and V. Mittal, "Endothelial progenitor cells control the angiogenic switch in mouse lung metastasis," *Science*, vol. 319, no. 5860, pp. 195–198, 2008.

[31] A. Veeravagu, S. R. Bababeygy, M. Y. S. Kalani, L. C. Hou, and V. Tse, "The cancer stem cell-vascular niche complex in brain tumor formation," *Stem Cells and Development*, vol. 17, no. 5, pp. 859–867, 2008.

[32] D. Schiffer, A. Chiò, M. T. Giordana, A. Mauro, A. Migheli, and M. C. Vigliani, "The vascular response to tumor infiltration in malignant gliomas. Morphometric and reconstruction study," *Acta Neuropathologica*, vol. 77, no. 4, pp. 369–378, 1989.

[33] P. Wesseling, R. O. Schlingemann, F. J. R. Rietveld et al., "Early and extensive contribution of pericytes/vascular smooth muscle cells to microvascular proliferation in glioblastoma multiforme:

an immuno-light and immuno-electron microscopic study," *Journal of Neuropathology and Experimental Neurology*, vol. 54, no. 3, pp. 304–310, 1995.

[34] S. Song, A. J. Ewald, W. Stallcup, Z. Werb, and G. Bergers, "PDGFR beta+ perivascular progenitor," *Cell Biology*, vol. 7, no. 9, pp. 870–879, 2005.

[35] J. M. Heddleston, Z. Li, R. E. McLendon, A. B. Hjelmeland, and J. N. Rich, "The hypoxic microenvironment maintains glioblastoma stem cells and promotes reprogramming towards a cancer stem cell phenotype," *Cell Cycle*, vol. 8, no. 20, pp. 3274–3284, 2009.

[36] I. Fischer, J.-P. Gagner, M. Law, E. W. Newcomb, and D. Zagzag, "Angiogenesis in gliomas: biology and molecular pathophysiology," *Brain Pathology*, vol. 15, no. 4, pp. 297–310, 2005.

[37] Y. Rong, D. L. Durden, E. G. van Meir, and D. J. Brat, "'Pseudopalisading' necrosis in glioblastoma: a familiar morphologic feature that links vascular pathology, hypoxia, and angiogenesis," *Journal of Neuropathology and Experimental Neurology*, vol. 65, no. 6, pp. 529–539, 2006.

[38] O. Kargiotis, J. S. Rao, and A. P. Kyritsis, "Mechanisms of angiogenesis in gliomas," *Journal of Neuro-Oncology*, vol. 78, no. 3, pp. 281–293, 2006.

[39] D. Schiffer, *Brain Tumor Pathology: Hotspots and Pitfalls on Current Histological Histological Diagnosis*, Springer, Dordrecht, The Netherlands, 2006.

[40] L. Annovazzi, M. Mellai, V. Caldera, G. Valente, and D. Schiffer, "SOX2 expression and amplification in gliomas and glioma cell lines," *Cancer Genomics and Proteomics*, vol. 8, no. 3, pp. 139–147, 2011.

[41] L. Conti, L. Crisafulli, V. Caldera et al., "REST controls self-renewal and tumorigenic competence of human glioblastoma cells," *PLoS ONE*, vol. 7, no. 6, Article ID e38486, 2012.

[42] S. A. Llaguno, J. Chen, C.-H. Kwon et al., "Malignant astrocytomas originate from neural stem/progenitor cells in a somatic tumor suppressor mouse model," *Cancer Cell*, vol. 15, no. 3, p. 240, 2009.

[43] T. S. Jacques, A. Swales, M. J. Brzozowski et al., "Combinations of genetic mutations in the adult neural stem cell compartment determine brain tumour phenotypes," *The EMBO Journal*, vol. 29, no. 1, pp. 222–235, 2010.

[44] K. Masui, S. O. Suzuki, R. Torisu, J. E. Goldman, P. Canoll, and T. Iwaki, "Glial progenitors in the brainstem give rise to malignant gliomas by platelet-derived growth factor stimulation," *Glia*, vol. 58, no. 9, pp. 1050–1065, 2010.

[45] S. Sugiarto, A. I. Persson, E. G. Munoz et al., "Asymmetry-defective oligodendrocyte progenitors are glioma precursors," *Cancer Cell*, vol. 20, no. 3, pp. 328–340, 2011.

[46] C. Persson, F. Petritsch, J. Swartling et al., "Non-stem cell origin for oligodendroglioma," *Cancer Cell*, vol. 18, no. 6, pp. 669–682, 2010.

[47] J. C. Liu, M. Sage, R. Miller et al., "Mosaic analysis with double markers reveals tumor cell of origin in glioma," *Cell*, vol. 146, no. 2, pp. 209–221, 2011.

[48] D. Zipori, "The nature of stem cells: state rather than entity," *Nature Reviews Genetics*, vol. 5, no. 11, pp. 873–878, 2004.

[49] A. L. Vescovi, R. Galli, and B. A. Reynolds, "Brain tumour stem cells," *Nature Reviews Cancer*, vol. 6, no. 6, pp. 425–436, 2006.

[50] D. Schiffer, M. Mellai, L. Annovazzi, A. Piazzi, I. Monzeglio, and V. Caldera, "Glioblastoma cancer stem cells: basis for a functional hypothesis," *Stem Cell Discovery*, vol. 2, no. 3, pp. 122–131, 2012.

[51] R. Chen, M. C. Nishimura, S. M. Bumbaca et al., "A hierarchy of self-renewing tumor-initiating cell types in glioblastoma," *Cancer Cell*, vol. 17, no. 4, pp. 362–375, 2010.

[52] S. Mazzoleni, L. S. Politi, M. Pala et al., "Epidermal growth factor receptor expression identifies functionally and molecularly distinct tumor-initiating cells in human glioblastoma multiforme and is required for gliomagenesis," *Cancer Research*, vol. 70, no. 19, pp. 7500–7513, 2010.

[53] S. G. M. Piccirillo, R. Combi, L. Cajola et al., "Distinct pools of cancer stem-like cells coexist within human glioblastomas and display different tumorigenicity and independent genomic evolution," *Oncogene*, vol. 28, no. 15, pp. 1807–1811, 2009.

[54] S. G. Piccirillo, S. Dietz, B. Madhu et al., "Fluorescence-guided surgical sampling of glioblastoma identifies phenotypically distinct tumour-initiating cell populations in the tumour mass and margin," *British Journal of Cancer*, vol. 107, no. 3, pp. 462–468, 2012.

[55] R. Pallini, L. Ricci-Vitiani, G. L. Banna et al., "Cancer stem cell analysis and clinical outcome in patients with glioblastoma multiforme," *Clinical Cancer Research*, vol. 14, no. 24, pp. 8205–8212, 2008.